2008

# SELECTIVE NON-PEPTIDE MU-OPIOID RECEPTOR ANTAGONIST: DESIGN, SYNTHESIS AND BIOLOGICAL STUDIES

Lindsey Aschenbach
*Virginia Commonwealth University*

# SELECTIVE NON-PEPTIDE MU-OPIOID RECEPTOR ANTAGONISTS:

# DESIGN, SYNTHESIS AND BIOLOGICAL STUDIES

A thesis submitted in partial fulfillment of the requirements for the degree of Masters at Virginia Commonwealth University.

by

LINDSEY C. K. ASCHENBACH
Bachelors of Science in Biochemistry, Virginia Tech, 2004

Director: Yan Zhang, Ph.D.
Department of Medicinal Chemistry
School of Pharmacy

Virginia Commonwealth University
Richmond, Virginia
December 2008

# Acknowledgement

I would like to take this opportunity to thank my advisor, Dr. Yan Zhang, for his assistance and guidance over the course of my research experience here at VCU. His support and insight have been invaluable in the progression of my research. During my research experiences at VCU, I have had the opportunity expand my chemistry background by working in a number of different departments. I would like to thank Dr. Dana Selley and Dr. Laura Sim-Selley of the Department of Pharmacology and Toxicology for not only their guidance but also for the opportunity to work in their labs and gain valuable experience that I would not have found in an organic chemistry lab. I would like to thank Dr. Dukat and Dr.Nagamasi for being in my committee and all of their help with my thesis. I would also like to thank the School of Pharmacy for their support during my time in the Department of Medicinal Chemistry. While I have received a lot of research assistance while at VCU, I would like to specifically thank Mike Cassidy for his assistance and guidance with the bioassays, Catherine He for her assistance and guidance with cell culture and bioassays and Jerry Hernandez for his assistance with teaching me how to culture cells. I would also like to thank the members of Dr. Zhang's lab group for their comradely as well as their assistance with my research progression. I would especially like to thank Dr. Guo Li for his help in organic synthesis and Mika Shima for her assistance with the bioassays. Most importantly, I would like to thank all of my family and friends. My friend and husband, Jeremy Allen, has been extremely supportive and helpful in the progression of my research here at VCU as well as there for me in some very difficult times that I have encountered since starting at VCU. I especially want to thank my mother, father, and sister for all of their unending love and support throughout my life and all of my educational endeavors. Without the encouragement of my family, but especially my late father, I would not have been able to achieve all that I have achieved academically. Thank you to all of those people named and unnamed here that have prepared me for this achievement as well as for those challenges to come.

# Table of Contents

Page

# List of Tables

Page

# List of Figures

Page

# List of Schemes

Page

## List of Abbreviations

| | |
|---|---|
| Å | angstroms |
| $^3H$ | tritiated |
| α | alpha |
| β | beta |
| δ | delta |
| δ (experimental) | chemical shift |
| °C | degrees Celcius |
| γ | gamma |
| κ | kappa |
| μ | mu |
| μg | micrograms |
| μL | microliter |
| % | percent |
| aq | aqueous |
| BBB | blood brain barrier |
| Bmax | receptor density |
| $CD_3OD$ | deuterated methanol |
| CHO | Chinese hamster ovary |
| CNS | central nervous system |
| $CO_2$ | carbon dioxide |
| d | doublet |
| DI | deionized |
| DMEM | Dulbecco's modified Eagles's medium |
| DMF | dimethylformamide |
| DMSO | dimethyl sulfoxide |
| DMT | 2',6'-dimethylthrosine |
| DOR | delta-opioid receptor |
| DPM | disintegrations per minute |
| $EC_{50}$ | molar concentration producing half maximal response |
| EDTA | ethylenediaminoacetic acid |
| EGTA | ethylene glycol tetraacetic acid |
| EL | extracellular loop |
| Emax | maximum response |
| FBS | fetal bovine serum |

| | |
|---|---|
| g | grams |
| g's | g force |
| G148 | geneticin |
| GDP | guanosine diphosphate |
| GPCR | G-protein coupled receptor |
| GRK | G-protein Coupled receptor kinase |
| GTP | guanosine triphosphate |
| GTPγS | guanosine gamma thio-phosphate |
| h | hours |
| HAT | hypoxanthine, aminopterin, and thymidine |
| HBSS | Hank's balanced salt solution |
| HEK | human embryonic kidney |
| HEPEs | 4-(2-hydroxyethyl)-1-piperazineethanesulonic acid |
| $IC_{50}$ | molar concentration producing half inhibition response |
| IL | intracellular loop |
| IR | infrared spectroscopy |
| $K_2CO_3$ | potassium carbonate |
| Ke | dissociation constant |
| Ki | inhibition constant |
| KOR | kappa-opioid receptor |
| m | multiplet |
| M | molar |
| mg | milligram |
| mHz | megahertz |
| mL | milliliter |
| mm | millimeter |
| mmol | millimole |
| mM | millimolar |
| mp | melting point |
| mRNA | message ribonucleic acid |
| MOR | mu-opioid receptor |
| MS | mass spectrometry |
| $N_2$ | nitrogen gas |
| $Na^+$ | sodium ion |
| NG108-15 | mouse neuroblastoma x rat glioma hybrid |
| $NH_4OH$ | ammonium hydroxide |

| | |
|---|---|
| NLX | naloxone |
| nM | nanimolar |
| NMDA | N-methyl-D-aspartic Acid |
| NMR | nuclear magnetic resonance |
| NTI | naltrindole |
| Nor-BNI | nor-binaltorphimine |
| $pA_2$ | apparent affinity |
| PBS | phosphate buffer solution |
| pmol | picomole |
| POMC | pro-opiomelanocortin |
| rpm | rotations per minute |
| s | singlet |
| SAR | structure-activity relationship |
| SCWRL | side chain placement with a rotamer library |
| $SOCl_2$ | thionylchloride |
| SSRI | serotonin reuptake inhibitor |
| TEA | triethylamine |
| THF | tetrahydrofuran |
| TM | transmembrane |
| Tris | trihydroxymethylaminomethane |
| VTA | ventral tegmental area |

# Abstract

SELECTIVE NON-PEPTIDE MU-OPIOID RECEPTOR ANTAGONISTS:

DESIGN, SYNTHESIS AND PHARMACOLOGICAL STUDIES

By Lindsey C. K. Aschenbach, M.S.

A thesis submitted in partial fulfillment of the requirements for the degree of Masters of Science at Virginia Commonwealth University.

Virginia Commonwealth University, 2008

Major Director: Dr. Yan Zhang, Assistant Professor
Department of Medicinal Chemistry

There are currently many opioid agonists available for clinical use as analgesics. However, many of these opioid agonists have notorious side effects including respiratory depression and may lead to addiction and dependence. Problems associated with these opioid agonists are determined to come from their interactions with the mu-opioid receptor. Opioid antagonists, such as naltrexone, have shown to aid in the treatment of opioid addiction. Although naltrexone has high affinity to the mu-opioid receptor, it lacks selectivity. Novel selective mu-opioid receptor antagonists were designed based on the identification of important pharmacophore elements in several known mu-opioid receptor agonists and antagonists. These compounds were synthesized and in vitro biological assays were conducted to determine their affinity to

all three opioid receptors. Also, molecular modeling studines were conducted to help visualize the interactions between the mu-opioid receptor and these ligands. Finally, four lead compounds have been identified for further optimization.

# I. Introduction

Ancient civilizations have used extracts from the poppy flower for analgesic purposes. Around 300 B.C. Theophrastus described the analgesic use of opium in the "Inquiry of Plants". Opium was a crude extract from the unripe seedpod of the poppy flower, *Papaver Somniferum*. Morphine is the main active ingredient of opium and was isolated by Serturner in 1803. Later, other morphine-like alkaloids, such as thebaine and codeine, were isolated from the same resource. Morphine is still the most commonly used opioid analgesic in clinical settings.[1]

Morphine produces many effects including analgesia, which makes it useful to treat post-operation and chronic pain. However, morphine also has adverse side effects such as respiratory depression, pancreatitis, renal failure, chemical toxicity for patients with low tolerability, and raised intracranial pressure that can lead to head injuries. Most significantly, morphine is highly addictive both physically and psychologically.[2]

Opioids have been associated with abuse and addiction problems for a long time. However, it has become more prominent over the last couple of centuries, especially since the introduction of the hypodermic needle in the 1950s. Long-term use of opioids may lead to addiction that can result in a compulsive need for opioids. According to the National Survey on Drug Use and Health (NSDUH), in 2005 about 2.2 million people

used prescription analgesics for non-medical purposes for the first time.[3] As of 2007, it is estimated about 16 million people worldwide abuse opioids.[4] Opioid dependency and addiction can be treated through detoxification or drug replacement therapy.

Morphine, as well as other opioids, mainly acts on the opioid receptors in the central nervous system. There are three major opioid receptors including mu, kappa and delta. All three opioid receptors are involved in analgesia. However, it has been shown that the analgesic effect and adverse side effects of morphine are primarily due to its interaction with the mu-opioid receptor. For example, it was found that the analgesic and addictive properties of morphine is abolished in mu-opioid receptor knock-out mice.[5] Therefore, the characterization of the mu-opioid receptor is essential for understanding of morphine's analgesic mechanism and addictive potential.

Opioid antagonists have played important roles in the pharmacological studies of opioid receptors. Receptor selective antagonists are preferred in characterizing each type of opioid receptors. Due to the role of the mu-opioid receptor in analgesia and drug addiction, highly selective mu-opioid receptor antagonists are very useful pharmacological tools in the study of the mu-opioid receptor structure-activity relationship.

Naltrexone, a non-peptide opioid antagonist, is a long-acting and reversible opioid ligand used for the management of alcohol and opioid dependence. Naltrexone can also be used to treat other types of addiction including compulsive shopping and gambling. It has been shown to promote abstinence and prevent relapse.[6] However, naltrexone may also carry some side effects including dysphoria, depression, pulmonary edema and

cardiac arrhythmias.[7,8] These side effects may be related to the low selectivity of naltrexone to the opioid receptors.[9] On the other hand, there are a couple of selective peptidyl mu-opioid receptor antagonists available, including CTOP and CTAP. However, these two compounds are peptides and may undergo metabolic inactivation.[10] Therefore, the development of highly selective non-peptide mu-opioid receptor antagonists is needed to help alleviate any adverse effects seen by opioid antagonists with low selectivity.

The ability for these ligands to be reversible is also very important in the design of opioid antagonists. Reversible opioid antagonists will temporarily block the opioid receptor and can be easily washed out of the binding locus during pharmacological studies. However, irreversible antagonists will covalently bind to the receptor and will inactivate the receptor indefinitely. Therefore, in certain cases reversible mu-opioid receptor antagonists are preferred in order to study the mu-opioid receptor.

Although naltrexone has some problems associated with its low selectivity to the opioid receptors, it may be an ideal template for the design of selective mu-opioid receptor antagonists. Naltrexone has subnanomolar to nanomolar affinity to the three opioid receptors and shows mild selectivity for the mu- and kappa-opioid receptors over the delta-opioid receptor. It may be helpful to maintain the high affinity for the mu-opioid receptor by utilizing naltrexone as the backbone in the design of new mu-opioid receptor antagonists.

Previous site-directed mutagenesis and molecular modeling studies have shown that certain amino acid residues are critical for ligand selectivity. For example, amino

acid residue Trp318 located in extracellular loop (EL) 3 of the mu-opioid receptor is a major contributor to the selectivity of mu-opioid receptor antagonists to the mu-opioid receptor.[11] It is important to note that Trp318 is not conserved in the delta- and kappa-opioid receptors.[11] Therefore, the addition of certain structural features to the backbone of naltrexone that might interact with EL3 of the receptor may lead to some novel antagonists with high selectivity to the mu-opioid receptor.

The focus of this project is the design, chemical synthesis and pharmalogical evaluation of selective and reversible non-peptide mu-opioid receptor antagonists that carry structural features to interact with EL3 of the mu-opioid receptor. The molecular design of the compounds is based on our previous molecular modeling studies of some selective mu-opioid receptor agonists and irreversible mu-opioid receptor antagonists. Based on the information obtained from the molecular modeling studies, a series of new ligands will be designed as mu-opioid receptor antagonists. The newly designed ligands will be chemically synthesized and further characterized through various in vitro pharmacology studies, including competition radioligand binding assays for the three opioid receptors and functional assays to determine the possible efficacy of the ligands.

The development of highly selective, non-peptidyl, and reversible mu-opioid receptor antagonists will benefit the treatment of dependence and addiction on opioids with fewer side effects. Furthermore, these compounds can be used as probes to characterize the mu-opioid receptor and in the long run benefit the development of new analgesics with decreased adverse side effects.

# II. Background

## 1. Brief Introduction to the Mu-Opioid Receptor

The existence of different types of opioid receptors was proposed in 1973 by Terenius and later confirmed by other research groups using stereospecific radioligand binding assays.[12-14] In 1981, three distinct types of opioid receptors were identified and classified as mu-, delta- and kappa-opioid receptors based on results of the behavioral and bioassay studies.[15,16] All three opioid receptors have been cloned and the amino acid residue sequences of their cDNA has been determined between 1993 and 1994.[17] Further pharmacological characterization revealed that the mu-opioid receptor mediates the analgesic effect of morphine.[18,19]

### 1.1 Structure and Signal Transduction of the Opioid Receptor

The opioid receptors belong to the G-protein coupled receptor (GPCR) superfamily in the rhodopsin subclass. Opioid receptors (**Figure 1**) are integral membrane proteins made up of seven transmembrane (TM) spanning alpha-helices connected by three intracellular loops (IL) and three extracellular loops (EL).[20]

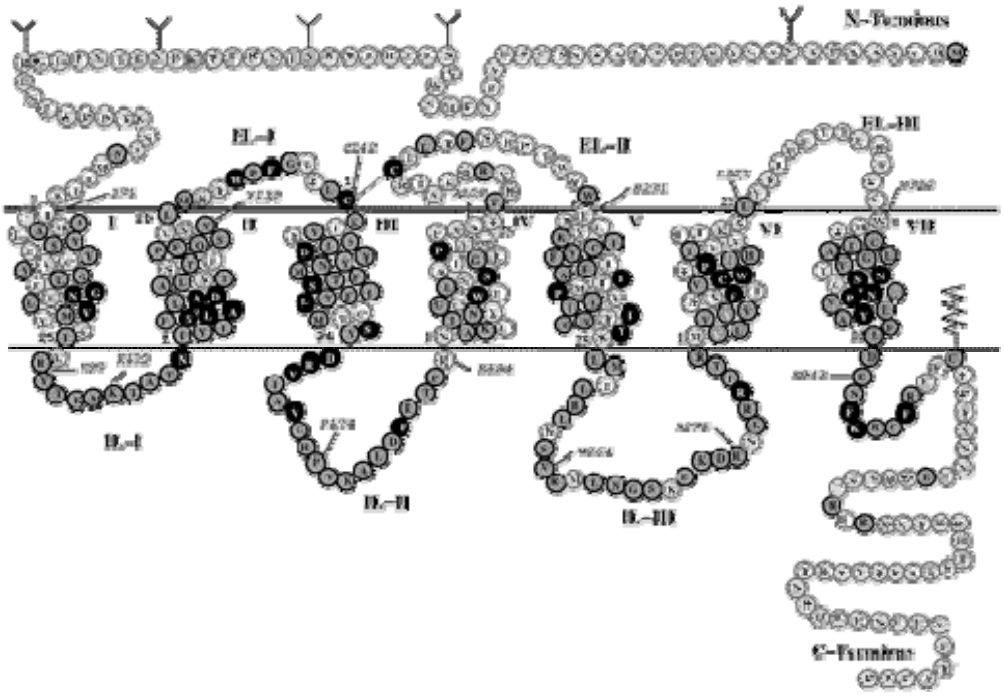

**Figure 1.** Model of the human mu-opioid receptor.[21]

The seven transmembrane regions of the receptor allow signal transduction for many small molecules, peptide transmitters, and modulators. The interaction of the receptor with the guanine nucleotide-binding proteins (G-proteins) mediates signaling for opioid receptors.[22] The G-protein is a heterotrimeric protein composed of three subunits, the $G_\alpha$, $G_\beta$ and $G_\gamma$ subunits. Opioid receptors interact preferentially with the pertussis toxin sensitive G-proteins of the $G_{i\alpha}$ and $G_{o\alpha}$ families.[22]

The $G_\alpha$, $G_\beta$ and $G_\gamma$ subunits activate when an agonist binds to the receptor and a conformational change takes place (**Figure 2**). This conformational change promotes the exchange of GDP with GTP at the $G_\alpha$ subunit. The G-protein dissociates into a GTP-bound $G_\alpha$ subunit and a $G_{\beta\gamma}$ subunit and both will activate downstream second messenger

pathways. Deactivation of the receptor occurs when GTPase located in the $G_\alpha$ domain hydrolyzes the GTP subunit to a GDP subunit followed by re-association with the $G_{\beta\gamma}$ subunit.[23]

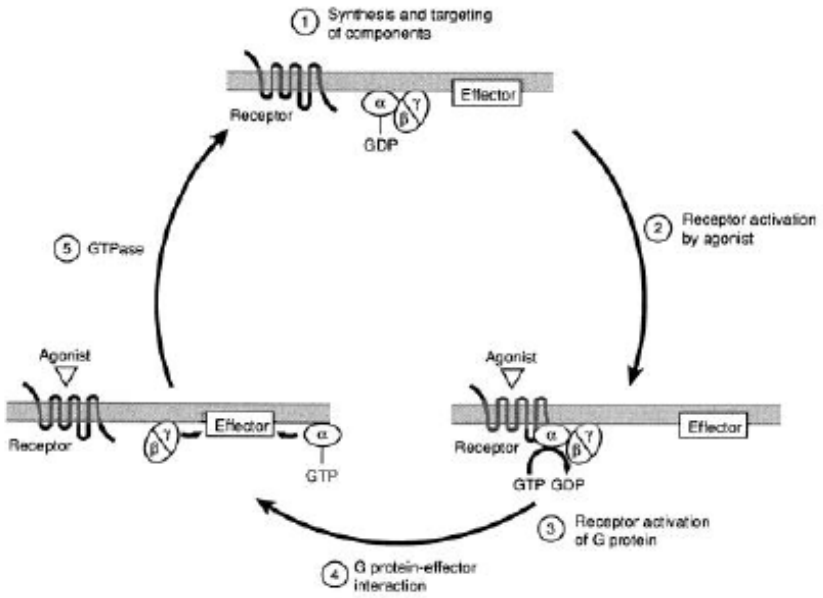


**Figure 2.** The activation cycle of a GPCR.[24]

Activation of the opioid receptor mediates the inhibition of adenylyl cyclase activity caused by the GTP-bound $G_\alpha$ subunit.[25] The acute inhibition of adenylyl cyclase reduces the production of cyclic adenosine monophosphate (cAMP) resulting in the reduction of voltage-dependent current and neurotransmitter release. The threshold of voltage-dependent ion channels shifts to more negative potentials when cAMP levels decrease. Therefore, there is a decrease in neuron excitability.[26] In addition, the $G_{\beta\gamma}$ subunit of opioid receptors mediates the reduction of cellular excitability through

membrane hyperpolarization caused by the activation of potassium conductance and the inhibition of voltage-gated calcium channels.[27,28]

## 1.2 Distribution of the Mu-Opioid Receptor in the CNS

Anatomical localization of opioid receptors was first investigated using radioligand autoradiography techniques.[29] Later, cloning technology and immunohistochemical analysis has allowed higher resolution to investigate anatomical distributions and expression levels of opioid receptors at the plasma membrane.[30,31] The opioid receptors are widely distributed in the central nervous system (CNS) and in the peripheral sensory and autonomic nerves.[32] Studies have shown that the mu-opioid receptor is expressed throughout the CNS including the cortex, hypothalamus, midbrain periaqueductal gray (PAG) matter, and rostral ventromedial medulla (RVM).[33,34] Mu-opioid receptors control the pain transmission pathway directly by acting in the superficial layers of the dorsal horn.[34] At the same time, the mu-opioid receptor as well as the kappa-opioid receptors are widely distributed on the wall of the gastrointestinal tract.[35]

## 1.3 Pharmacological Effects Mediated by the Mu-Opioid Receptor

Activation of opioid receptors by endogenous peptides is involved in regulation of both behavioral and homeostatic functions, including nociception, food intake, respiration, reward mechanisms, and gastrointestinal motility.[36] Through the use of transgenic mice lacking each opioid receptor, the mu-opioid receptor was confirmed to

mediate the acute effects of most clinically relevant opioid drugs including analgesia, respiratory depression, locomotor stimulation, and chronic effects such as physiological withdrawal signs.[37] The activation of mu-opioid receptors specifically mediates the analgesic actions of opioid agonists.[34] The role of endogenous opioids in pain suppression provides an important insight into the biology of opioid analgesics. Morphine, the prototypical opioid analgesic, does not simply inhibit the pain-transmission pathways; it mimics the action of the endogenous opioid peptides released in response to a specific stimulus such as pain.[34]

It is well known that the chronic use of opioid analgesics results in the development of tolerance, which is defined as a loss of effect following repeated treatments such that a higher dose is required for an equivalent effect.[34] Dependence is another result from chronic use of opioid analgesics. Interestingly, it has been proposed that dependence occurs with the discontinuation of opioid drugs and will manifest itself as a withdrawal syndrome.[18]

## 2. Mu-Opioid Receptor Antagonists

Mu-opioid receptor agonists like morphine have been used for many years and are still used as the first line therapy in the treatment of moderate to severe pain.[36] Despite the clear benefits from the use of mu-opioid receptor agonists, severe side effects have been associated with these drugs. These side effects, including respiratory depression, addiction and dependence, associated with opioid agonists have been determined to come from the interactions with the mu-opioid receptor.

At present, there are several pharmacotherapies available for maintenance treatment of opioid addiction. These pharmacotherapies include opioid receptor antagonists with low selectivity like naltrexone and naloxone. Although they are commonly used for treatment of the adverse effects associated with mu-opioid receptor agonists, naloxone and naltrexone have some side effects due to their lack of selectivity. Therefore, selective opioid antagonists are important in order to eliminate interactions with other opioid receptors.

Cyprodime is another opioid antagonist used mainly in pharmacological studies due to its moderate selectivity to the mu-opioid receptor. However, cyprodime has lower affinity to the mu-opioid receptor compared to naloxone and naltrexone. Other types of mu-opioid receptor antagonists include peptide ones, such as CTAP and CTOP, and irreversible non-peptidyl ones, e.g. β-FNA. These peptides and irreversible non-peptidyl compounds are not used for medicinal purposes due to various issue associated including rapid metabolism and inactivation of the receptor indefinitely. Therefore, the development of reversible and selective non-peptidyl mu-opioid receptor antagonists will be beneficial in the treatment of the adverse effects associated with opioid agonists.

## 2.1 Prototypical Mu-Opioid Receptor Agonist: Morphine

Activation of the mu-opioid receptor by opioid agonists has been associated with various undesirable side effects. Some of these side effects include dependence, sedation, respiratory depression, seizure, constipation, and opioid bowel dysfunction.[38] Despite these serious effects associated with opioid agonists such as morphine (**1**; **Figure**

**3**), the rate of their use for moderate to severe pain has steadily increased in recent years.[39]

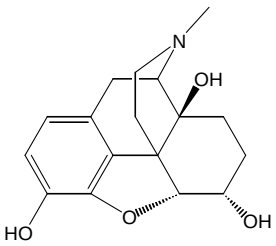


**1**

**Figure 3.** Structure of the mu-opioid receptor agonist: morphine (**1**).

Morphine is the principal active agent of opium and is a very potent mu-opioid receptor agonist (**Table 1**).[36] Morphine acts directly in the CNS to relieve pain and is the gold standard used to judge the analgesic properties of other mu-opioid receptor agonists.[38]

**Table 1.** Binding affinities of morphine (**1**) for the opioid receptors.[36]

| | Ki $_{\mu}$ (nM) | Ki $_{\delta}$ (nM) | Ki $_{\kappa}$ (nM) | Ratio δ/μ | Ratio κ/μ |
|---|---|---|---|---|---|
| **1** | 1.80 | 160 | 47.0 | 88.9 | 26.1 |

The discovery of new pain medications has occupied both the academic community and pharmaceutical industry for the past two decades with little success.[38] Morphine and related compounds remain the drugs of choice for the treatment of

moderate to severe pain in the U.S. Furthermore, many of the newer drugs are either in clinical trials or currently on market in alternative dosage forms of classical opioids.[40]

## 2.2 Naltrexone and Naloxone: Non-selective Opioid Receptor Antagonists

Opioid antagonists are commonly used as rescue medications to counteract the adverse side effects induced by opioid agonist overdose, mainly respiratory depression. They are also used clinically in the treatment of opioid dependence and alcoholism.[41] To this date, there are only two FDA approved mu-opioid receptor antagonists, naloxone and naltrexone, for the treatment of adverse effects associated with opioid agonists.[38]

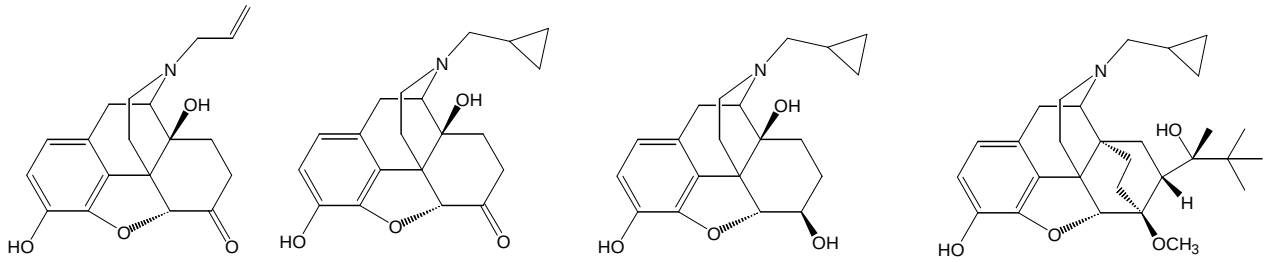


**Figure 4.** Structures of naloxone (**2**), naltrexone (**3**), naltrexone's metabolite 6β-naltrexol (**4**), and buprenorphine (**5**).

Naltrexone (**3**; **Figure 4**) is a competitive opioid receptor antagonist with low selectivity that falls into the morphinan structural series of opioids. Naltrexone promiscuously binds with high affinity to the mu- and kappa-opioid receptors and binds with lower affinity to the delta-opioid receptor (**Table 2**).[42] Naltrexone has been found to

be orally active with greater potency and longer duration of action than its counterpart naloxone (**2**; **Figure 4**).[43] When naltrexone is administered orally, about 60% is eliminated within 42 h after administration.[44] The mean naltrexone plasma levels decline very slowly and naltrexone still can be seen in the plasma 96 h after administration.[45] These properties make naltrexone suitable for the treatment of opioid dependence and provide an effective treatment for addicted patients.[46] For over a decade, naltrexone has also been an approved treatment for alcohol addiction, although oral administration leads to poor patient compliance.[47] When administered to an opioid-dependent person, acute withdrawal effects will precipitate.[4] When naltrexone is administered orally, only 40% of the dose is bioavailable due to the first pass metabolism.[48] In addition, poor compliance may be due to elevated plasma concentrations of the first pass metabolite 6β-naltrexol (**4**; **Figure 4**). This metabolite has been linked to increased incidence of side effects and treatment dropout.[49]

Naloxone is administered intravenously to reverse respiratory depression associated with overdose and analgesia from opioid agonists. Although naloxone has lower affinity to the mu-opioid receptor compared to naltrexone, it still has the ability to precipitate withdrawal effects similar to naltrexone. The oral bio-availability of naloxone is poor (only 2%) due to extensive first pass metabolism.[50]

**Table 2.** Binding affinities of naloxone (**2**) and naltrexone (**3**) for the opioid receptors.[42,51]

| | Ki $_{\mu}$ (nM) | Ki $_{\delta}$ (nM) | Ki $_{\kappa}$ (nM) | Ratio δ/μ | Ratio κ/μ |
|---|---|---|---|---|---|
| **2** | 1.90 | 32.6 | 3.06 | 17.2 | 1.61 |
| **3** | 0.11 | 60.0 | 0.19 | 545 | 1.72 |

The FDA recently approved Vivitrol, an extended-release formulation of naltrexone that is administered intramuscularly, for the treatment of alcohol addiction. The administration of Vivitrol results in lower plasma concentration of 6β-naltrexol, which leads to better patient compliance and a reduced side effect profile.[47] Other treatments for opioid addiction include combination of naltrexone and buprenorphine. Buprenorphine (**5**; **Figure 4**) is a mu-opioid receptor partial agonist and allows a decrease in withdrawal symptoms during opioid detoxification since naltrexone may displace buprenorphine from the mu-opioid receptor more gradually due to similar affinities.[52]

Although naloxone and naltrexone are effective treatments for a large number of disorders, including alcoholism and opioid dependence, they still have several pharmacokinetic issues. Naloxone has very poor oral bioavailability and a short half-life.[53] On the other hand, naltrexone is associated with poor compliance due to the formation of the metabolite 6β-naltrexol.[49] Both naltrexone and naloxone show low selectivity to the mu-opioid receptor exclusively and this may lead to other complications. Cardiac arrhythmias and pulmonary edema may be linked to naloxone's interaction with the kappa-opioid receptors.[54] Also patients receiving naltrexone for opioid dependence exhibited higher than expected rates of overdose and suicide while

some reports have been linked to depression and dysphoria due to naltrexone's interaction with the delta-opioid receptor.[55]

## 2.3 Cyprodime: Moderately Selective Mu-Opioid Receptor Antagonist

Unlike naloxone and naltrexone that lack selectivity to the mu-opioid receptor, cyprodime (**6**; **Figure 5**) is a moderately selective mu-opioid receptor antagonist in vivo (**Table 3**).[56] Cyprodime has been labeled with tritium resulting in a selective mu-opioid receptor radioligand with high affinity that has potential to be used as tool in probing mu-opioid receptor mechanisms. Although cyprodime is more selective for the mu-opioid receptor over the delta- and kappa-opioid receptors, it shows lower affinity for the mu-opioid receptor compared to naloxone and naltrexone. Further studies based on the structure profile of cyprodime did not yield any more selective mu-opioid receptor antagonists with higher affinity to the mu-opioid receptor.[57]

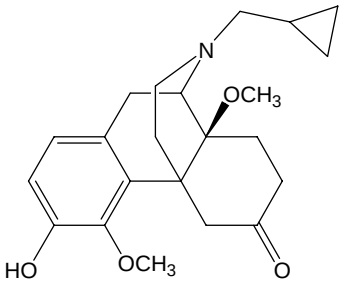


**6**

**Figure 5.** Structure of the mu-opioid receptor antagonist: cyprodime (**6**).

**Table 3.** Binding affinities of cyprodime (**6**) for the opioid receptors.[56]

| | Ki $_{\mu}$ (nM) | Ki $_{\delta}$ (nM) | Ki $_{\kappa}$ (nM) | Ratio δ/μ | Ratio κ/μ |
|---|---|---|---|---|---|
| **6** | 5.40 | 245 | 2187 | 45.4 | 405 |

## 2.4 Selective and Irreversible Mu-Opioid Receptor Antagonists

Through the use of selective or irreversible opioid antagonists as probes, opioid receptors and their functional mechanisms can be characterized. The use of selective or irreversible antagonists allows for elimination of a particular receptor type. Then the pharmacological properties of the remaining receptor types can now be observed.[58,59] Selective irreversible antagonists can be used in combination with agonists to estimate the relative efficacy and affinity of opioid agonists. The most widely used irreversible mu-opioid receptor antagonist is beta-funaltrexamine.[60]

β-Funaltrexamine (β-FNA, **7**; **Figure 6**) was described by Portoghese in 1981 as the first selective mu-opioid receptor antagonist.[61] β-FNA binds to all three opioid receptors with high affinity. However, β-FNA is an irreversible opioid antagonist only at the mu-opioid receptor in vitro, which acts as a site-directed alkylating agent that binds covalently to the mu-opioid receptor.[61] The ability of β-FNA to alkylate the mu-opioid receptor selectively leads to depletion of the mu-opioid receptor population.[38] β-FNA has been widely employed as a tool in the investigation of opioid receptor mechanisms.[62]

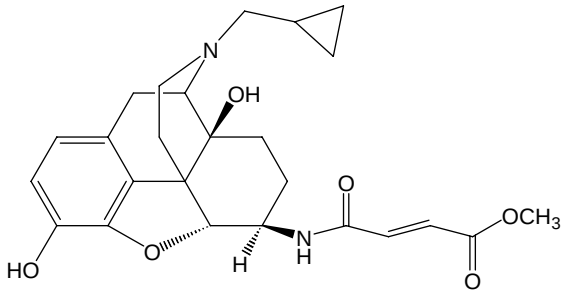


**7**

**Figure 6.** Structure of β-FNA (**7**).

Highly selective and irreversible ligands such as β-FNA are widely used as affinity labels. The design of β-FNA involved the attachment of chemically selective Michael acceptor group to a naltrexone-derived antagonist pharmacophore.[63] Several factors need to be considered when creating an affinity label. These factors include affinity of the ligand for the receptor recognition site, the location of the electrophilic center of the ligand, and the reactivity and selectivity of the electrophilic group.[62] Therefore, two consecutive recognition steps are involved in the covalent bonding and the proper orientation of the ligand with the receptor.[64] The use of β-FNA illustrates that mu-opioid receptor agonists and antagonists have different binding sites. The pre-treatment with a mu-opioid receptor agonist, such as morphine, did not protect the receptor from β-FNA. However, the introduction of a reversible mu-opioid receptor antagonist, such as naltrexone, effectively protected the receptor from alkylation by β-FNA.[65]

The replacement of the 14-hydroxyl group of naltrexone with an amino group creates 14-aminonaltrexone (**8**; **Figure 7**), which displays potent antagonist activity both

in vivo and in vitro.[38] The acylation of the 14-amino group leads to two more irreversible mu-opioid receptor antagonists, clocinnamox (C-CAM, **9**; **Figure 7**) and methocinnamox (M-CAM, **10**; **Figure 7**).[66] Unlike β-FNA, both C-CAM and M-CAM act as potent opioid antagonists to all three of the opioid receptors.[65]

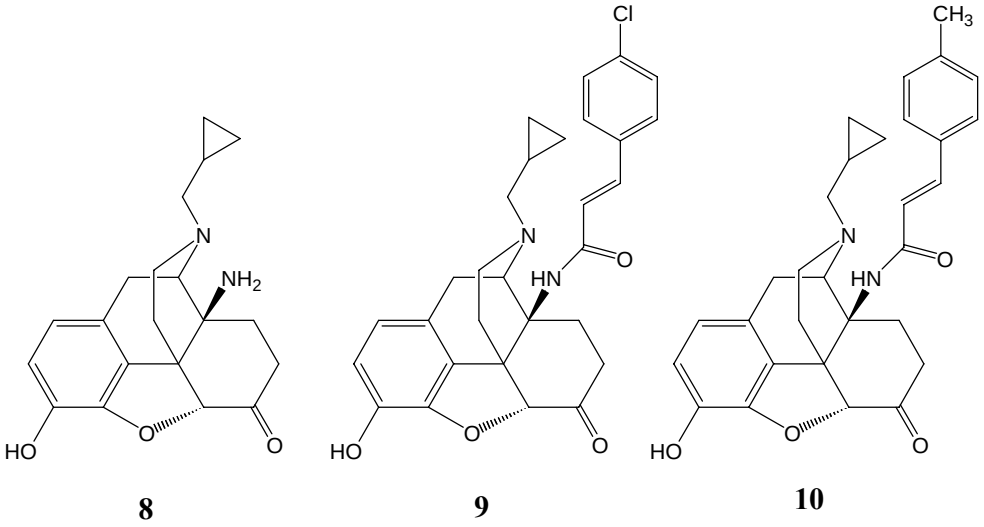


**Figure 7.** Structure of irreversible mu-opioid receptor antagonists: 14-aminonaltrexone (**8**), clocinnamox (**9**), and methocinnamox (**10**).

The use of selective and irreversible antagonists for the mu-opioid receptor limits their use since they bind covalently with the receptor. Therefore, reversible antagonists would be preferred since they temporarily "knock-out" the receptors during pharmacological studies and can be washed out from the binding locus to revive the receptor.

## 2.5 Selective Peptidyl Mu-Opioid Receptor Antagonists

Somatostatin is a widely distributed regulatory peptide that binds to various somatostatin receptors within the CNS and peripheral nervous system and is involved in many biological processes including binding to the mu-opioid receptor.[67,68] Somatostatin was used as a conformational template centered on the tetrapeptide sequence Phe-D-Trp-Lys-Thr for the design of a series of compounds that contains a β-turn that was found to be potent to the mu-opioid receptor.[69] From the conformational template of somatostatin two compounds of penicillamine-containing octapeptides were designed and synthesized, D-Phe-C[Cys-Tyr-D-Trp-Orn-Thr-Pen]-Thr-$NH_2$ (CTOP, **11**; **Figure 8**) and D-Phe-C[Cys-Tyr-D-Trp-Arg-Thr-Pen]-Thr-$NH_2$ (CTAP, **12**; **Figure 8**).[70] Both compounds contain a disulfide linkage between the cysteine and penicillamine that provided a useful approach in improving selectivity of flexible peptides.[70] The additional conformational constraint allows for an increase in molecular rigidity and an increase in metabolic stability compared with other endogenous opioid peptides.[10] Radiolabeled CTAP has been shown to be stable in the blood and serum of rats with a half-life of 500 min. The increased stability of CTAP is probably due to the penicillamine-cysteine disulfide linkage that allows for CTAP to become conformationally constrained and biologically active.[71]

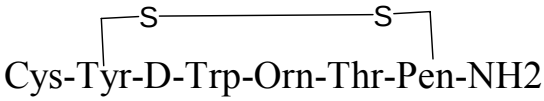


**11**

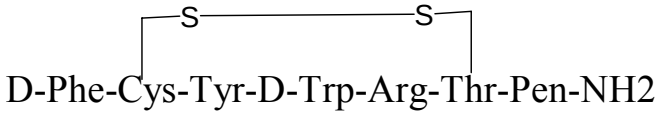


**12**

**Figure 8.** Structure of selective peptidyl mu-opioid receptor antagonists: CTOP (**11**) and CTAP (**12**).

Although CTOP and CTAP are based on the somatostatin hormone, they both act as mu-opioid receptor antagonists with low affinity to the somatostatin receptor (**Table 4**).[72] CTAP has shown to reduce antinociception in mice and block the mu-opioid receptor without causing severe withdrawal symptoms.[73] The use of radiolabeled CTAP has demonstrated its ability to cross the blood brain barrier (BBB) at therapeutic levels.[71] Although CTAP has shown some promise as a selective mu-opioid receptor antagonist compared to natural peptides, however, CTAP is also selective to the somatostatin receptor. Even though CTAP is more stable compared to endogenous opioid peptides, it is still vunerable to enzymatic degradation to a lesser extent.[10,74]

**Table 4.** Binding affinities of CTOP (**11**) and CTAP (**12**) for the opioid receptors.[75,76]

| | Ki $_{\mu}$ (nM) | Ki $_{\delta}$ (nM) | Ki $_{\kappa}$ (nM) | Ratio δ/μ | Ratio κ/μ |
|---|---|---|---|---|---|
| **11** | 0.18 | >1,000 | >1,000 | >5,555 | >5,555 |
| **12** | 2.30 | 365 | >10,000 | 159 | >4,348 |

Since pharmacological studies require both in vivo and in vitro activity, the use of selective mu-opioid receptor peptides such as CTOP and CTAP are not as desirable as non-peptidyl mu-opioid receptor antagonists since they have a shorter half-life. Therefore, non-peptidyl mu-opioid receptor antagonists are preferred since they have the ability to penetrate the CNS and are less vunerable to metabolic inactivation compared to peptides.

### 3. Application of the "Message-Address" Concept in the Design of Kappa-Opioid Antagonists

Progress in opioid research has relied on the use of non-selective opioid antagonists like naloxone and naltrexone. Both, naloxone and naltrexone are frequently used in the verification of opioid receptor interactions since they can induce antagonism with all three opioid receptors.[77] Since the recognition of multiple opioid receptor types, the development of selective antagonists as tools to determine the selectivity of opioid agonists has become increasingly important.[9]

The "message-address" concept has been used to design non-peptidyl selective kappa-opioid receptor antagonists like norbinaltorphine (Nor-BNI, **13**; **Figure 9**) and GNTI (**14**; **Figure 9**) as tools in opioid research.[9] Following this concept may allow the design of new selective mu-opioid receptor antagonists.

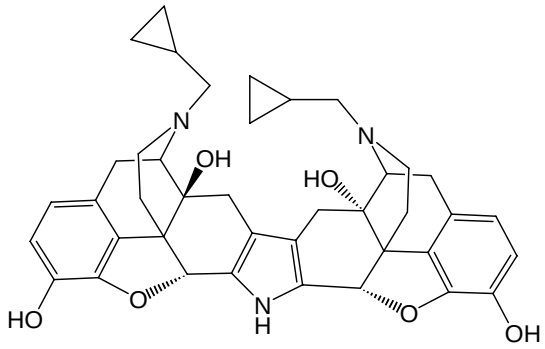


**13**

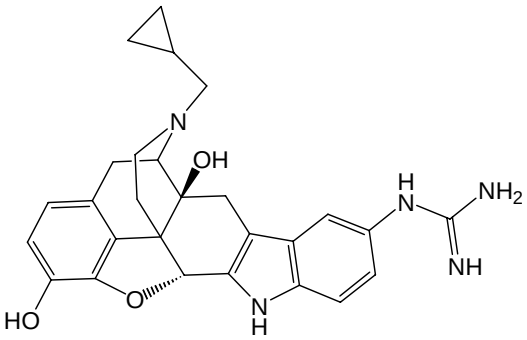


**14**

**Figure 9.** Selective kappa-opioid receptor antagonists: norBNI (**13**) and GNTI (**14**).

### 3.1 Message-Address Concept

Schwyzer first proposed the "message-address" concept in his analysis of the structure-activity relationship of ACTH, adrenocorticotropic hormone, and related hormones.[78] Peptide hormones within the same class contain a "message" sequence and an "address" sequence of amino acid residues, each being sequential and close to one another in the peptide chain. The message component is responsible for signal transduction, while the address component provides additional binding affinity and is not essential for the transduction process.[79] Therefore, each compound will contain a unique address component linked to a common message recognition component (**Figure 10**).[80,81]

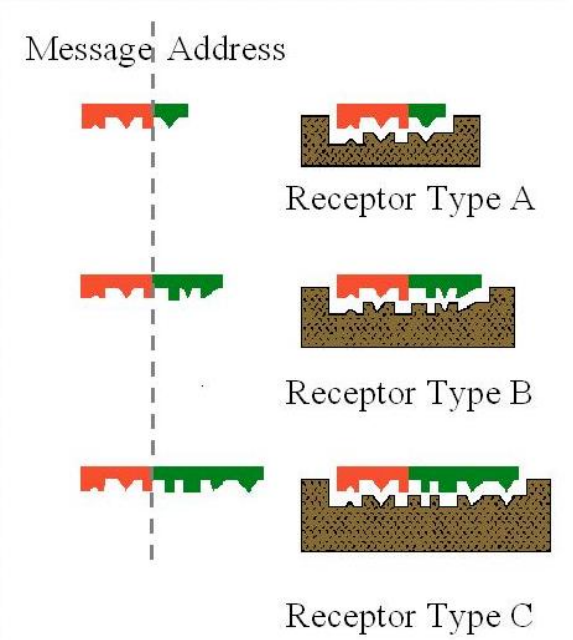


**Figure 10.** Message-address concept. This concept is the basis for selectivity for ligands to a particular subtype of receptor.[82]

### 3.2 Design of Selective Kappa-Opioid Receptor Antagonist

The "message-address" concept has been used to demonstrate opioid ligand selectivity. First, this concept was enriched so that the "message" component is similar for all the opioid receptor subtypes. Second, the "address" component is the primary determinant of selectivity among receptor subtypes. GNTI (**14**, **Figure 11**), 5'-guanidinonaltrindole, was one of the first selective kappa-opioid receptor antagonists designed utilizing the "message-address" concept.[83]

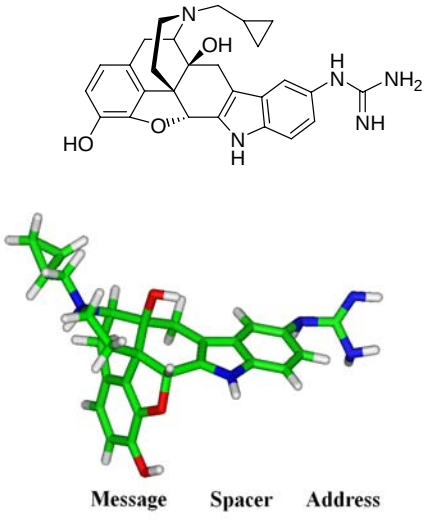


**Figure 11.** The conformational analysis of GNTI (**14**).

The "message" component of GNTI consists of the morphinan moiety; the "address" component consists of the guanidine moiety. The guanidine moiety confers the selectivity of GNTI to the kappa-opioid receptor. The indole ring acts as a "spacer" used to connect the "message" and "address" components. GNTI is 5-fold more potent and selective than the prototypical kappa-opioid receptor antagonist norBNI.[82]

Molecular modeling studies of GNTI with the kappa-opioid receptor suggested the involvement of Glu297 in the binding locus, which is located on the top of TM6. Since Glu297 is an acidic amino acid residue, it may interact with the guanidine moiety of GNTI. The mutation of Glu297 to an alanine amino acid residue dramatically reduced the affinity of GNTI to the kappa-opioid receptor.[59,84] Therefore, Glu297 is important for the recognition and selectivity of GNTI in the binding pocket of the kappa-opioid receptor.[85]

Another site-directed mutagenesis study was conducted to determine the significance of the acidic amino acid residue Glu297 for the selectivity of GNTI and norBNI to the kappa-opioid receptor over the mu-opioid receptor. The study involved the mutation of the amino acid residue Lys303 in the mu-opioid receptor into a glutamate residue (K303E). Lys303 in the mu-opioid receptor was found to be in an equivalent position compared to Glu297 in the kappa-opioid receptor. It was found that the replacement of the lysine residue with the glutamate residue allowed the binding of norBNI and GNTI with much higher affinity to the mutated mu-opioid receptor then to the wild mu-opioid receptor.[84]

Alternatively, when Glu297 was mutated to a lysine residue in the kappa-opioid receptor (E297K), the binding affinities for both GNTI and norBNI were diminished to the mutated kappa-opioid receptor (**Table 5**). These studies suggest that the kappa-opioid receptor and the mutated mu-opioid receptor contain similar binding sites that may be the recognition or "address" site. These binding sites were able to recognize the positively charged group in GNTI and norBNI.[84] This study highlights the significant role of the acidic amino acid residue, Glu297, of the kappa-opioid receptor in conferring ligand selectivity.

**Table 5.** Effects on the binding affinity of mutated amino acid residues Glu297, in kappa-opioid receptor, and Lys303, in mu-opioid receptor using norBNI (**13**) and GNTI (**14**).[84]

| | $Ki_{\kappa}$ (nM) | $Ki_{\kappa}$ [E297K] (nM) | $Ki_{\mu}$ (nM) | $Ki_{\mu}$ [K303E] (nM) |
|---|---|---|---|---|
| **13** | 0.12 | 12.5 | 101.9 | 0.77 |
| **14** | 0.75 | 12.9 | 9.23 | 0.06 |

This successful application of "message-address" concept in the design and development of kappa-opioid receptor selective antagonists gives an insight in the development of mu-opioid receptor selective antagonists.

## 4. Summary

The application of ligands with high selectivity for each type of the opioid receptors is crucial for the understanding of the mechanism of opioid actions. There are currently many mu-opioid receptor agonists available but morphine is still the most commonly used agonist. Morphine acts at the mu-opioid receptor to produce analgesic effects. However, it can cause other adverse effects including respiratory depression, dependence, and addiction.[38] Therefore, the development of mu-opioid receptor antagonists is important in the maintenance treatment of opioid addiction.

Currently, only two mu-opioid receptor antagonists, naloxone and naltrexone, are approved by the FDA for the treatment of adverse effects associated with opioid agonists.[38] However, both naloxone and naltrexone carry low selectivity to the mu-opioid receptor and may cause other adverse side effects due to their low selectivity.[42,52]

Other types of mu-opioid receptor antagonists have been developed including peptide ones and irreversible non-peptidyl ones. However, peptides can undergo metabolism easier than non-peptides and irreversible antagonists limit the use of the compounds since they inactivate the receptor indefinitely.[58,71]

The development of a non-peptide, reversible mu-opioid receptor antagonists is important for the treatment of dependence and addiction to opioid agonists. These drugs seem to be more promising because they will have less interference with the normal function of the delta- and kappa-opioid receptors. Such mu-opioid receptor selective antagonists may also be useful in the characterization of the mu-opioid receptor structure-function relationship.

# III. Project Design

The project, the development of selective non-peptidyl mu-opioid receptor antagonists, consists of four parts: molecular design, chemical synthesis, biological evaluation, and molecular modeling study. The novel ligands will be designed based on the identification of important pharmacophore elements in several known opioid agonists and antagonists. Chemical synthesis will be conducted to prepare the designed ligands. Next, in vitro pharmacology studies will be pursued in order to determine the affinity of these compounds for three types of opioid receptors. Finally, molecular modeling studies will be carried out in order to visualize the binding modes of the ligands in the mu-opioid receptor.

## 1. Molecular Design

Applying the "message-address" concept, a comparative conformational analysis of several known mu-opioid receptor agonists and antagonists will be conducted to identify major pharmacophore elements, followed by docking studies of these ligands in a homology model of mu-opioid receptor to identify the unique amino acid residues in the binding locus. To be noted, previous studies have shown that extracellular loops, especially EL2 and EL3, may be involved in the determination of ligand selectivity

for opioid receptors based on the relatively low sequence homology level in the EL domains among the three opioid receptors.[86]

## 1.1 Comparative Conformational Analysis of Mu-Opioid Receptor Agonists and Antagonists

The design of novel selective mu-opioid receptor antagonists will be based on a comparative conformational study utilizing highly selective mu-opioid receptor agonists such as fentanyl (**15**, **Figure 12**) and endomorphin 2 (**16**, **Figure 12**).

As shown in figure **12**, the phenylethyl moiety in fentanyl is orientated the same way as the tyrosine (Tyr) residue at the first position of endomorphin 2. This suggests that it may be related to their agonist activity for the mu-opioid receptor and belongs to the "message" component of the molecule. The *N*-phenyl ring connected to the propanamide group in fentanyl may overlap with the third amino acid residue, phenylalanine (Phe), of endomorphin 2. This might be the "address" part of these molecules to recognize the mu-opioid receptor (please refer to message-address concept in the background on pages 20-23).

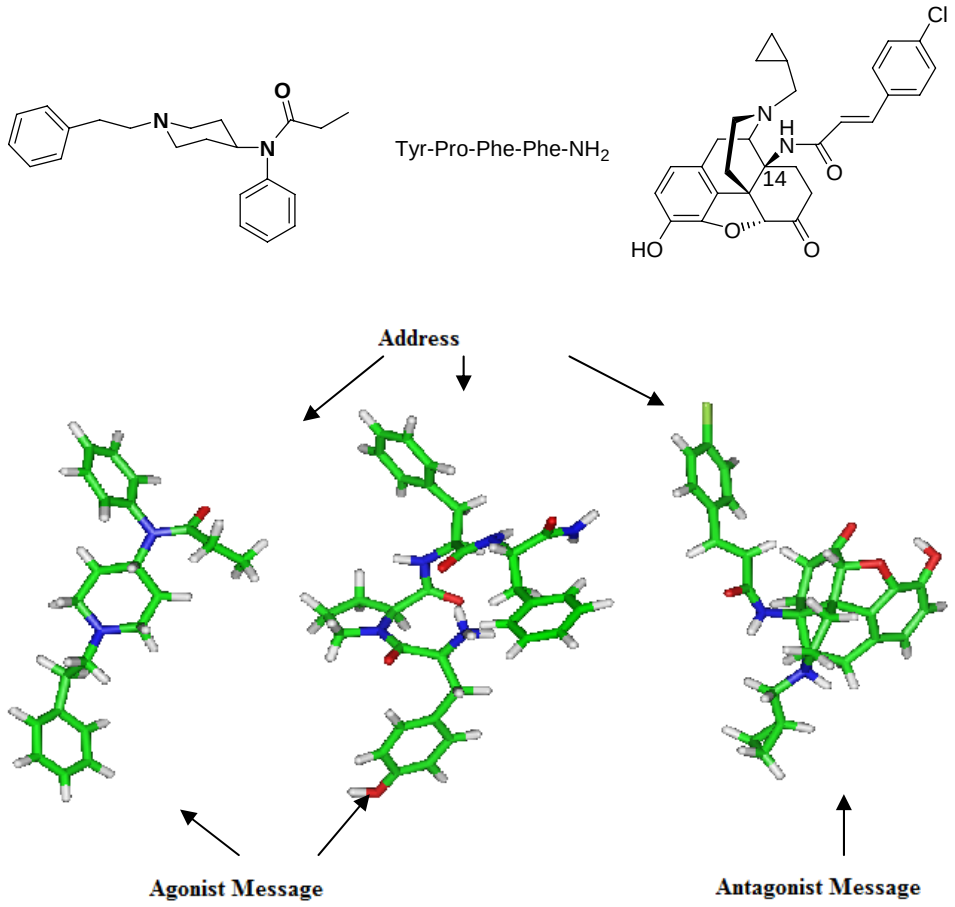


**Fentanyl (15)** **Endomorphin 2 (16)** **Clocinnamox (9)**

**Figure 12.** Comparative conformational analysis of selective mu-opioid receptor agonists and antagonists.

The conformational analysis of clocinnamox (**7**), an irreversible mu-opioid receptor antagonist, shows a correlation with the above results. The 17-cyclopropylmethyl group in clocinnamox may be positioned similarly to the phenylethyl moiety of fentanyl and belongs to the "message" component of the molecule. To be noticed, many mu-opioid receptor antagonists including GNTI, naltrexone, nalorphine

and clocinnamox carry similar size substitutions at the 17-position. This may help explain why clocinnamox acts as an antagonist to the mu-opioid receptor while fentanyl acts as an agonist. Therefore, the "message" component of these antagonists may be the cyclopropylmethyl group. However, the *p*-chlorophenyl moiety at the 14-position of clocinnamox may overlap with the *N*-phenyl ring of fentanyl, the "address" component of the molecule. This suggests that agonists and antagonists may share similar "address" components that confer their common selectivity to the mu-opioid receptor, while their "message" components are different due to the opposite signal transductions.

## 1.2 Docking Studies in a Homology Model of the Mu-Opioid Receptor

The results of the comparative conformational study between fentanyl, endomorphin 2, and clocinnamox will be verified using a homology model of the mu-opioid receptor. This model will be built based on the X-ray crystal structure of bovine rhodopsin. Bovine rhodopsin, also a member of the GPCR superfamily, has a 30% sequence identity compared to the opioid receptors.[87] Although the sequence homology level between opioid receptors and bovine rhodopsin are not very high, it is possible to build a plausible homology model of the mu-opioid receptor based on rhodopsin's X-ray crystal structure.[87]

Previously, a homology model was built for the mu-opioid receptor based on a X-ray crystal structure of the dark state bovine rhodopsin (**Figure 13**). The homology model of the mu-opioid receptor was further optimized in a membrane-aqueous system.[87]

The interactions between naltrexone and the homology model of the mu-opioid receptor have been well characterized.[16]

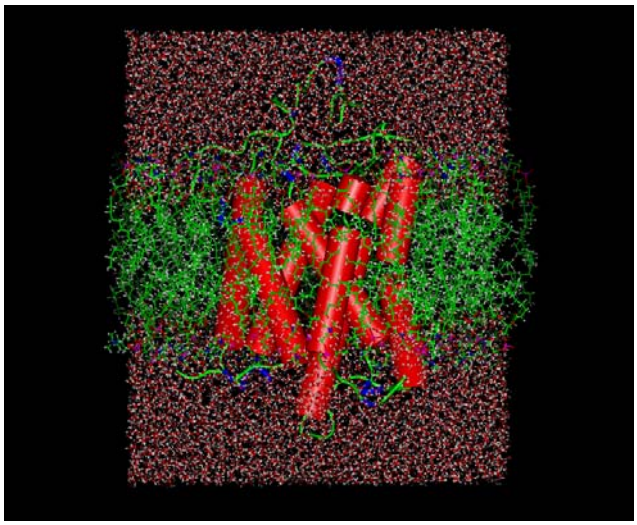

**Figure 13.** Homology model of the mu-opioid receptor in a membrane-aqueous interface.[87]

The comparative conformational analysis study has been verified using docking studies where clocinnamox is docked into the binding pocket of the homology model of the mu-opioid receptor. We have noticed that there is significantly low sequence homology in the EL2 and the EL3 in the three opioid receptors while these regions are important in the recognition and binding of opioid ligands.[16,87] Docking studies of clocinnamox show that the 14-*p*-chlorophenyl moiety of clocinnamox (address part) is located in an aromatic area of the binding pocket at EL2 and EL3 locus (**Figure 14**).

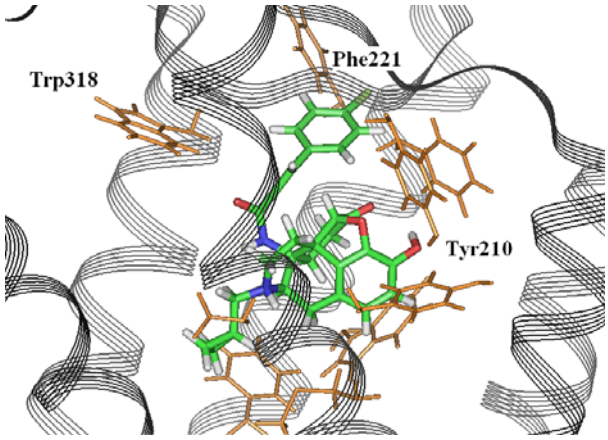


**Figure 14.** Docking study of clocinnamox in the mu-opioid receptor homology model.

The 14-*p*-chlorophenyl moiety in clocinnamox is located in an aromatic binding pocket of the mu-opioid receptor and is considered the "address" component of clocinnamox. The amino acid residues Tyr210, Phe313, and Trp318, are not conserved in the delta- and kappa-opioid receptors. Therefore, similar aromatic binding pockets may not exist in the delta- and kappa-opioid receptors. Trp318 in EL3 has been determined, through site-directed mutagenesis studies and chimera opioid models, to be a significant contributor to the selectivity of the mu-opioid receptor agonists and antagonists.[88]

Therefore, the hypothesis for this study is that a mu-opioid receptor ligand carrying an aromatic structural feature that may interact with EL3 of the receptor might lead to its high selectivity to the mu-opioid receptor. Based on this hypothesis, a series of new ligands that may satisfy the requirements of the mu-opioid receptor binding pocket will be designed and synthesized to test their affinity towards the mu-, delta- and kappa-opioid receptors.

## 1.3 Design of Selective Mu-Opioid Receptor Antagonists

Based on the previous studies and analysis, a series of novel ligands as 14-*O*-heterocylic substituted naltrexone derivatives are designed as mu-opioid receptor selective antagonists (**Figure 15**). The hetero-aromatic moieties include pyridine, quinoline and isoquinoline, which are attached to 14-*O*-position of naltrexone by an ester bond. The nitrogen atom in the hetero-aromatic moieties may act as hydrogen bond acceptors towards the extracellular binding locus of the mu-opioid receptor, since certain amino acid residues on EL2 and EL3, e.g. Tyr210 and Trp318, were found to be essential for ligand recognition through site-directed mutagenesis studies.[87] It is also important to note that Trp318 is a significant contributor to the selectivity of the mu-opioid receptor agonists and antagonists.[87]

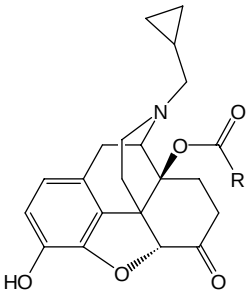


| Compounds Set 1 | R |
|---|---|
| **17** | 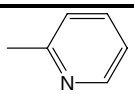 |
| **18** | 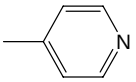 |
| **19** | 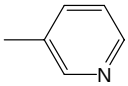 |
| **20 (Control)** | 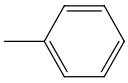 |

| Compounds Set 2 | R |
|---|---|
| **21** | 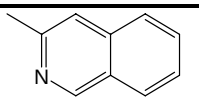 |
| **22** | 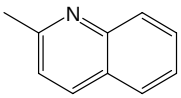 |
| **23** | 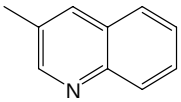 |
| **24 (Control)** | 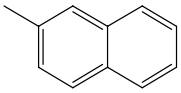 |

**Figure 15.** Designed 14-*O*-heterocyclic substituted derivatives of naltrexone.

A second series of selective mu-opioid receptor antagonists, 6-*N*-heterocyclic substituted naltrexamines, were previously designed and synthesized in our laboratories for a similar purpose (manuscript submitted to the Journal of Medicinal Chemistry).[89] These antagonists contain a heterocylic moiety including pyridine, quinoline, and isoquinoline, linked at the 6-position of naltrexone through an amide bond (**Figure 16**). The ligands carrying either the α- or β-configuration have been chemically synthesized to determine if stereochemical arrangement plays an important role in the affinity and selectivity for the mu-opioid receptor.

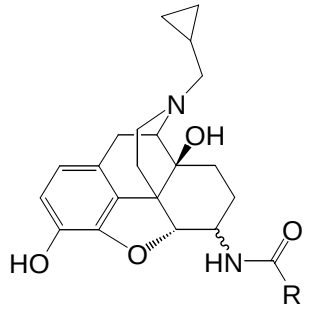


| Compound Set 3 | Configuration | R |
|---|---|---|
| **25** | **α** | 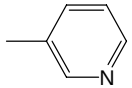 |
| **26** | **β** | |
| **27** | **α** | 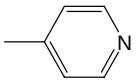 |
| **28** | **β** | |
| **29** | **α** | 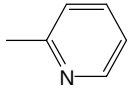 |
| **30** | **β** | |
| **31 (Control)** | **α** | 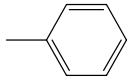 |
| **32 (Control)** | **β** | |

| Compound Set 4 | Configuration | R |
|---|---|---|
| **33** | **α** | 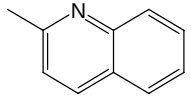 |
| **34** | **β** | |
| **35** | **α** | 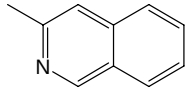 |
| **36** | **β** | |
| **37** | **α** | 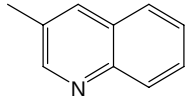 |
| **38** | **β** | |
| **39** | **α** | 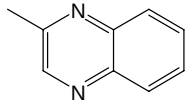 |
| **40** | **β** | |
| **41 (Control)** | **α** | 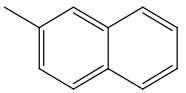 |
| **42 (Control)** | **β** | |

**Figure 16.** 6-*N*-heterocyclic substituted derivatives of naltrexamine.

The aromatic character of the heterocyclic moiety helps to provide an aromatic interaction to the aromatic binding pocket in the mu-opioid receptor. The nitrogen atom may act as a hydrogen bond acceptor to probe possible formations of hydrogen bonds with the amino acid residue Trp318 of EL3 of the mu-opioid receptor. Also, the stereochemical arrangement may play a very important role for the affinity, as well as the selectivity, of the ligand, based on previous compounds such as α-FNA and β-FNA.[90] Although β-FNA binds to the mu-opioid receptor irreversibly, its epimer α-FNA does not bind to the mu-opioid receptor irreversibly. However, α-FNA can protect against β-FNA induced irreversible antagonism.[91] This suggests that both α- and β-FNA interact with the same site in the mu-opioid receptor but only β-FNA properly aligns and binds in the mu-opioid receptor.[90]

Both sets of compounds, 14-*O*-heterocyclic substituted naltrexone and 6-*N*-heterocyclic substituted naltrexamine, have a phenyl and naphthalenyl compound designed to act as controls in order to test the hydrogen bonding hypothesis.

Both series of compounds have been designed to test the hypothesis that the addition of a heteroaromatic moiety to the backbone of naltrexone and naltrexamine may allow for the formation of a hydrogen bonding interaction with Trp318 in EL3 of the binding pocket of the mu-opioid receptor. This additional interaction may allow for the creation of more selective mu-opioid antagonists.

## 2. Chemical Synthesis

Chemical synthesis of the 14-*O*-heterocyclic substituted naltrexone derivatives will be conducted using synthetic pathways adapted from literature.[92,93] The basic scheme consists of the direct coupling of the heterocyclic moiety to the 3- and 14-position of naltrexone. This is followed by the selective removal of the heterocyclic moiety at the 3-position of naltrexone (**Scheme 1**).

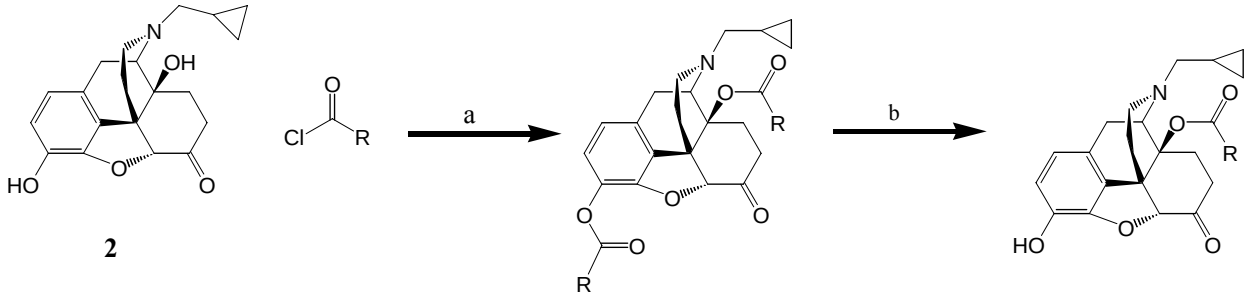


**Scheme 1.** The synthetic route of 14-*O*-heterocyclic substituted naltrexone derivatives. The heterocyclic moieties are represented by "R". Reagents and conditions: a. DMF, TEA, $N_2$(g); b. 4% $H_2SO_4$ (aq), MeOH, $NH_4OH$.

## 3. Biological Evaluation of the 6-*N*-Heterocyclic Substituted Naltrexamine and 14-*O*- Heterocyclic Substituted Naltrexone Derivatives

Following the synthesis of the two series of naltrexone derivatives, bioassays will be conducted to study the selectivity of these ligands for the opioid receptors. Mono-cloned opioid receptor expressed CHO and HEK293 cells will be utilized to conduct these assays. The affinities of the ligands will be determined by conducting binding assays utilizing tritiated radioligands, [$^3$H]DAMGO, [$^3$H]NTI and [$^3$H]Nor-BNI, for the mu-, delta-, and kappa-opioid receptors, respectively. Functional assays, i.e. [$^{35}$S]GTPγS

binding assay, will be applied to the naltrexone derivatives with at least 10-fold selectivity for mu- over delta- and kappa-opioid receptors to determine whether the compounds act as full agonists, partial agonists or antagonists. Ideally, a lead compound will be identified as a mu-opioid receptor antagonist with high selectivity for the mu-opioid receptor over delta- and kappa-opioid receptors.

**4. Molecular Modeling Study**

A homology model of the mu-opioid receptor will be adapted to illustrate the possible docking modes of the 14-*O*-heterocyclic substituted naltrexone derivatives in the mu-opioid receptor. The mu-opioid receptor homology model will be reconstructed and revisited by the author of the thesis based on the X-ray crystal structure of the dark state bovine rhodopsin.[94] Site-directed mutagenesis data and chimera opioid receptor data will be used to identify important amino acid residues in the binding pocket. The 14-*O*-heterocyclic substituted naltrexone derivatives will be docked into the hypothetical binding pocket using GOLD to visualize the interactions of the ligands with the mu-opioid receptor. The GOLD scores from the docking studies of these naltrexone derivatives will be analyzed together with the binding affinities obtained from the biological studies.

## 5. Summary of the Project Design

In summary, a series of novel opioid ligands as 14-*O*-heterocyclic substituted naltrexone derivatives, will be designed based on molecular modeling studies on known mu-opioid receptor selective agonists and antagonists. These naltrexone derivatives will contain heteroaromatic moieties including pyridine, quinoline, and isoquinoline moieties at the 14-*O*-position of naltrexone that may form a hydrogen bonding interaction with an aromatic binding locus in EL domain of the mu-opioid receptor. Next, compounds in this series, will be synthesized and the affinities will be determined for all three opioid receptors using in vitro biological assays. Finally, a homology model of the mu-opioid receptor will be built based on the X-ray crystal structure of the dark state bovine rhodopsin. Docking studies of the 14-*O*-heterocyclic substituted naltrexone derivatives will be conducted in order to visualize the interactions between the mu-opioid receptor and these ligands.

In conclusion, the purpose of this study is the molecular design, chemical synthesis, biological evaluation and molecular modeling study of selective non-peptidyl mu-opioid receptor antagonists. This project may lead to the development of more selective mu-opioid receptor antagonists with reduced adverse effects seen with other opioid antagonists like naltrexone and naloxone.

# IV. Results and Discussion

## 1. Chemical Synthesis of 14-*O*-Heterocylic Substituted Naltrexone Derivatives

### 1.1 Chemical Synthesis Routes

Depending on commercially availability of the precursors of the 14-*O*-heterocyclic moiety of naltrexone, one of the two synthetic routes is adapted from literature to synthesize the 14-*O*-heterocyclic substituted naltrexone derivatives.[92,93] The first synthetic pathway involves the direct coupling reaction of an acyl chloride with naltrexone (**Scheme 2A**), while the second involves the in situ conversion of a carboxylic acid to an acyl chloride prior to the coupling reaction (**Scheme 2B**).

The heterocyclic moiety is first added to both the 3- and 14-positions of naltrexone, 17-(cyclopropylmethyl)-4,5α-epoxy-3,14-dihydroxymorphinan-6-one, to generate the di-substituted naltrexone intermediate (**Scheme 2**). The following step involves the chemoselective removal of the heterocyclic moiety at the 3-position. After the purification of the naltrexone derivatives by column chromatography, the target products are converted into hydrochloride salts. The final yields of these compounds vary between 10 and 70% (**Table 6**).

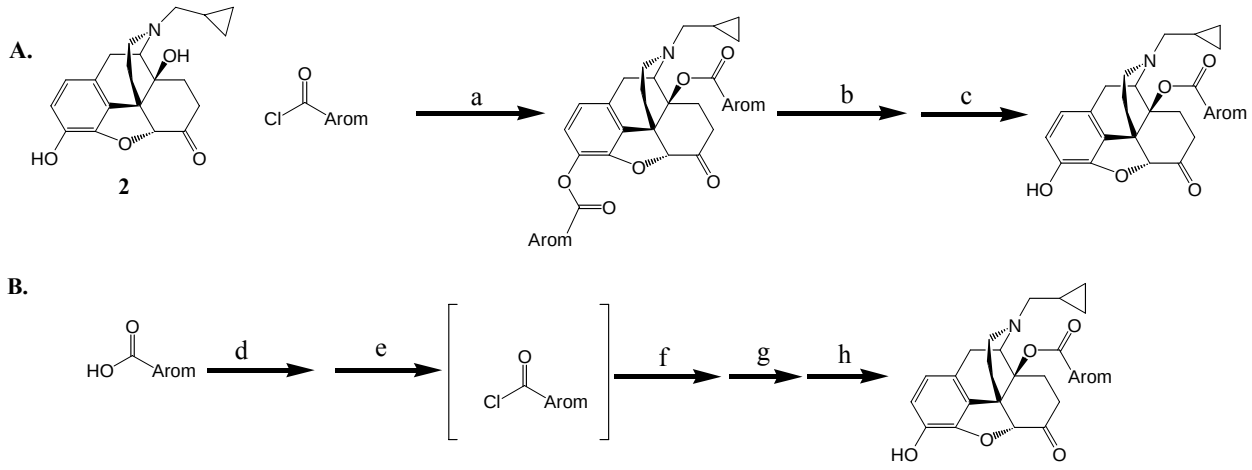


**Scheme 2.** The synthetic route for the 14-*O*-heterocyclic substituted naltrexone derivatives.
A. The direct coupling of an acyl chloride heterocyclic moiety with naltrexone.
B. The conversion of a carboxylic acid heterocyclic moiety to an acyl chloride moiety, in situ followed by coupling with naltrexone.
Reagents and conditions: a. DMF, TEA, $N_2$ (g), 100 ºC, 4 h; b. 4% $H_2SO_4$ (aq), MeOH, rt, 4h;
c. $NH_4OH$, pH 7; d. $SOCl_2$ ex., $N_2$ (g), 80 ºC, 3 h; e. toluene, *in situ*; f. **2**, DMF; g. $H^+$; h. pH 7.

The next step is the same for both routes A and B for all of the compounds. The acyl chloride, commercially available or prepared *in situ*, is heated at reflux with naltrexone and TEA in DMF (solvent) for up to 4 h at 100 °C under nitrogen atmosphere. The solvent is then removed and the residue is dissolved in methanol and a 4% $H_2SO_4$ aqueous solution, to selectively remove the heterocyclic moiety attached to the 3-position of naltrexone skeleton. This step of the reaction took up to 4 h at room temperature. A weak base ($NH_4OH$) is then applied to neutralize the mixture. The solvent is then removed and column chromatography is conducted to separate out the final product. The yields for these compounds vary (**Table 6**).

**Table 6.** Percent yield of 14-*O*-heterocyclic substituted naltrexone derivatives.

| Compound | 14-*O*-heterocyclic Substituent | Route | Percent Yield (%) |
|---|---|---|---|
| **17** | 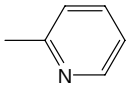 | B | 50 |
| **18** | 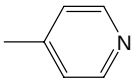 | A | 69 |
| **19** | 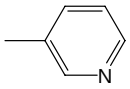 | A | 24 |
| **20** | 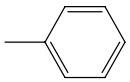 | A | 10 |
| **21** | 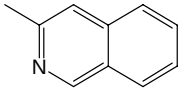 | A | 24 |
| **22** | 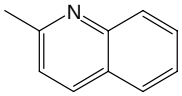 | A | 17 |
| **23** | 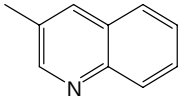 | B | 22 |
| **24** | 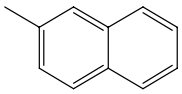 | A | 7 |

## 1.2 The Synthesis of Acyl Chloride

In route B, the conversion of a carboxylic acid to an acyl chloride is necessary because acyl chlorides are good electrophiles, and therefore very reactive. Both the oxygen and chlorine on the carbonyl carbon of the acyl chloride are strong electron withdrawing groups, allowing the carbonyl carbon to carry partial positive charge. This will allow a weak nucleophile to attack the carbonyl carbon atom. The hydroxyl group on carboxylic acids are not very good leaving groups and do not react in nucleophilic substitution reactions except when the hydroxyl group is protonated to give water, a good leaving group.[94] To prevent protonation of the carboxylic acid, the environment is made

basic with the use of triethylamine (TEA), which contains a tertiary amine that can neutralize hydrochloric acid generated from the reaction through the formation of the salt triethylamine hydrochloride.[92,93]

The conversion reaction in step d in scheme 2 involves heating at reflux the carboxylic acid with thionyl chloride ($SOCl_2$) under a nitrogen atmosphere.[95] All the components are pre-dried in order to ensure the reaction was free of water. The reaction mixture is heated with an excess amount of $SOCl_2$ at 80 °C for about 3 h.[96] Then, toulene is added and distilled in order to remove any excess of $SOCl_2$.[92,93]

### 1.3 Chemoselective Deprotection of 3-*O*-Substitution

The addition of the heterocylic moiety to the skeleton of naltrexone is a "one-pot" reaction. Therefore, both the 3- and 14-positions contain the heterocyclic moiety after the direct coupling reaction of the substituent with naltrexone. A mildly acidic solution (dilute $H_2SO_4$ solution) is used to selectively cleave the substituent at the 3-position but still maintain the substitution on the 14-position of the naltrexone skeleton. The phenyl ester moiety on the 3-position is highly unstable in acidic and in basic conditions, and can be readily cleaved.[97] However, the substituent at the 14-position is only stable under mild acidic conditions and very labile in basic conditions. This is due to the 14-position being a tertiary ester and is very unstable to basic hydrolysis.

Substitution on both the 3- and 14-positions requires a 2:1 ratio of acyl chloride substituent to naltrexone. This is due to the 3-position of naltrexone having more accessibility to the substitution compared to the 14-position. The 14-position contains a

tertiary alcohol and is also hindered by the methylcyclopropyl group. Therefore, the 3-position is substituted first followed by the 14-position.

### 1.4 Methods for the Synthesis and Deprotection of Compounds 17, 20 and 24

Although most of the compounds are synthesized in the above manner, some difficulty is encountered in the synthesis of compounds **17**, **20** and **24**. The synthesis of compound **17** involves the conversion of picolinic acid to an acyl chloride. The first few attempts produced a thick black residue and the reaction mixture probably is degraded. Therefore, conversion of the carboxylic acid to an acyl chloride is ran overnight followed by heating at reflux with naltrexone under a nitrogen gas atmosphere. Instead of adding the dilute acid to cleave the substitution on the 3-position of naltrexone, column chromatography is used to separate out the target compound. The final compound is isolated as a dark brown residue and not a powder like most of the other 14-*O*-heterocyclic substituted naltrexone derivatives.

Compounds **20** and **24** are the control compounds. Problems are found in the deprotection step. After these two compounds are heated at reflux with naltrexone, a di-substituted product was formed and there was difficulty in the removal of the heterocyclic moiety at the 3-position. This may be due to the overall stability of the compound. Several different attempts have been made to try to remove the heterocyclic moiety at the 3-position (**Table 7**).

**Table 7.** Deprotection conditions used to prepare compounds **20** and **24**.

| Attempt | Condition | Reaction Time | Overall Results |
|---|---|---|---|
| 1 | Dilute acid ($H_2SO_4$) | 24 hours | Di-substituted product |
| 2 | Titration of sample from attempt 1 from pH 4 to 1 with addition of 1N $H_2SO_4$ | Overnight | Di-substituted product |
| 3 | Heat mixture to 50 °C under nitrogen protection | Overnight | Di-substituted product |
| 4 | Addition of 5 mg sodium bicarbonate and dissolved in THF | Overnight | Di-substituted product |
| 5 | Dissolve in THF and potassium carbonate at room temperature | Overnight | Final mono-substituted product |

Attempts 1 to 4 (**Table 7**) did not accomplish the removal of the substituent at the 3-position. However, the final attempt was successful. Basically, THF and potassium carbonate mixture is separated into two layers: $K_2CO_3$ saturated water layer and THF layer. The compound is isolated from the water layer and purified using column chromatography.

All the compounds are converted into dihydrochloride salts and completely dried using the vacuum pump prior to characterization by nuclear magnetic resonance (NMR), infrared spectroscopy (IR), mass spectrometry (MS) and melting point determination. All the compounds are evaluated for their affinity to all three opioid receptors through radiolabeled competition binding assays, and their efficacy for the mu-opioid receptor through [$^{35}$S] GTPγS binding assay.

## 1.5 Verification of Dihydrochloride Salts

After the synthesis of the 14-*O*-heterocylic substituted naltrexone derivatives, they are converted into dihydrochloride salts through the addition of 2.2 equivalents of 1.25 M hydrochloric acid in methanol. However, the control compounds **20** and **24** are converted to mono-hydrochloride salts. In order to verify whether these compounds are in the mono- or dihydrochloride salt form, $^{1}$H-NMRs are taken for both the free base and salt form of each compound. If the compound is a di-hydrochloric salt, then there should be a difference in the chemical shifts between the free base and salt form in the heterocyclic substituent of the compounds. For each compound, the differences between the chemical shifts in the free base versus the salt form of the heterocylic substituent are observed (**Table 8** and **Table 9**). The chemical shifts of the heterocyclic substituent in the salt form are shifted down field compared to the free base form. There is no major difference in the chemical shifts of the salt form and free base form of the two control compounds **20** and **24**.

**Table 8.** The difference of the chemical shifts between the salt and free base forms of the first series of 14-*O*-heterocyclic substituted naltrexone derivatives.

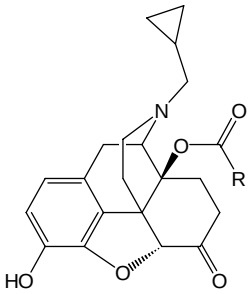


| Compound | **17** | **18** | **19** | **20** |
|---|---|---|---|---|
| | | Substituent (R) | | |
| | 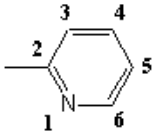 | 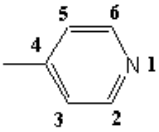 | 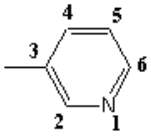 | 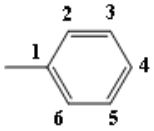 |
| Positions: | | | | |
| 2 | - | 0.34 | 0.07 | 0.00 |
| 3 | 0.90 | 0.72 | - | 0.12 |
| 4 | 0.60 | - | 0.69 | 0.11 |
| 5 | 0.91 | 0.72 | 0.76 | 0.12 |
| 6 | 0.36 | 0.34 | 0.42 | 0.00 |

* The change in the chemical shifts of the salt and free base was determined by $\delta_{salt}$-$\delta_{free\ base}$.

**Table 9.** The difference of the chemical shifts between the salt and free base forms of the second series of 14-*O*-heterocyclic substituted naltrexone derivatives.

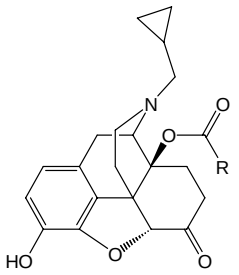


| Compound | **21** | **22** | **23** | **24** |
|---|---|---|---|---|
| | | Substituent (R) | | |
| | 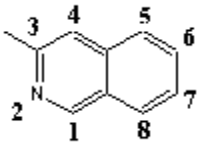 | 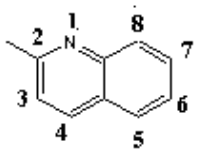 | 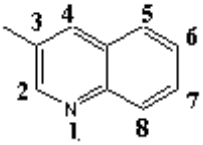 | 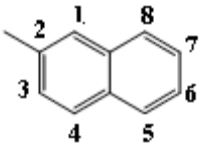 |
| Positions: | | | | |
| 1 | 0.14 | N | N | 0.16 |
| 2 | N | - | 0.03 | - |
| 3 | - | 0.86 | - | 0.10 |
| 4 | 0.04 | 0.89 | 0.51 | 0.11 |
| 5 | 0.12 | 0.95 | 0.40 | 0.19 |
| 6 | 0.12 | 1.16 | 0.26 | 0.19 |
| 7 | 0.12 | 1.29 | 0.49 | 0.10 |
| 8 | 0.19 | 1.12 | 0.17 | 0.10 |

* The change in the chemical shifts of the salt and free base was determined by $\delta_{salt}$-$\delta_{free}$

base·

All the compounds show a difference greater than 0.30 ppm in the chemical shifts between the salt and free base form except for compound **21**. Therefore, according to the data it can be assumed that all compounds are dihydrochloride salts except that compound **21** and the controls **20** and **24** are mono hydrochloride salts.

It has been reported that environmental change can cause the complete conformational conversion of an amide skeleton upon the addition of acid.[98] An *N*-methyl amide containing *N*- 2,6-pyridinedicarboxamide moieties (**43**) that can switch its conformation depending upon the acceptor ability of the solvent. With the addition of trifluoroacetic acid (TFA) to the amides, a lower field shift in the aromatic protons can be observed (**Figure 17**). The addition of TFA to compound **43** causes the nitrogen atom in the pyridine ring to lie in the *syn* position with respect to the carbonyl group due to hydrogen bond formantion.[98]

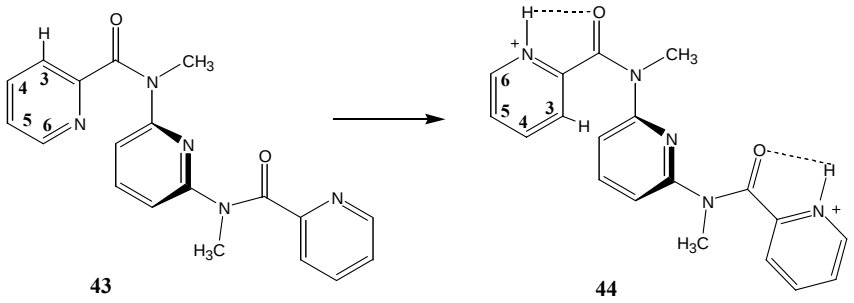

43 44

| Proton Assignment | Proton Shift (ppm) 43 | 44 | Difference in chemical shifts |
|---|---|---|---|
| 3 | 7.60 | 7.60 | 0.00 |
| 4 | 7.73 | 8.43 | 0.70 |
| 5 | 7.24 | 8.04 | 0.80 |
| 6 | 7.31 | 7.91 | 0.60 |

**Figure 17.** Difference in proton chemical shifts for *N*-2,6-pyridinedicarboxamide moieties with the addition of TFA (150 equiv).[98] The difference in chemical shifts was determined by $\delta_{44}$-$\delta_{43}$.

Mass spectrometry was also conducted for all of the compounds. The major peak was found to be the mono-protonated 14-*O*-heterocyclic substituted naltrexone derivatives. The second major peak was determined to be mono-protonated naltrexone conjugated with the chloride ion. For some of the compounds the di-protonated product can be seen but the relative intensity was low.

## 2. Pharmacological Studies of 14-*O*-Heterocyclic Substituted Naltrexone Derivatives

In order to determine the affinities of these newly synthesized derivatives of naltrexone, several different radiolabeled binding assays were conducted. First, a

saturation binding assay was used to determine the affinity of the radioligand used for each receptor and the approximate amount of receptors in the different monoclonal receptor expressed cell lines. This was followed by competition binding assays to all three opioid receptors to determine the 14-*O*-heterocyclic substituted naltrexone derivatives' affinity and selectivity. Finally, the compounds underwent a functional assay to determine their potential agonist activity.

## 2.1 Cell Culture of Cell Lines Over-expressing Opioid Receptors

Before any of the compounds were evaluated in the different binding assays, cell lines expressing the three opioid receptors were cultured and harvested for use in the assays. For the mu- and kappa-opioid receptors, CHO cell lines were used. For the delta-opioid receptor several different cell lines were used including HEK293, CHO and NG108-15 cell lines. The CHO cell lines were cultured in DMEM/F12 media containing 5% fetal bovine serum (FBS), 0.2 mg/mL geneticin (G418) and 1% penicillin-streptomycin except 10% FBS was used for the DORCHO cell lines. The HEK cell lines were cultured in DMEM media with 8% FBS, 0.2mg/mL G418, 1% penicillin-streptomycin, and 1.5 mM HEPES. The NG108-15 cell lines used DMEM media with 10% FBS, 1% penicillin-streptomycin, 0.2 mg/mL G418 and 100x HAT.[99,100]

## 2.2 Saturation or Scatchard Radiolabeled Binding Assay

In order to characterize the receptors, a saturation or scatchard binding assay was used to determine the Bmax of the receptors for each cell line and Kd for the radiolabeled

ligands for their respective receptors. Bmax is the maximum number of binding sites that can be bound by the radioligand and is a measure of receptor density in the tissue reported in pmol/mg.[101] Kd is the affinity of the radioligand for the particular receptor and is the concentration of radioactive ligand required to occupy 50% of the receptors. Kd is reported in molar concentration units, in this case all of the Kd values were reported in nanomolar concentration units. The saturation assay was performed for the CHO cell lines expressing the delta-opioid receptor (DORCHO) and the kappa-opioid receptor (KORCHO), and HEK cell lines expressing the delta-opioid receptor (DORHEK) all from the University of Minnesota. For all the other cells lines, NG108-15 (delta-opioid receptor) and mu-opioid receptor (MORCHO) from Virginia Commonwealth University (VCU) and delta-opioid receptor (DORCHO) from Temple University, the Bmax had already determined and used without further testing (**Table 10**).

The radioligands used in all the assays are highly selective for their corresponding receptors.[102] For the mu-, delta- or kappa-opioid receptors [$^3$H] NLX, [$^3$H] NTI or [$^3$H] Nor-BNI were used respectively. The saturation assay involves the competition of the radiolabeled ligand at different concentrations with the same drug, except it is unlabeled (cold), in excess for the corresponding receptors. However, the cold drug used for the mu-opioid receptor was naltrexone.

Naltrexone can be used as the cold ligand instead of naloxone because naltrexone has about 10-fold higher affinity for the mu-opioid receptor compared to naloxone.[42,51] The cold ligand used to determine the non-specific binding needs to have high affinity for

its receptor. Also, naltrexone and naloxone have comparable affinity to all three opioid receptors.[42,51]

**Table 10.** Bmax and Kd for the different mono-cloned opioid expressed cell lines determined by saturation binding assay.

| Cell Line | Bmax (pmol/mg) | Kd (nM) |
|---|---|---|
| MORCHO | 3.00 | 2.00 |
| DORCHO (Temple) | 5.80 | * |
| DORCHO (Minnesota) | 1.21 | 0.46 |
| DORHEK | 1.51 | 0.36 |
| KORCHO | 3.37 | 0.65 |

* Saturation assay was not completed for the DORCHO cells from Temple University. The Bmax was already determined and the Kd was assumed to be similar to the other cells that express the delta-opioid receptor.

## 2.3 Competition Binding Assay

The competition binding assays were conducted for all the three opioid receptors in order to determine the binding affinities for naltrexone and the naltrexone derivatives. From this assay, $IC_{50}$ values were determined and converted to Ki values using the Cheng-Prusoff equation.[103] The same radioligands and cold drugs from the saturation binding assays were used in this assay. However, this time the concentration of the naltrexone derivatives were varied, while the radioligand concentration was between 1 to 2 times their Kd values.

### A. Mu-Opioid Receptor

The selectivity of the 14-*O*-heterocyclic substituted naltrexone derivative for the mu-opioid receptor was determined using [$^3$H]NLX as the radioligand (2 nM) to compete with the naltrexone derivatives. The non-specific binding was determined by an excess

of cold naltrexone at a concentration of 10 μM. The MORCHO (from Dr. Selley's laboratory at VCU) cells were used to determine the affinity of the naltrexone derivatives to the mu-opioid receptor. About 10 to 15 μg of protein was added to each tube. A Bradford protein determination assay was used to determine and adjust the concentration of protein required for the assay.[104] The total volume of this assay was 500 μL. The incubation time for this assay was 120 minutes in a 37 °C water bath. Various concentrations of the naltrexone derivatives were tested to determine their Ki values. After incubation, the reaction was quenched with cold tris buffer. A Brandel harvester was used to separate the bound from the free radioligand. The results were determined utilizing a scintillation counter. Ki values are the result of triplicate determinations.

**B. Delta-Opioid Receptor**

The selectivity of the 14-*O*-heterocyclic substituted naltrexone derivative for the delta-opioid receptor was determined using [$^3$H]NTI as the radioligand (0.5 nM) to compete with the naltrexone derivatives. The non-specific binding was determined by an excess of cold naltrindole (NTI) at a concentration of 10 μM. Although several different cell lines were utilized in this assay, only the DORCHO (from Temple University) cells were used to determine the ligands affinity. About 10 to 20 μg of protein was added to each tube. A Bradford protein determination assay was used to determine and adjust the concentration of protein required for the assay.[104] The total volume of this assay was 1000 μL. The incubation time for this assay was 120 minutes in a 37 °C water bath. Various concentrations of the naltrexone derivatives were tested to determine their Ki

values. After incubation, the reaction was quenched with cold tris buffer. A Brandel harvester was used to separate the bound from the free radioligand. The results were determined utilizing a scintillation counter. Ki values are the result of duplicate determinations.

**C. Kappa-Opioid Receptor**

The selectivity of the 14-*O*-heterocyclic substituted naltrexone derivative for the kappa-opioid receptor was determined using [$^3$H]Nor-BNI as the radioligand at a concentration of 0.6 to 1.2 nM, about 1 to 2 times the Kd value determined in the saturation assay. The non-specific binding was determined by an excess of cold nor-BNI at a concentration of 10 μM. The KORCHO cells were used and about 20 to 30 μg of protein was added to each tube. A Bradford protein determination assay was used to determine and adjust the concentration of protein required for the assay.[104] The incubation time for this assay was 120 minutes in a 37 °C water bath. The total volume of this assay was 500 μL. Various concentrations of the naltrexone derivatives were tested to determine their Ki value. After incubation, the reaction was quenched with cold tris buffer. A Brandel harvester was used to separate the bound from the free radioligand. The results were determined utilizing a scintillation counter. Ki values are the result of triplicate determinations.

There were a couple problems in the assay dealing with the radioligand. [$^3$H]Nor-BNI is very unstable and was kept cold in the presence of nitrogen gas. Also, the [$^3$H]Nor-BNI was dissolved in 5:2 toulene:ethanol. Toulene at very high

concentrations can disrupt cellular membranes.[105] Therefore, the toluene:ethanol solvent was removed from the radioligand under vacuum pressure in an ice water bath for about 8 to 10 h. After the radioligand was completely dry, it was re-dissolved in ethanol. Also a small amount of cold nor-BNI was added in order to dilute the concentration of [$^3$H]Nor-BNI to a lower specific activity since it is very unstable at a high specific activity. Nitrogen gas was added to the [$^3$H]Nor-BNI in ethanol to help prevent further degradation. This process was conducted for small batches of [$^3$H]Nor-BNI, about 100 to 150 μL, at a time.

Another problem seen in the assay was that the total amount of radioligand bound was between 15 to 20% of the total amount of radioligand added (standards). In order to compensate for this problem, the total volume was increased from 0.5 to 1 mL and the amount of [$^3$H]Nor-BNI was doubled from 0.6 to 1.2 nM, 2 times the Kd value. This helps reduce the radioligand bound to between 7 to 8%.

### 3. [$^{35}$S]GTPγS Functional Binding Assay for the Mu-Opioid Receptor

A functional assay was used to compare the agonist activity of the naltrexone derivatives to the mu-opioid receptor compared to DAMGO, a full mu-opioid receptor agonist. From this assay, the potency, $EC_{50}$, and the intrinsic efficacy, Emax, can be determined. The $EC_{50}$ is the molar concentration of an agonist to produce 50% of the maximal possible effect. The Emax is the maximum effect of the agonist.[106] DAMGO has an Emax value of 366% stimulation of receptor and represents 100% agonist activity.

All the naltrexone derivatives were compared to DAMGO's Emax value in order to determine whether these compounds are agonists, partial agonists, and antagonists.

The agonist activity of the naltrexone derivatives for the mu-opioid receptor was determined using [$^{35}$S]GTPγS as the radioligand. [$^{35}$S]GTPγS was diluted so the final DPM count is about 125,000. The non-specific binding was determined using an excess of cold gamma-GTP at a concentration of 20 μM. GDP was also added to all the tubes at a concentration of 10 μM in order to obtain optimal agonist-stimulated binding. The MORCHO cells were used and the approximate amount of protein added to each tube is between 9 to 10 μg in the assay. A Bradford protein determination assay was used to determine and adjust the concentration of protein required for the assay.[104] Finally, TME buffer with $Na^+$ was utilized to improve agonist stimulated binding.[107] The incubation time for this assay was 90 minutes in a 37 °C water bath. The concentration of the naltrexone derivatives tested was between 0.0001 nM to 10,000 nM.

## 4. Competition Binding Assay Results for 14-*O*-Heterocyclic Substituted Naltrexone Derivatives

### 4.1 14-*O*-Pyridinyl Substituted Naltrexone Derivatives

The results for the first set of compounds, 14-*O*-pyridinyl substituted naltrexone derivatives, show that all of the compounds have nanomolar and subnanomolar affinity for the mu-opioid receptor. More importantly, the first set of naltrexone derivatives display higher selectivity for the mu-opioid receptor over the kappa- and delta-opioid receptors (**Table 11**).

**Table 11.** Binding assay results for the 14-*O*-pyridinyl substituted naltrexone derivatives.

| Cmpd | R | μKi (nM) +/- SEM | δKi (nM) +/- SEM | κKi (nM) +/- SEM | Ratio δ/μ | Ratio κ/μ | Comparison of Agonist Percent Stimulation to DAMGO |
|---|---|---|---|---|---|---|---|
| Naltrexone | | 0.260 +/- 0.017 | 117.058 +/- 8.945 | 5.150 +/- 0.264 | 450 | 8 | |
| **17** | 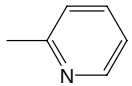 | 0.14 +/- 0.03 | 4610+/- 821 | 255 +/- 64.8 | 33650 | 1859 | 0.00 |
| **18** | 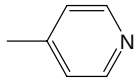 | 5.58 +/- 1.34 | 1144+/- 99.7 | 775 +/- 256 | 205 | 139 | 0.00 |
| **19** | 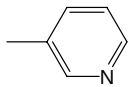 | 1.59 +/- 0.61 | 1310 +/- 306 | 565+/- 109 | 55 | 355 | 0.00 |
| **20** | 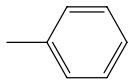 | 123+/- 38.2 | >10,000 | 729+/- 144 | >81 | 6 | 0.00 |

The Ki values for the mu- and kappa-opioid receptors are n=3 and the Ki value for the delta-opioid receptor is n=2. The averages are reported along with their standard error of the means (SEM) for each compound. The comparison to percent stimulation of DAMGO is the Emax of the compound compared to the Emax of DAMGO using a [$^{35}$S]GTPγS functional assay. Note the abbreviations are Cmpd – compound; R – substituent; SEM - standard error of the mean.

Based on the results, compound **17** was determined to be the lead compound for the first series of 14-*O*-pyridinyl substituted naltrexone derivatives. Compound **17** has the highest affinity and selectivity for mu-opioid receptor compared to the other derivatives in the first series of 14-*O*-pyridinyl substituted naltrexone derivatives (**Figure 18**). Compared to naltrexone, **17** has comparable affinity to the mu-opioid receptor, but much higher selectivity for the mu-opioid receptor over the kappa- and delta-opioid receptors. Compared to the control compound **20**, it is clear that the nitrogen is necessary for higher binding affinity to the mu-opioid receptor. Also, the GTPγS functional assay showed no agonist activity for the mu-opioid receptor for up to 10,000 nM of compound **17**.

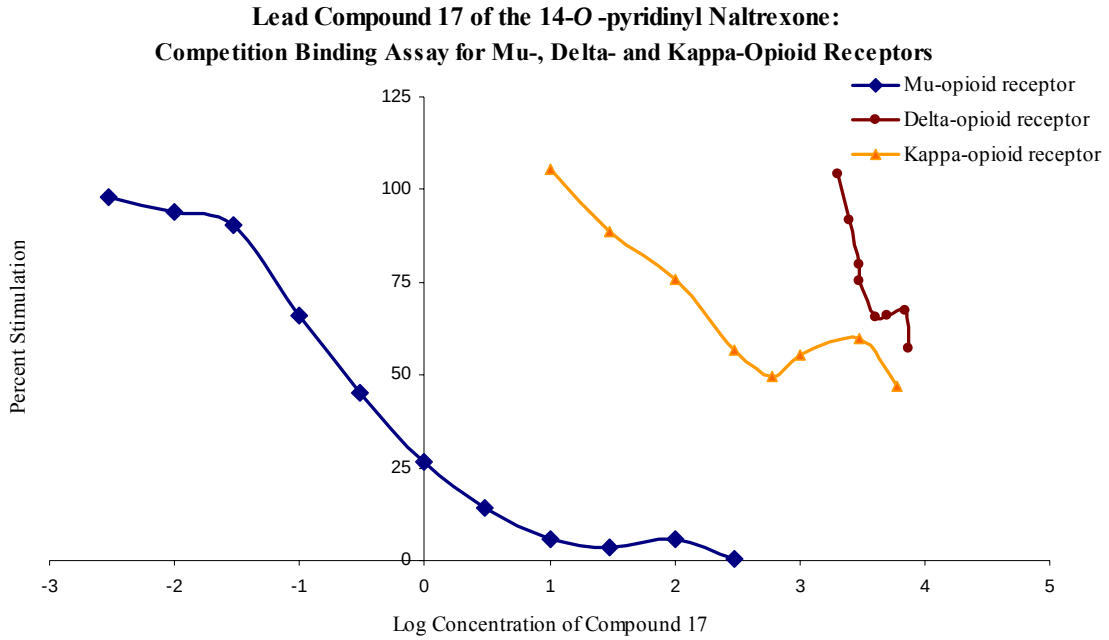


**Figure 18.** Competition binding curve for lead compound **17** for the mu-, delta-, and kappa-opioid receptors.

Compound **18** displays high selectivity for the mu-opioid receptor over the delta- and kappa-opioid receptors. When compared to naltrexone, **18** has one-tenth the affinity of naltrexone but is much more selective for mu- over kappa-opioid receptors. Compared to the lead compound **17**, **18** shows lower selectivity to the mu-opioid receptor. Also, the GTPγS functional assay shows no agonist activity for the mu-opioid receptor for up to 10,000 nM of compound **18**.

Compound **19** shows a similar binding profile compared to compound **18.** It has high affinity and selectivity for the mu-opioid receptor compared to the delta- and kappa-opioid receptors. However, it has about one-tenth the affinity to the mu-opioid receptor compared to naltrexone and compound **17**. Both compounds **18** and **19** have higher affinity to the mu-opioid receptor compared to the control **20** suggesting that the nitrogen may be playing an important role for binding to the mu-opioid receptor. Additionally, the GTPγS functional assay shows negative results of the mu-opioid receptor for up to 10,000 nM of compound **19**.

The control compound **20** displays very low affinity to the mu-opioid receptor compared to naltrexone (about one-hundredth the affinity) and to the other compounds in this series. Therefore, the nitrogen atom in compounds **17** to **19** seems to play an important role in affinity and selectivity of these naltrexone derivatives to the mu-opioid receptor.

## 4.2 14-*O*-Quinolinyl and 14-*O*-Isoquinolinyl Substituted Naltrexone Derivatives

The results for the second set of 14-*O*-heterocyclic substituted naltrexone compounds show that all of the compounds are more selective for the mu-opioid receptor over the kappa- and delta-opioid receptors (**Table 12**). Also, these compounds have nanomolar level affinity for the mu-opioid receptor.

**Table 12.** Binding assay results for the 14-*O*-quinolinyl and 14-*O*-isoquinolinyl substituted naltrexone derivatives.

| Cmpd | R | μKi (nM) +/- SEM | δKi (nM) +/- SEM | κKi (nM) +/- SEM | Ratio δ/μ | Ratio κ/μ | Comparison of Agonist Percent Stimulation to DAMGO |
|---|---|---|---|---|---|---|---|
| Naltrexone | | 0.260 +/- 0.017 | 117.058 +/- 8.945 | 5.150 +/- 0.264 | 450 | 8 | |
| **21** | 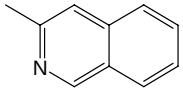 | 68.40 +/- 6.04 | > 10,000 | >10,000 | >146 | >147 | 0.00 |
| **22** | 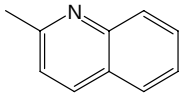 | 1.44 +/- 0.32 | 1362+/- 111 | 1377+/- 112 | 947 | 957 | 0.00 |
| **23** | 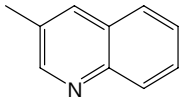 | 2.60 +/- 0.72 | 2824+/- 14.6 | 665 +/- 98.2 | 901 | 247 | 22.0 +/- 10.3 |
| **24** | 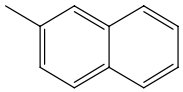 | 225 +/- 46.6 | > 10,000 | 474 +/- 176 | >44 | 2 | 0.00 |

The Ki values for the mu- and kappa-opioid receptor are n=3 and the Ki value for delta-opioid receptor is n=2. The averages are reported along with their standard error of the mean (SEM) for each compound. The comparison to percent stimulation of DAMGO is the Emax of the compound compared to the Emax of DAMGO using a [$^{35}$S]GTPγS functional assay. Note the abbreviations are Cmpd – compound; R – substituent; SEM - standard error of the mean.

From the second series of naltrexone derivatives, **22** is determined to be the lead compound. Compound **22** has lower affinity (about one-tenth) for the mu-opioid receptor compared to naltrexone, however it has much higher selectivity for the mu-opioid receptor over the kappa- and delta- opioid receptors. Naltrexone has comparable affinity for the mu- and kappa-opioid receptors (**Figure 19**). Compared to compound **24**, compound **22** also shows much higher affinity and selectivity to the mu-opioid receptor. Therefore, the nitrogen plays an important role in the binding of these naltrexone derivatives to the mu-opioid receptor. Additionally, compound **22** displayed no agonist activity for up to 10,000 nM concentration in the GTPγS functional assay.

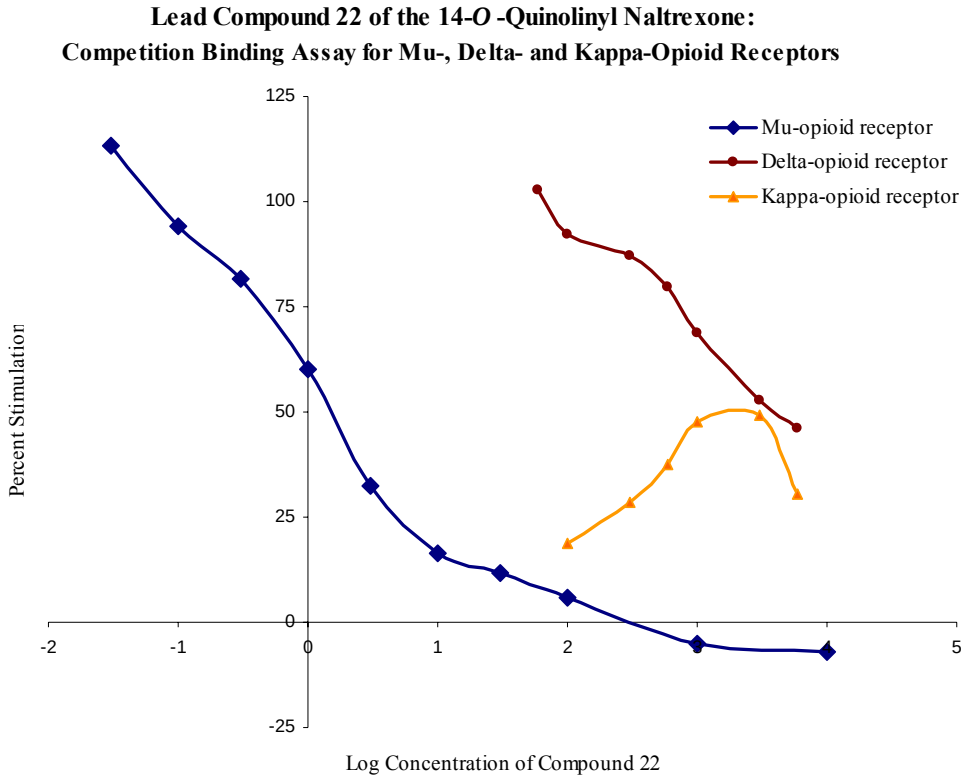


**Figure 19.** Competition binding curve for lead compound **22** for the mu-, delta-, and kappa-opioid receptors.

Compound **21** shows lower affinity to the mu-opioid receptor compared to naltrexone. However, **21** still shows selectivity for the mu-opioid receptor over the delta- and kappa-opioid receptors. Compared to the control **24**, compound **21** has higher selectivity for the mu-opioid receptor compared to the delta- and kappa-opioid receptors. However, both compounds **21** and **24** display similar affinity to the mu-opioid receptor. The addition of the two-ring system may be too bulky to fit well in the binding pocket of the mu-opioid receptor, and this may explain the lower affinity seen with the quinoline series compared to the pyridine series. Additionally, compound **21** displayed no agonist activity for up to 10,000 nM concentration in the GTPγS functional assay.

Compound **23** shows lower affinity to the mu-opioid receptor compared to naltrexone. However, **23** displays selectivity for the mu-opioid receptor over the delta- and kappa-opioid receptors. Compared to the lead compound **22**, compound **23** shows similar affinity to the mu-opioid receptor. Compared to the control **24**, compound **23** has higher selectivity and affinity for the mu-opioid receptor compared to the delta- and kappa-opioid receptors. Additionally, compound **23** displayed no agonist activity for up to 10,000 nM concentration in the GTPγS functional assay.

The control compound **24** shows low affinity to the mu-opioid receptor compared to naltrexone and to the other compounds in this series. The nitrogen seems to play an important role in affinity and selectivity of these naltrexone derivatives to the mu-opioid receptor. The decrease in affinity may be due to the addition of the second ring. The substitution may be too bulky and may not be situated properly into the binding pocket.

## 4.3 Comparison between the Lead Compounds 17 and 22

Compound **17** and **22** are determined to be the lead compounds for the pyridinyl and quinolinyl series of the 14-*O*-heterocylic substituted naltrexone derivatives. Both compounds contain a nitrogen atom next to the ester linkage. The nitrogens in compounds **17** and **22** may arrange themselves in similar conformations in the binding pocket of the mu-opioid receptor. Also, compound **17** has 10-times higher affinity for the mu-opioid receptor compared to compound **22**. This may be due to the addition of the second ring, making compound **22** more bulky.

Further in vitro studies need to be conducted on these two lead compounds such as a Schild regression analysis to determine their apparent affinities, or $pA_2$, values for the mu-opioid receptor. The Schild regression is used to determine the nature of antagonist either competitive or non-competitive. Schild regression is used to compare the change in dose ratios, the ratio of the $EC_{50}$ of an agonist alone compared to the $EC_{50}$ in the presence of an antagonist. By altering the concentration of the antagonist, the dose ratio is altered.[108]

Additionally, in vivo studies should be conducted to see how they act in the body and what kind of effects they produce in the body. Finally, further optimization may be conducted in order to explore the possibility of an amide linkage over the ester linkage to the 14-position of naltrexone.

## 5. Molecular Modeling Study of the 14-*O*-Heterocyclic Substituted Naltrexone Derivatives in the Mu-Opioid Receptor

Molecular modeling studies have been conducted on the 14-*O*-heterocyclic substituted naltrexone derivatives, as well as naloxone and naltrexone, to gain insight on the interactions of the compounds in the binding pocket of the mu-opioid receptor. A homology model of the mu-opioid receptor was built based on the X-ray crystal structure of the dark state of bovine rhodopsin (1U19; resolution of 2.2 Å).[109] Clustal X was applied to align the sequences of human mu-, delta- and kappa-opioid receptors with bovine rhodopsin (**Figure 20**).[110] Furthermore, the conserved residues found throughout most of the GPCRs were used to identify the helical regions of the opioid receptors and rhodopsin.[109]

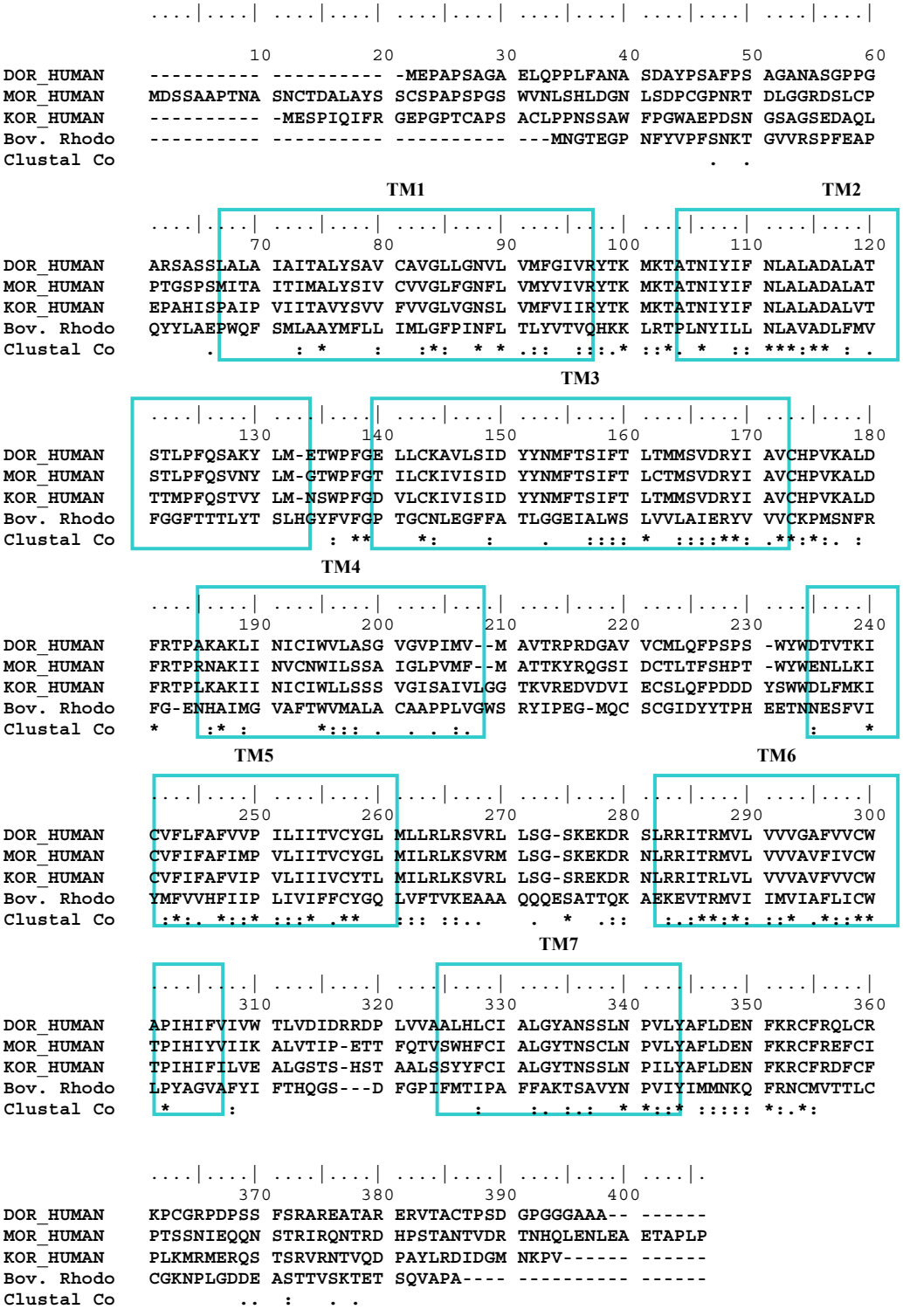


**Figure 20.** Sequence alignment of the human mu-, delta-, and kappa-opioid receptors to bovine rhodopsin (1U19) using Clustal X. The boxes represent the transmembrane (TM) regions. The * represents conserved amino acid residues found among all GPCRs. Abbreviations: MOR=mu-opioid receptor, DOR=delta-opioid receptor, KOR=kappa-opioid receptor, Bov. Rhodo=bovine rhodopsin.

First, the N and C termini of the mu-opioid receptor were cleaved off before Ile68 and after Pro355 since the N and C termini have very low sequence homology among the three opioid receptors and bovine rhodopsin. The helices of bovine rhodopsin were directly mutated with the residues of mu-opioid receptor. Loop searches were conducted for the gaps found in EL2, EL3 and IL3 in order to maintain the conformation of the three-dimensional structure of the rhodopsin loops. Since EL2 is important in the interaction of the opioids in the binding pocket, maintaining the conformation and integrity of EL2 was important. Before minimization was conducted, side chain placement with a rotamer library (SCWRL) was used to check and fix improper positioning of the amino acid residues.[111] The disulfide bond between cysteine residues 130 of TM3 and 180 of EL2 was rejoined, and hydrogens were added and lone pairs were removed. The receptor was minimized with Gasteiger-Hückel charges with a dielectric constant of 4.0 and 100,000 iterations. Procheck was also performed to validate acceptable phi and psi angles in the protein and all of the residues were found to be in acceptable angle conformations.

Initial docking studies were conducted for the 14-*O*-heterocylic substituted naltrexone derivatives using GOLD 3.1.[112] A distance constraint was set at 4Å between the positively charged nitrogen atom at the 17-position of naltrexone to the oxygen O1278 of the amino acid residue Asp149 of the mu-opioid receptor. It turned out that the binding pocket is not large enough to incorporate the bulky heterocyclic side chain at the 14-position of the naltrexone derivatives. In order to accommodate the larger naltrexone

derivatives, compound **22** was interactively docked into the homology model of the mu-opioid receptor.

Based on site-directed mutagenesis data, compound **22** was positioned in a similar manner as naltrexone. First, the positively charged amino group at the 17-position of the compound was positioned between 3 to 4Å away from the amino acid residue Asp149 since it has been shown to form a hydrogen bond with one of the oxygens of Asp149.[87] Next the phenol moiety at the 3-position of naltrexone and was placed about 3 to 4Å apart from the aromatic amino acid residues, Tyr212 and Phe223, of EL2.[87] The amino acid residue Tyr150 of TM3 may also form a hydrogen bond with the phenol oxygen at the 3-position of the naltrexone backbone.[88] The final hydrophobic interaction is between Leu221, Trp320 and Ile324 that can also interact with piperidinyl and cyclohexanoyl in naltrexone backbone. Trp320 in EL3 was found to be critical in the binding of mu-opioid receptor.[11] When Trp320 was mutated to leucine and lysine, the affinity of naltrexone significantly decreased in the mutated mu-opioid receptor.[87,88]

By satisfying these interactions, compound **22** was docked into the binding pocket and the receptor-ligand complex was minimized. Compound **22** was used because it showed satisfactory binding affinity and selectivity for the mu-opioid receptor. After the minimization was complete, molecular dynamics simulation was conducted in Sybyl 7.1.

The dynamics simulation was done in order to allow the formation of a larger binding pocket by moving amino acid residue side chains out of the binding pocket. The dynamic simulations used Gasteiger-Hückel charges, a dielectric constant of 4.0, an aggregate with a 10Å radius around the ligand and a distance constraint of 4Å between

the positively charged amino group at the 17-position of naltrexone backbone to one of the oxygens of the amino acid residue Asp149 of the receptor. Dynamic simulation involves the heating of the receptor, allowing the movement of side chains and stretching the binding cavity. After the dynamics simulation the homology model of the mu-opioid receptor was minimized. The final binding cavity was analyzed and the compound was removed (**Figure 21**).

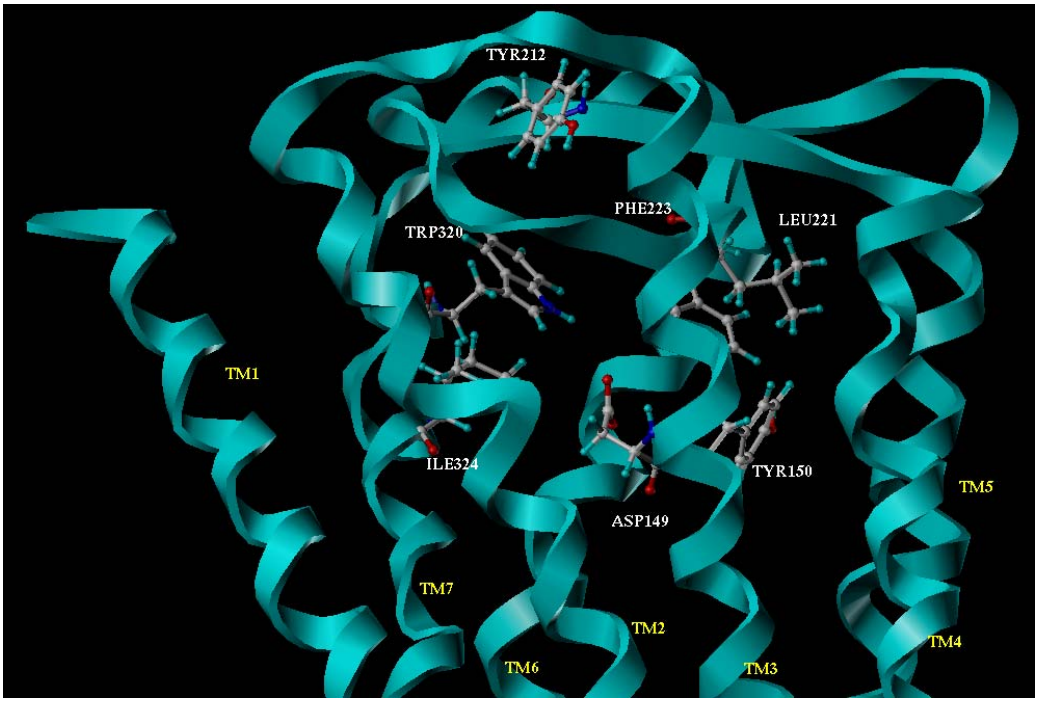


**Figure 21.** Binding pocket of the mu-opioid receptor with the critical amino acid residues.

The docking studies were conducted using GOLD 3.1 for each of the 14-*O*-heterocyclic substituted naltrexone derivative and two mu-opioid receptor antagonists, naltrexone and naloxone, with the newly formed homology model of the mu-opioid receptor.[112] Default settings were used in GOLD with a distance radius set to 10Å where

the central residues were set to oxygen O1278 of Asp149. Also, a distance constraint of 4Å was set between the 17-nitrogen atom of naltrexone with one of the oxygen O1278 of Asp149. The GOLD scores for naltrexone and naloxone are 54.71 and 53.88, respectively. The GOLD scores for the **17** to **20** derivatives range from 68.39 to 82.20 and for the **21** to **24** derivatives range from 69.38 to 73.98. The gold scores for all of the compounds are summarized in Table 13.

**Table 13.** Gold docking scores for opioid antagonists, naloxone and naltrexone, and 14-*O*-heterocyclic substituted naltrexone docked into the binding cavity of the homology model of the mu-opioid receptor.[51]

| Cmpd | R | Ki $_{\mu}$ (nM) | Gold Score | S (hb_ext) | S (vdw_ext) | S (hb_int) | S (int) | S (con) |
|---|---|---|---|---|---|---|---|---|
| Naltrexone | | 0.26 | 54.71 | 6.48 | 37.82 | 0.00 | -3.77 | -0.00 |
| Naloxone | | 1.90 | 53.88 | 6.48 | 37.17 | 0.00 | -3.69 | -0.00 |
| **17** | 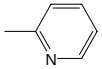 | 0.14 | 70.19 | 6.60 | 48.04 | 0.00 | -2.47 | -0.00 |
| **18** | 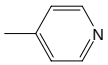 | 5.58 | 69.38 | 5.83 | 48.88 | 0.00 | -3.67 | -0.00 |
| **19** | 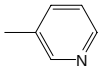 | 1.59 | 73.98 | 7.10 | 49.88 | 0.00 | -1.70 | -0.00 |
| **20** | 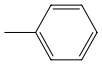 | 123 | 71.86 | 6.54 | 49.44 | 0.00 | -2.66 | -0.00 |
| **21** | 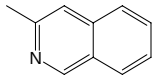 | 68.4 | 71.92 | 6.14 | 52.16 | 0.00 | -5.93 | -0.00 |
| **22** | 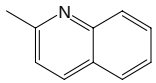 | 1.44 | 82.20 | 3.05 | 60.71 | 0.00 | -4.33 | -0.00 |
| **23** | 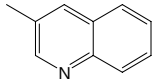 | 2.69 | 68.89 | 6.73 | 53.92 | 0.00 | -10.97 | -0.00 |
| **24** | 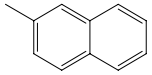 | 225 | 68.39 | 6.28 | 55.45 | 0.00 | -14.14 | -0.00 |

Abbreviations include Cmpd – Compound; R – substituent; S – Gold score component; hb – hydrogen bonding; vdw – Van der Waals interactions; ext – external interactions, int – internal interactions. The score components for constraints indicates a negative score depending on the ability of the docking solution to meet the defined constraints.

The docking scores do not seem to correlate well with the actual binding data obtained from the competition binding assays for the mu-opioid receptor. First, naloxone and naltrexone are known opioid antagonist but are not selective for the mu-opioid receptor. They both show similar selectivity for the mu- and kappa-opioid receptors. Their GOLD scores are the lowest among all of the compounds docked into the homology model of the mu-opioid receptor. This may be due to the homology model being optimized with one of the 14-*O*-heterocyclic substituted naltrexone derivatives aligned in its binding pocket.

From the first series, pyridinyl series of compounds (**17** to **20**), the GOLD scores range from 69.38 to 73.98. This may be due to the binding pocket of the homology model being explored around these naltrexone derivatives. There is no significant difference in the GOLD scores between all four ligands. However, there are some significant differences seen in their affinities for the mu-opioid receptor shown in the in vitro binding assays. Therefore, the homology model does not display an accurate depiction of what is really occurring in the binding pocket. These homology models are hypothetical pictures of how the compounds might bind.

From the second series, quinolinyl series of compounds (**21** to **24**), the GOLD scores range from 68.39 to 82.20. This may be due to the binding pocket of the homology model being explored around these naltrexone derivatives. Also, compound **22** has the highest GOLD score of all the naltrexone derivatives showing that the binding pocket of the homology model was optimized with this compound. Again, there is no significant difference in the GOLD scores between all four ligands. But, there are some

significant differences seen in their affinities for the mu-opioid receptor shown in the in vitro binding assays. Therefore, the homology model does not display an accurate depiction of what is really occurring in the binding pocket. These homology models are hypothetical pictures of how the compounds might bind.

The docking solutions for several of these compounds including the two lead compounds, **17** and **22**, as well as naloxone and naltrexone are shown in figures 22 to 24.

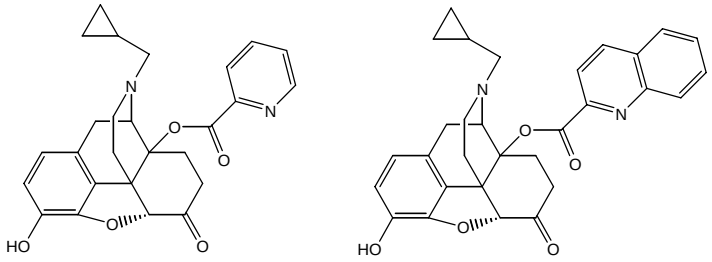


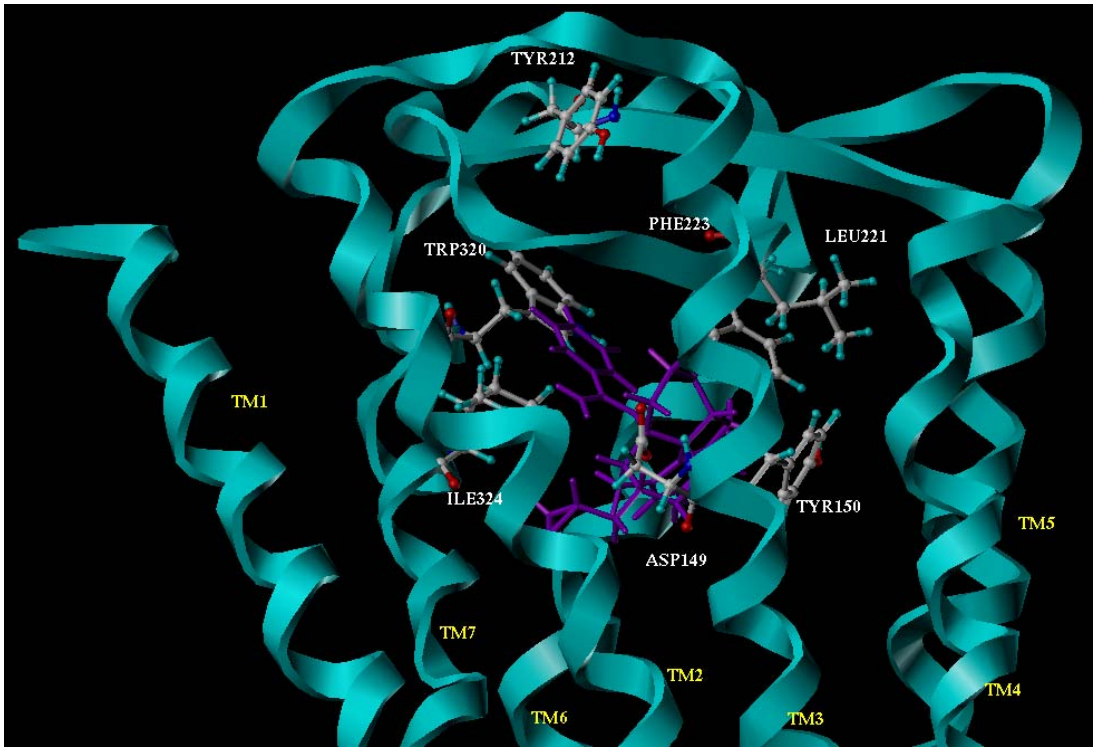


**Figure 22.** Lead compound **17** best ranked docking solution in the binding cavity of the mu-opioid receptor homology model.

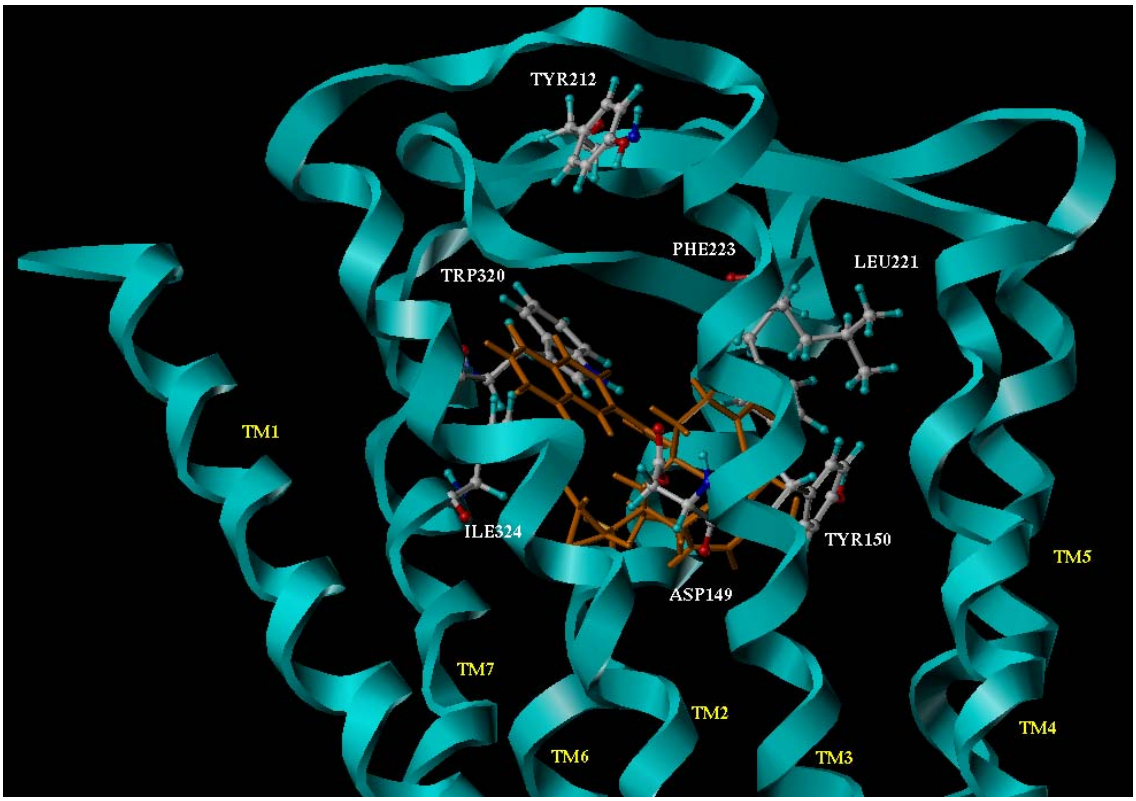


**Figure 23.** Compound **22**, highest Gold score of all derivatives, best ranked docking solution in the binding cavity of the mu-opioid receptor homology model.

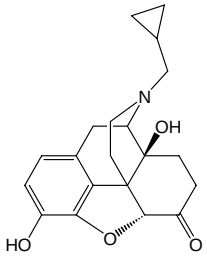


Naltrexone

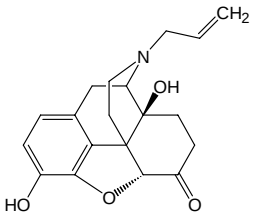


Naloxone

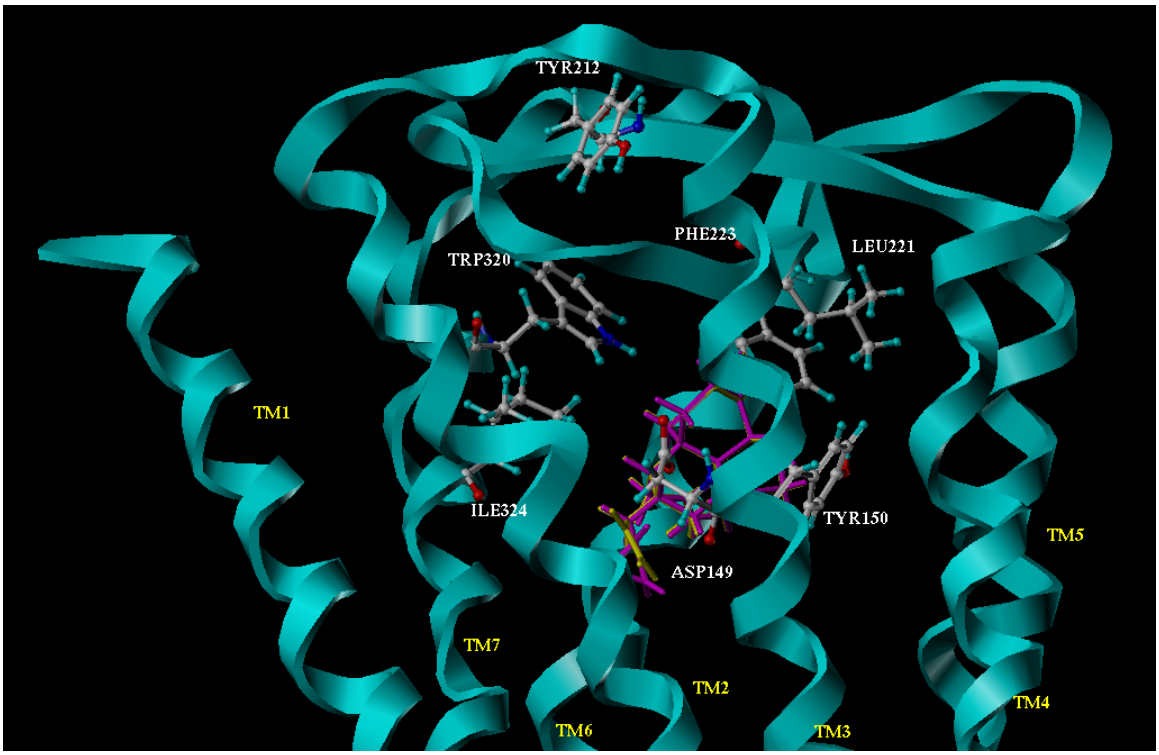


**Figure 24.** Opioid antagonists naltrexone (purple) and naloxone (yellow) best ranked docking solutions in the binding cavity of the mu-opioid receptor homology model.

In the homology model of the mu-opioid receptor binding pocket, naloxone and naltrexone seem to be overlapping each other (**Figure 24**). Compared to the lead compound, **17**, of the 14-*O*-heterocyclic substituted naltrexone derivatives, naltrexone is not interacting with the amino acid residue Trp320, which seems to interact with the

pyridine substituent on the lead compound, **17** (**Figure 25**). This may help explain the high Van der Waals contributions for the 14-*O*-heterocyclic substituted naltrexone derivatives and the lower GOLD scores of naloxone and naltrexone. Also, the poor correlation seen between the affinities of the 14-*O*-heterocyclic substituted naltrexone derivatives and the GOLD score values may be due to the small sample size.

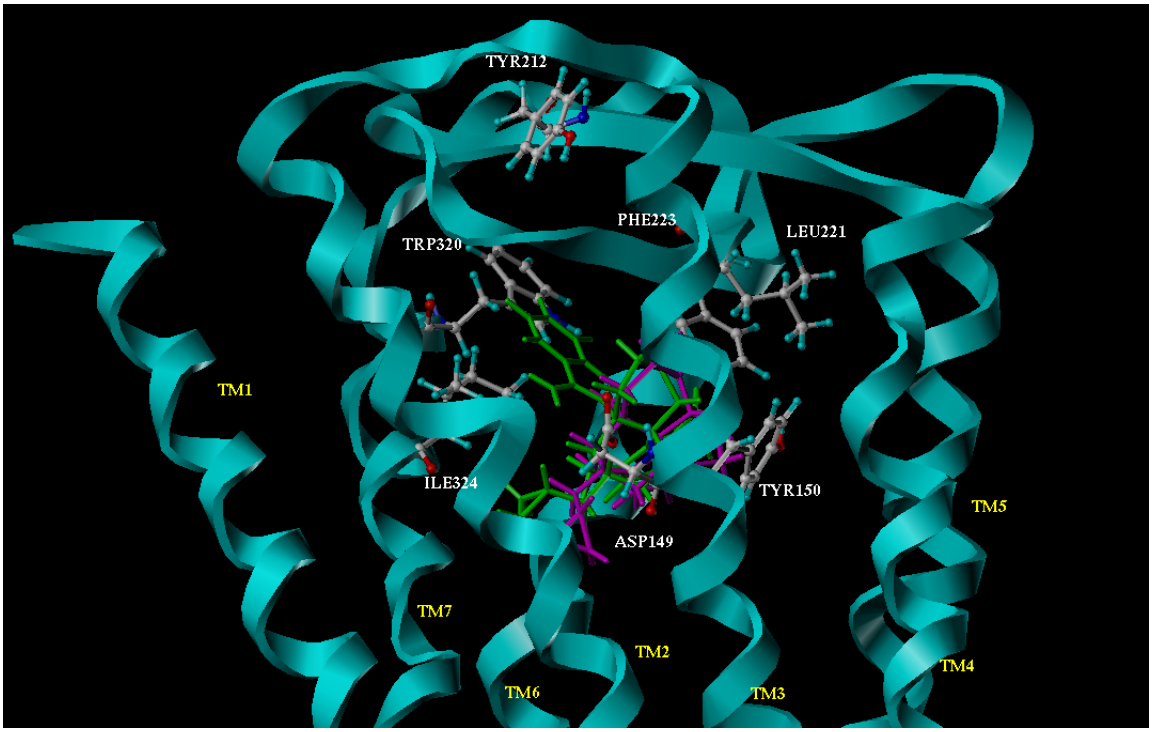


**Figure 25.** Opioid antagonist naltrexone (purple) and lead compound **17** (green) best ranked docking solutions in the binding cavity of the mu-opioid receptor homology model.

## 6. Competition Binding Assay Results for the 6-*N*-heterocyclic Substituted Naltrexamine Derivatives

Two different sets of 6-*N*-heterocyclic substituted naltrexamine derivatives were designed (see **Figure 16** on page 30). The first set carries a pyridinyl ring and the second set carries a quinolinyl or isoquinolinyl ring. Also, the α and β configurations at the 6-position of the naltrexone were investigated to determine if stereochemical arrangement altered their affinities towards the mu-opioid receptor.

A hetero-aromatic moiety was introduced to the 6-position of naltrexamine in order to design selective mu-opioid antagonists. An amide bond was used as the linkage of the side chain moiety to the skeleton of naltrexamine. Both the α and β stereochemical configurations of these compounds were synthesized to determine if stereochemical arrangement plays an important role in affinity and selectivity for the mu-opioid receptor. The nitrogen in the aromatic system acts as a hydrogen bond acceptor to probe the possibility of hydrogen bond formation with amino acid residues Tyr210 or Trp318. Control compounds with phenyl and naphthalene rings were also designed and synthesized as control compounds to test the hydrogen bonding hypothesis.

### 6.1 6-*N*-Pyridinyl Substituted Naltrexamine Derivatives

The first set of compounds, 6-*N*-pyridinyl substituted naltrexamine derivatives, all show nanomolar to subnanomolar affinity for the mu-opioid receptor (**Table 14**). Stereochemical arrangements did not seem to be a major factor in the determination of affinity and selectivity of these compounds for the mu-opioid receptor. The controls, **31**

and **32**, display little selectivity between the mu- and kappa-opioid receptors. This suggests that the nitrogen in the substitution may play an important role in the binding of these naltrexamine derivatives.

From the pyridinyl series of compounds, compound **26** is determined to be a lead compound (**Figure 26**). Compound **26** has similar binding affinity to the mu-opioid receptor compared to naltrexone. However, **26** is much more selective to the mu-opioid receptor compared with naltrexone. Compound **26** has higher selectivity to the mu-opioid receptor compared to the control compound **32**. However, control compound **31** seems to have similar binding and selectivity characteristics as compound **26**. Additionally, the GTPγS functional assay was conducted and the Emax of compound **26** was compared with the Emax of DAMGO. From these results, it seems that compound **26** acts as a partial opioid antagonist to the mu-opioid receptor compared with DAMGO. However, the control compound **31** also seems to act as a partial antagonist for the mu-opioid receptor, while compound **31** shows higher agonist activity compared with compound **26**.

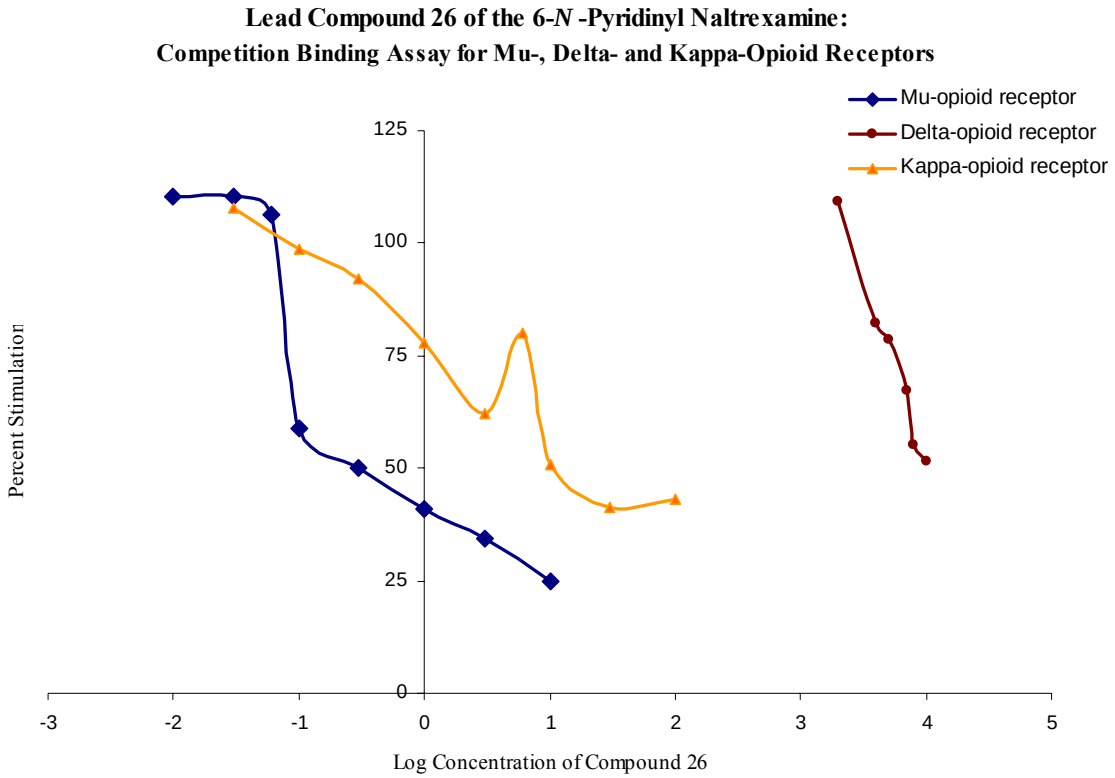


**Figure 26.** Competition binding curve for lead compound **26** for the mu-, delta-, and kappa-opioid receptors.

**Table 14.** Binding assay results for the 6-*N*-pyridinyl substituted naltrexamine derivatives.

| Cmpd | 6-Config. | 6-*N* R | μKi (nM) +/- SEM | δKi (nM) +/- SEM | κKi (nM) +/- SEM | Ratio δ/μ | Ratio κ/μ | Comparison of Agonist Percent Stimulation to DAMGO |
|---|---|---|---|---|---|---|---|---|
| Naltrexone | | | 0.260 +/- 0.017 | 117.058 +/- 8.945 | 5.150 +/- 0.264 | 450 | 8 | |
| **25** | α | 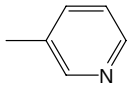 | 0.16 +/- 0.08 | 450 +/- 92.6 | 85.2 +/- 24.8 | 2728 | 517 | 44.82 +/- 4.50 |
| **26** | β | | 0.15 +/- 0.04 | 3667 +/- 34.8 | 5.98 +/- 1.30 | 24779 | 40 | 29.11 +/- 5.00 |
| **27** | α | 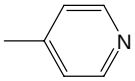 | 0.59 +/- 0.11 | 2060 +/- 354 | 21.6 +/- 10.0 | 3515 | 37 | 37.32 +/- 4.87 |
| **28** | β | | 0.41 +/- 0.08 | 3063 +/- 87.7 | 59.5 +/- 8.31 | 7398 | 144 | 22.72 +/- 0.84 |
| **29** | α | 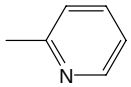 | 2.79 +/- 0.44 | 678 +/- 168 | 234 +/- 12.6 | 243 | 84 | 37.79 +/- 2.68 |
| **30** | β | | 6.46 +/- 1.56 | 2375 +/- 232 | 307 +/- 74.8 | 367 | 47 | 41.09 +/- 4.32 |
| **31 (Control)** | α | 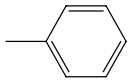 | 0.13 +/- 0.04 | 443 +/- 56.4 | 46.0 +/- 6.68 | 3464 | 359 | 41.24 +/- 7.48 |
| **32 (Control)** | β | | 1.02 +/- 0.34 | 820 +/- 57.6 | 8.75 +/- 1.72 | 801 | 8 | 67.29 +/- 3.96 |

The Ki values for the mu- and kappa-opioid receptor are n=3 and the Ki value for the delta-opioid receptor is n=2. The averages are reported along with their standard error of the means (SEM) for each compound. The comparison to percent stimulation of DAMGO is the Emax of the compound compared to the Emax of DAMGO using a [$^{35}$S]GTPγS functional assay. Note the abbreviations are Cmpd – compound; R – substituent; SEM - standard error of the mean; Config – configuration.

Another type of [$^{35}$S]GTPγS functional assay was conducted to determine if these compounds are antagonists and the amount of antagonism they produce. Therefore, an assay was conducted to generate a dose-response curve of DAMGO, a mu-opioid receptor agonist, with and without the naltrexamine derivatives. An antagonist is supposed to produce a right shift in the curve and the shift in the curve is measured to demonstrate the relative antagonist activity of the compound.

To further characterize compound **26**, a functional assay was conducted to determine whether or not it displays antagonistic effects on the interaction of DAMGO with the mu-opioid receptor. Compound **26** produces a right shift in the stimulation curve produced by DAMGO activation of the receptor (**Figure 27**). The $EC_{50}$ and Emax for DAMGO alone is 68.3 nM and 424.66% stimulation, respectively. The addition of 7.5 nM of compound **26**, about 30-times the $IC_{50}$ (0.26 nM) of compound **26,** alters the $EC_{50}$ and Emax for DAMGO to 118.0 nM and 408.48% stimulation, respectively. There is a 2-fold increase in the $EC_{50}$ and a slight almost negligible decrease in the stimulation of [$^{35}$S]GTPγS. The dissociation constant, or Ke, for compound **26** is 16.089 +/- 8.640 nM. The reported dissociation constant or Ke for naltrexone is 0.33 nM.[113] In order to make a better comparison with naltrexone, a $pA_2$ value needs to be determined using a Schild regression analysis with varying concentrations of antagonist. The $pA_2$ value for naltrexone is reported to be about 8.9 when given intravenously to rats given DAMGO.[114]

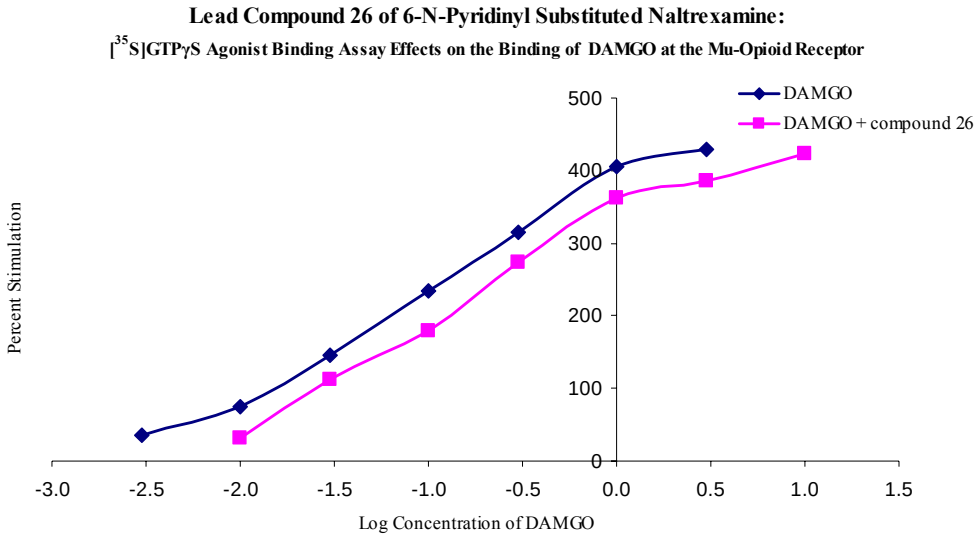


**Figure 27.** Stimulation of [$^{35}$S]GTPγS by DAMGO and the effects of **26** on the stimulation produced by DAMGO at the mu-opioid receptor. The concentration of **26** used in this assay is 7.5 nM. The averages of the data was produced from an n=2.

## 6.2 6-*N*-quinolinyl and 6-*N*-isoquinolinyl Substituted Naltrexamine Derivatives

The second set of compounds, 6-*N*-quinolinyl and 6-*N*-isoquinolinyl substituted naltrexamine derivatives, subnanomolar to nanomolar affinity to the mu-opioid receptors (**Table 15**). Stereochemical arrangements did not seem to be a major factor in the determination of affinity and selectivity of these compounds for the mu-opioid receptor. The control compound **42**, displays no selectivity between all three opioid receptors, while control compound **41** shows some selectivity to the mu-opioid receptor compared to the delta- and kappa-opioid receptor. However, it also displays lower affinity to the mu-opioid receptor compared to naltrexone and the other heterocyclic compounds in this

series. The control compounds display a decrease in affinity to the mu-opioid receptor and may suggest that the nitrogen in the substitution may play an important role in the binding of these naltrexone derivatives.

**Table 15.** Binding assay results for the 6-*N*-quinolinyl and 6-*N*-isoquinoline substituted naltrexamine derivatives.

| Cmpd | Config. | 6-*N* R | μKi (nM) +/- SEM | δKi (nM) +/- SEM | κKi (nM) +/- SEM | Ratio δ/μ | Ratio κ/μ | Comparison of Agonist Percent Stimulation to DAMGO |
|---|---|---|---|---|---|---|---|---|
| Naltrexone | | | 0.260 +/- 0.017 | 117.058 +/- 8.945 | 5.150 +/- 0.264 | 450 | 8 | |
| **33** | α | 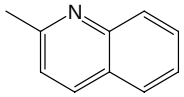 | 0.23 +/- 0.12 | 2161+/- 125 | 10.6 +/- 1.03 | 9398 | 46 | 40.9 +/- 7.20 |
| **34** | β | | 0.10 +/- 0.03 | 186 +/- 2.58 | 5.14 +/- 1.33 | 1775 | 49 | 65.4 +/- 6.13 |
| **35** | α | 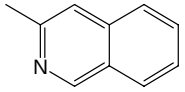 | 0.56 +/- 0.15 | 1108 +/- 103 | 26.9 +/- 5.32 | 1997 | 49 | 15.8 +/- 2.53 |
| **36** | β | | 0.11 +/- 0.04 | 578 +/- 5.28 | 1.75 +/- 0.76 | 5349 | 16 | 33.0 +/- 2.46 |
| **37** | α | 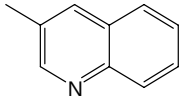 | 0.13 +/- 0.03 | 360 +/- 11.3 | 2.00 +/- 0.12 | 2791 | 15 | 44.8 +/- 3.96 |
| **38** | β | | 0.08 +/- 0.02 | 125 +/- 32.3 | 0.62 +/- 0.22 | 1527 | 8 | 53.4 +/- 8.74 |
| **39** | α | 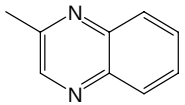 | 0.71 +/- 0.27 | 338 +/- 54.2 | 6.84 +/- 2.62 | 473 | 10 | 75.7 +/- 17.8 |
| **40** | β | | 0.14 +/- 0.04 | 352.8 +/- 10.6 | 1.29 +/- 0.23 | 2613 | 10 | 53.0 +/- 6.75 |
| **41 (Control)** | α | 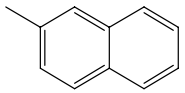 | 8.78 +/- 1.80 | 861 +/- 168 | 641 +/- 166 | 98 | 73 | 72.8 +/- 6.07 |
| **42 (Control)** | β | | 57.4 +/- 0.26 | 30.2 +/- 4.80 | 67.3 +/- 17.8 | 0.52 | 1 | 11.9 +/- 0.69 |

The Ki values for the mu- and kappa-opioid receptor are n=3 and the Ki value for delta-opioid receptor is n=2. The averages are reported along with their standard error of the means (SEM) for each compound. The comparison to percent stimulation of DAMGO is the Emax of the compound compared to the Emax of DAMGO using a [$^{35}$S]GTPγS functional assay. Note the abbreviations are Cmpd – compound; R – substituent; SEM - standard error of the mean; Config - configuration.

From the second series of compounds, compound **35** is determined to be a lead compound to undergo further optimization. Compound **35** has comparable affinity with naltrexone to the mu-opioid receptor. However, this compound displays higher selectivity for the mu-opioid receptor over the delta- and kappa-opioid receptors not seen with naltrexone (**Figure 28**). Compared to the control compounds **41** and **42**, compound **35** displays both higher selectivity and affinity to the mu-opioid receptor suggesting that the nitrogen may play an important role in its binding to the mu-opioid receptor. Also, the GTPγS functional assay was conducted and the Emax value of compound **35** was compared with the Emax of DAMGO. From these results, it seems that compound **35** acts as a partial opioid antagonist to the mu-opioid receptor compared with DAMGO. However, the control compound **42** also seems to act as a partial antagonist for the mu-opioid receptor.

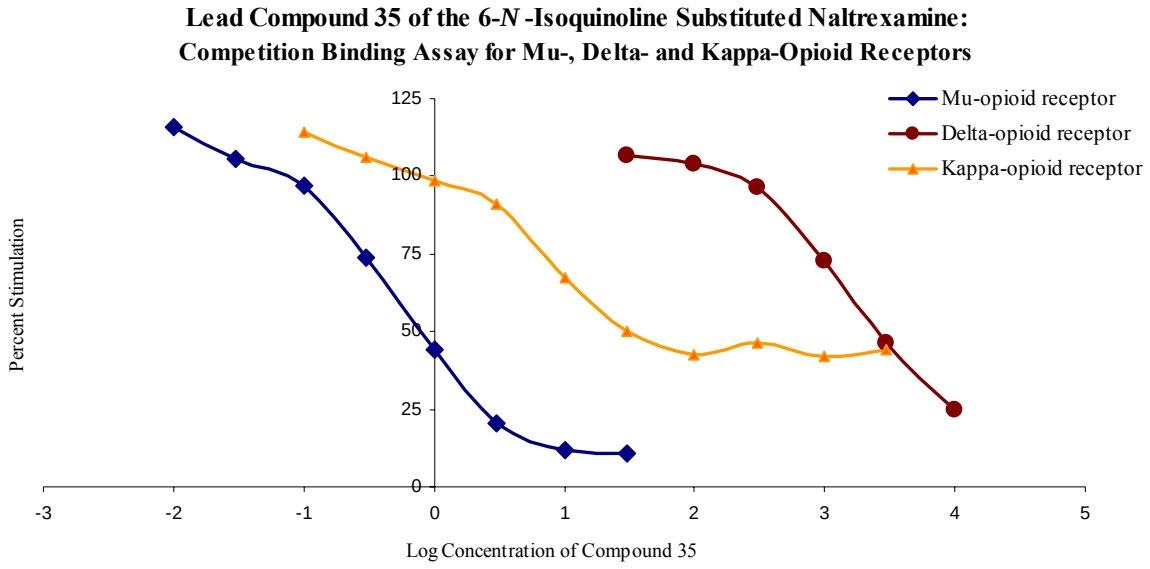


**Figure 28.** Competition binding curve for lead compound **35** for the mu-, delta-, and kappa-opioid receptors.

To further characterize compound **35**, a functional assay was conducted to determine whether or not it displays antagonistic effects on the interaction of DAMGO with the mu-opioid receptor. Stimulation of [$^{35}$S]GTPγS through binding of an agonist produces a sigmoidal concentration effect curve. Compound **35** produced a right shift in the stimulation of mu-opioid receptor by DAMGO (**Figure 29**). The $EC_{50}$ and Emax for DAMGO alone are 57.1 nM and 243.83% stimulation, respectively. The addition of 20.0 nM of naltrexamine derivative **35**, about 20-times the $IC_{50}$ (1.00 nM), altered the $EC_{50}$ and Emax for DAMGO to 73.5 nM and 221.45% stimulation, respectively. A 1.2-fold increase was seen in the $EC_{50}$ and a slight almost negligible decrease in the stimulation of [$^{35}$S]GTPγS. The dissociation constant, or Ke, for compound **35** is 74.204 +/- 5.260 nM and only a 1.2-fold shift increase was observed with a 20.0 nM concentration of compound **35**. A Schild regression analysis needs to be conducted where concentration-effect curves are constructed in the presence of increasing concentrations of antagonist in order to determine the apparent affinity, $pA_2$, for compound **35**.

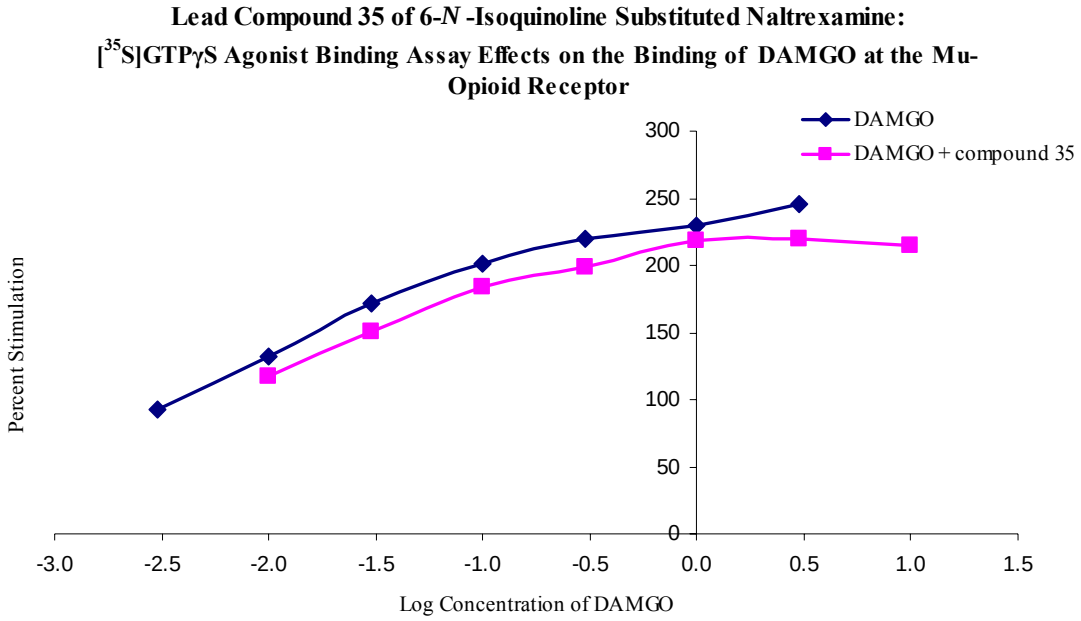


**Figure 29.** Stimulation of [$^{35}$S]GTPγS by DAMGO and the effects of **35** on the stimulation produced by DAMGO at the mu-opioid receptor. The concentration of **35** used in this assay is 20.0 nM. The averages of the data was produced from an n=2.

## 6.3 Comparison of the Lead Compounds 26 and 35

From the 6-*N*-heterocyclic substituted naltrexamine derivatives, two lead compounds were identified: **26** and **35**. In order to further characterize the antagonistic profile of these two compounds, a Schild regression analysis needs to be conducted with varying concentrations of the compounds in order to determine and compare their apparent affinities, $pA_2$ values. The two different configurations, α and β, shows no difference in their affinities towards the mu-opioid receptors. This may be explained by their three-dimensional structure between the α-configuration (**33**) and β-configuration (**34**) of the 6-*N*-heterocyclic substituted naltrexamine derivatives (**Figure 30**). The lead compounds can be further optimized by the addition of a third phenyl ring to compound

**35** in order to see if the increase in bulk is tolerated at this position. Compounds **39** and **40** have two nitrogen atoms in the quinoline ring and demonstrate partial agonist activity around 52.95% and 75.69% for the α and β configurations, respectively. Therefore, the addition of the second nitrogen atom showed no enhancement of affinity or antagonism.

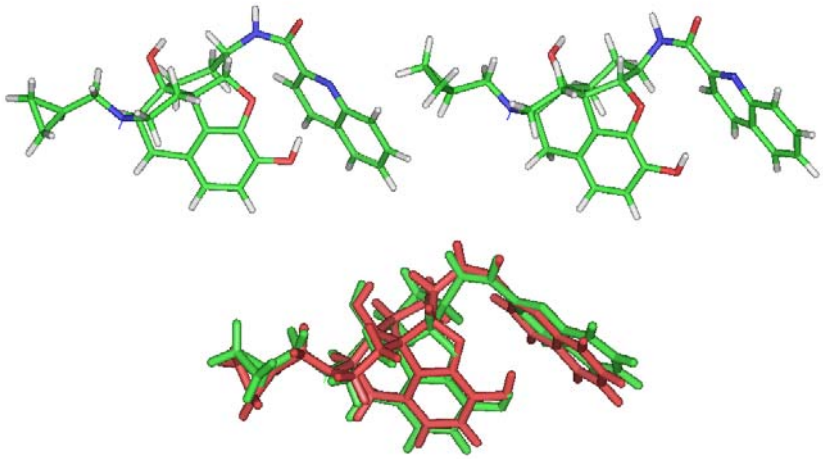

**Figure 30.** Overlay of the three-dimensional configurations of compounds **33** (left) and **34** (right).

# V. Conclusions

Currently there are many opioid agonists available for clinical use as analgesics that act in the centeral nervous system through the opioid receptors. There are three main opioid receptors, including the mu-, delta-, and kappa-opioid receptors. However, many of these agonists have been associated with notorious side effects including respiratory depression, tolerance and dependence. Morphine is the most commonly used opioid agonist in the treatment of chronic and post-operation pain. However, morphine is highly addictive both physically and psychologically.[2] It has been shown that the analgesic and adverse effects of morphine are due to its interactions with the mu-opioid receptor. Therefore, the characterization of the mu-opioid receptor is essential for understanding the addictive and analgesic actions of morphine.

The addiction and dependency of these opioid receptor agonists can be treated through detoxification or drug replacement therapy, including the application of opioid antagonists. Opioid antagonists also play important roles in the pharmacological study of opioid receptors. Due to the role of the mu-opioid receptor in analgesia and drug addiction, a highly selective mu-opioid receptor antagonist will be useful as a pharmacological tool in the study of the structure-activity relationships of mu-opioid receptors.

Naltrexone is a non-peptide mu-opioid receptor antagonist. It also is a long-acting and reversible opioid ligand in the treatment of opioid dependence and many other addictions. Although naltrexone has the ability to promote abstinence and prevent relapse, it also has many side effects due to its low selectivity to the opioid receptors.[6,9] On the other hand, CTAP and CTOP, two representative mu-opioid receptor selective peptidyl antagonists, are available but may undergo metabolic inactivation faster than the non-peptidyl opioid antagonists. Therefore, the development of selective non-peptidyl mu-opioid receptor antagonists is necessary to help alleviate any adverse effects seen by opioid antagonists with low selectivity.

Besides the antagonists being selective for the mu-opioid receptor, these compounds also need to be reversible. Irreversible antagonists will bind covalently to the receptor and inactivate the receptor indefinetly. Reversible antagonists would be preferred since they temporarily "knock-out" the receptors during pharmacological studies and can be washed out from the binding locus to revive the receptors.

This project involved the design of reversible and selective non-peptidyl mu-opioid receptor antagonists. Since naltrexone has high affinity to the mu-opioid receptor, it is an ideal template for the development of these antagonists. The molecular design of these antagonists was based on the identification of important pharmacophore elements found in several known opioid agonists and antagonists. By applying the "message-address" concept and comparative conformational studies, the major pharmacophore elements were identified in previous studies. From this study it was suggested that agonists and antagonists may share a similar "address" component that confers their

selectivity to the mu-opioid receptor while the "message" component is different due to opposite signal transductions.

Site-directed mutagenisis and molecular modeling studies have shown that certain amino acid residues are critical for ligand selectivity. Amino acid residues that comprise an aromatic binding pocket include Tyr210, Phe313, and Trp318 located in extracellular loops (EL) 2 and 3 are not conserved in the delta- and kappa-opioid receptors. Therefore, similar aromatic binding pockets may not exisit in the delta- and kappa-opioid receptors. More importantaly, Trp318 is a significant contributor to the selectivity of the mu-opioid receptor agonists and antagonists.[88]

Based on previous studies conducted in Dr. Zhang's laboratory, it was determined that a mu-opioid receptor antagonist with an aromatic structural feature may interact with EL3 and lead to higher selectivity to the mu-opioid receptor. Therefore, the specific hypothesis for this study was that a mu-opioid receptor antagonist with an aromatic structural feature may interact with EL3 and lead to higher selectivity to the mu-opioid receptor. A series of new ligands that satisfy the requirements of the mu-opioid receptor binding pocket were designed and synthesized to test their affinity towards the mu-, delta- and kappa-opioid receptors.

Two novel series of selective non-peptidyl mu-opioid receptor antagonists were developed. The first series are 14-*O*-heterocylic substituted naltrexone derivatives that were designed by the addition of hetero-aromatic moieties including pyridine, quinoline and isoquinoline moieties attached to the 14-position of naltrexone through an ester linkage. The addition of the hetero-aromatic to the 14-position of naltrexone may

provide essential hydrogen bonding to interact with Trp318 in the aromatic binding pocket in the mu-opioid receptor and confer higher selectivity to the mu-opioid receptor.

The second series of selective non-peptidyl mu-opioid receptor antagonists were 6-*N*-heterocylic substituted naltrexamines. These antagonists contain a heterocyclic moiety including pyridine, quinoline, and isoquinoline linked at the 6-position of naltrexamine through an amide bond. The aromatic character of the heterocylic moiety may help provide hydrogen bonding interaction with the aromatic binding pocket in the mu-opioid receptor. Also the α and β stereochemical arrangements were tested to determine if they play a role in selectivity to the mu-opioid receptor.

Finally, for both series of compounds, phenyl and napthalenyl compounds were used as controls to test the hypothesis that the addition of heterocyclic moieties to naltrexone and naltrexamine's backbone will provide hydrogen bonding with Trp318 in EL3 of the binding pocket of the mu-opioid receptor. Chemical synthesis of the 14-*O*-heterocylic substituted naltrexone derivatives was conducted in a "one-pot" reaction condition by the direct coupling of the heterocyclic moiety to the 3- and 14-positions of naltrecxone. This is followed by the selective removal of the heterocylic moiety at the 3-position of naltrexone. Finally these compounds were converted into dihydrochloride salts except for compound **21**. Although most compounds were synthesized easily in the above manner, some difficulty was encountered in the synthesis of compounds **17**, **20** and **24**.

Following chemical synthesis of the selective non-peptidyl mu-opioid receptor antagonist, biological evaluation was conducted to determine the affinity and selectivity

of these compounds for the mu-, delta-, and kappa-opioid receptors. Besides the test of their affinities, these compounds were also characterized for their potential agonist activity using a functional [$^{35}$S]GTPγS assay.

For the first series of compounds, the 14-*O*-heterocylcic substituted naltrexone derivatives, all of these compounds, except for the controls, displayed higher selectivity for the mu-opioid receptor compared to the delta- and kappa-opioid receptors. Additionally, all of the compounds displayed an antagonist activity profile. Compounds **17** and **22** were identified as lead compounds with comparable affinity with naltrexone for the mu-opioid receptor but much higher selectivity for the mu-opioid receptor over the kappa- and delta-opioid receptors. Although compound **17** has similar affinity to the mu-opioid receptor compared to naltrexone but it has much higher selectivity to the mu-opioid receptor compared to naltrexone. Compound **22** also carries higher selectivity to the mu-opioid receptor compared to naltrexone though its binding affinity is about ten times lower than that of naltrexone.

The second series of compounds, 6-*N*-heterocylcic substituted naltrexamine derivatives, display similar affinity and selectivity compared to the 14-*O*-heterocylcic substituted naltrexone derivatives. Compounds **26** and **35** have been identified as a lead compound with a 10-fold decrease in affinity compared with naltrexone for the mu-opioid receptor but higher selectivity, about 40- and 49-fold respectively, for the mu-opioid receptor over the kappa-opioid receptors. DAMGO, a full mu-opioid receptor agonist, has been used to compare and determine agonistic characteristics of all of the compounds. All of the compounds are partial mu-opioid receptor agonists while the lead

compounds **26** and **35** have about 29.11% and 15.83% agonist activity compared to DAMGO, respectively.

For both series of compounds it is important to note that the controls which lacks an heterocyclic moiety to provide hydrogen bonding with EL3 for the mu-opioid receptor also showed much lower selectivity to the mu-opioid receptor. Therefore, it is clear that the nitrogen in the aromatic moieties is necessary for higher binding affinity to the mu-opioid receptor compared to the delta- and kappa-opioid receptors.

In order to get a better understanding of how these compounds are binding to the mu-opioid receptor, a homology modeling study of the mu-opioid receptor was conducted. The homology model of the mu-opioid receptor was built using the crystal structure of the dark state bovine rhodopsin as the template. Docking simulations of each ligand in the homology model of the mu-opioid receptor were then conducted and Gold scores were determined for each ligand. The Gold docking scores did not correlate very well with the affinities determined in the biological evaluation studies. The lead compound **22** displayed the highest Gold score of all of these derivatives. Lead compound **17** also displays a high Gold score. Naltrexone showed one of the lowest Gold docking scores compared to the designed compounds and may be due to the weaker interaction of naltrexone in the binding pocket.

In summary, from the first series of 14-*O*-heterocylcic substituted naltrexone derivatives, compounds **17** and **22** were determined to be the lead compounds using both competition binding assays for all three opioid receptors and functional assays to determine their agonist activity profile. Although compounds 14-*O*-heterocylcic

substituted naltrexone derivatives **17** and **22** display similar or lower affinity to the mu-opioid receptor compared to naltrexone, they both displayed much higher selectivity. From the second series of 6-*N*-heterocylic substituted naltrexamine derivatives, two lead compounds were identified, **26** and **38**. Both of these compounds have high selectivity and affinity to the mu-opioid receptor. Both of these compounds also display partial agonist activity a the mu-opioid receptor compared to DAMGO in the [$^{35}$S]GTPγS functional binding assay. Further optimization of these lead compounds may lead us to a potent and highly selective mu-opioid receptor antagonist with diminished agonist activity.

# VI. Experimental

## 1. Chemical Synthesis of 14-*O*-Heterocyclic Substituted Naltrexone Derivatives

Two synthetic routes are applied to synthesize the 14-*O*-heterocyclic substituted naltrexone derivatives. The first synthetic route is adapted when the starting material is an acyl chloride while the second is for the starting material as a carboxylic acid.[92,93] All compounds are characterized by $^{1}$H-NMR, $^{13}$C-NMR, MS and IR. Melting points are determined by Fischer Scientific melting point apparatus. The $^{1}$H-NMR (300 MHz) and $^{13}$C-NMR (75 MHz) spectra are obtained on a Varian Gemini spectrometer and tetramethylsilane is used as the internal standard. Mass spectrometer spectra are obtained using direct-infusion ESI-MS-MS. Samples are diluted 1:100 with methanol and introduced into a Quattro II triple quadruple mass spectrometer with an electrospray ion source (Micromass, Altrincham, England) at a flow rate of 10 mL/min using a Harvard Apparatus Syringe Pump model 11 (Holliston, MA). The samples are analyzed in negative ion mode with a capillary voltage of 2.3 kV, cone 30V, and extractor 5V. IR spectra are obtained using a Nicolet 5ZDX FT-IR spectrometer with potassium bromide as the background. Column chromatography is performed by using silica gel (grade 60 mesh; Bodman Industries, Ashton, PA). Routine thin-layer chromatography (TLC) is performed on silica gel GHIF plates (250 μ, 2.5 x 10 cm, Analtech Inc. Newark, DE). All

the compounds are converted to salts with 2.2 equivalents of 1.25 molar hydrogen chloride acid in methanol (Fluka).

### 1.1 Synthetic Route A: Acyl Chloride

One equivalent of naltrexone (NTX) is dissolved in 5 mL of DMF. Then 2.2 equivalents of the acyl chloride and 4.4 equivalents of TEA are added. The reaction mixture is heated at reflux for 4 h under $N_2$ atmosphere. The reaction mixture is then cooled down and TLC is conducted to monitor the reaction (40:1:0.01 $CH_2Cl_2$:MeOH:$NH_3H_2O$).

The reaction mixture is transferred to a large round bottom flask; 20 mL of 4% $H_2SO_4$ and 20 mL of MeOH are added to the mixture and stirred for 4 h at room temperature. TLC is taken again to monitor the reaction. The reaction mixture is neutralized by adding a dilute solution of ammonium hydroxide in a dropwise manner until it reached a pH of 7. The solvents are evaporated under reduced pressure and the residue is purified by column chromatography (50:1:0.04 $CH_2Cl_2$:MeOH:$NH_3H_2O$). The final compound is converted into a hydrochloride salt and stored in the freezer.

### 1.2 Synthetic Route B: Carboxylic Acids

In order to convert the carboxylic acid to an acyl chloride, the carboxylic acid is dried using a vacuum pump and toluene is dried overnight under 4Å molecular sieves. An excess amount of thionyl chloride ($SOCl_2$) is added to the carboxylic acid and then heated at reflux continuously under $N_2$ atmosphere for 3 h. The reaction mixture is then

immediately distilled under $N_2$ atmosphere by the addition and distillation of dried toluene three times to remove all of the excess $SOCl_2$.

One equivalent of pre-dried NTX is added to the reaction mixture containing the acyl chloride and dissolved in 5 mL of DMF. Then 4.4 equivalents of TEA is added to the reaction mixture. The reaction mixture is heated at reflux at for 4 h under $N_2$ atmosphere. The reaction mixture is then cooled down and TLC was conducted to monitor the reaction (40:1:0.1 $CH_2Cl_2$:MeOH:$NH_3H_2O$).

Next, the reaction mixture is transferred to a large round bottom flask. Then 20 mL of 4% $H_2SO_4$ and 20 mL of MeOH are added to the reaction mixture and stirred for 4 h at room temperature. TLC is taken again to monitor the reaction. The reaction mixture is neutralized by adding a dilute solution of ammonium hydroxide in a dropwise manner till it reached a pH of 7. The solvents are evaporated under reduced pressure and the residue is purified by column chromatography (50:1:0.04 $CH_2Cl_2$:MeOH:$NH_3H_2O$). The final compound is converted to a hydrochloride salt and stored in the freezer.

## 2. Final Compounds

### 17-Cyclopropylmethyl-4,5α-epoxy-3-hydroxy-14β-*O*-(pyridinyl-2'carboxy)morphinan-6-one (17)

Following procedure B, picolinic acid (492 mg, 4.0 mmol), $SOCl_2$ (5 mL), DMF (5 mL), naltrexone (341 mg, 1.0 mmol) and TEA (1.12 mL, 809 mg, 8.0 mmol), are applied. The reaction mixture is heated at reflux overnight under a nitrogen atmosphere. A black residue is obtained and purified by column chromatography (200:1:0.04 and 100:1:0.04

$CH_2Cl_2$:MeOH:$NH_3H_2O$) system and 225 mg (50.0% yield) of a red oil is isolated and converted to hydrochloride salt. $^1$H-NMR (300 MHz, $CDCl_3$) (free base) δ 0.58 (m, 4H), 1.12 (m, 1H), 1.91 (m, 2H), 2.47 (m, 2H), 2.72 (m, 2H), 3.09 (m, 2H), 3.15 (m, 2H), 3.21 (m, 2H), 3.36 (m, 1H), 3.50 (b, 1H, $D_2O$ exchangeable), 4.68 (m, 1H), 6.61 (d, J=8.1 Hz, 1H), 6.74 (d, J=8.1 Hz, 1H), 7.27 (m, 1H), 7.63 (m, 1H), 7.80 (m, 1H), 8.60 (m, 1H); $^1$H-NMR (300 MHz, $CD_3OD$) (dihydrochloride salt) δ 0.86 (m, 4H), 1.25 (m, 1H), 1.35 (m, 1H), 1.72 (b, 1H, $D_2O$ exchangeable), 2.10 (b, 1H, $D_2O$ exchangeable), 2.28 (m, 2H), 2.32 (m, 2H), 2.84 (m, 2H), 3.05 (m, 2H), 3.21 (m, 2H), 3.33 (m, 1H), 4.11 (m, 1H), 4.89 (b, 1H, $D_2O$ exchangeable), 6.67 (d, J=6.6 Hz, 1H), 6.75 (d, J=6.6 Hz, 1H), 8.18 (m, 1H), 8.23 (m, 1H), 8.70 (m, 1H), 8.96 (m, 1H); $^{13}$C-NMR (75 MHz, $CD_3OD$) (dihydrochloride salt) δ 1.56, 4.34, 4.97, 22.49, 26.90, 27.89, 29.30, 30.23, 34.17, 37.51, 52.99, 56.92, 61.69, 69.52, 88.54, 117.95, 119.98, 125.40, 127.39, 129.90, 138.89, 139.87, 142.36, 146.38, 161.31, 207.59; IR ($cm^{-1}$) 794.26, 1259.60, 1660.32, 3411.85; MS *m/z* (relative intensity, ion): 447.0 (100%, $(M+H)^+$).

**17-Cyclopropylmethyl-4,5*α*-epoxy-3-hydroxy-14β-*O*-(pyridinyl-4'carboxy)morphinan-6-one (18)**

Following procedure A, isonicotinyl chloride (534 mg, 3.0 mmol, 3 equivalents), naltrexone (341 mg, 1.0 mmol), DMF (5 mL), and TEA (0.84 mL, 607 mg, 6.0 mmol, 6 equivalents), are applied. Product is isolated by column chromatography (60:1:0.04 $CH_2Cl_2$:MeOH:$NH_3H_2O$) and 310 mg (69.0% yield) of a bright yellow powder is obtained and converted to hydrochloride salt. mp 190-195 °C; $^1$H-NMR (300 MHz,

$CDCl_3$) (free base) δ 0.58 (m, 4H), 0.89 (m, 1H), 1.66 (m, 2H), 1.93 (m, 2H), 2.18 (m, 2H), 2.46 (m, 2H), 2.74 (m, 2H), 3.03 (m, 2H), 3.95 (m, 1H), 4.73 (b, 1H, $D_2O$ exchangeable), 5.30 (m, 1H), 6.75 (d, J=8.1 Hz, 1H), 6.96 (d, J=8.1 Hz, 1H), 8.02 (m, 2H), 8.84 (m, 2H); $^1$H-NMR (300 MHz, $CD_3OD$) (dihydrochloride salt) δ 0.82 (m, 4H), 1.18 (m, 1H), 1.76 (b, 1H, $D_2O$ exchangeable), 2.13 (m, 2H), 2.32 (b, 1H, $D_2O$ exchangeable), 2.83 (m, 2H), 2.97 (m, 2H), 3.10 (m, 2H), 3.19 (m, 2H), 3.46 (m, 2H), 4.08 (m, 1H), 4.20 (m, 1H), 5.10 (b, 1H, $D_2O$ exchangeable), 7.05 (d, J=8.1 Hz, 1H), 7.27 (d, J=8.1 Hz, 1H), 8.74 (m, 2H), 9.18 (m, 2H); $^{13}$C-NMR (75 MHz, $CD_3OD$) (dihydrochloride salt) δ 2.46, 5.23, 5.80, 23.81, 27.71, 30.97, 34.68, 57.76, 62.11, 69.69, 70.16, 90.43, 120.88, 121.02, 123.80, 127.02, 127.53, 129.13, 129.71, 132.56, 143.50, 145.32, 147.69, 149.17, 160.13, 207.27; IR ($cm^{-1}$) 748.57, 1241.13, 1270.34, 1724.55, 1755.48, 3385.42; MS *m/z* (relative intensity, ion): 446.8 (100%, $(M+H)^+$).

**17-Cyclopropylmethyl-4,5α-epoxy-3-hydroxy-14β-*O*-(pyridinyl-3'carboxy)morphinan-6-one (19)**

Following procedure A, nicotinyl chloride (356 mg, 2.0 mmol), naltrexone (300 mg, 0.9 mmol), DMF (5 mL), and TEA (0.56 mL, 405 mg, 4.0 mmol), are applied. Product is isolated by column chromatography (50:1:0.04 $CH_2Cl_2$:MeOH:$NH_3H_2O$) and 105 mg (24.1% yield) of a white fluffy powder is obtained and converted to hydrochloride salt. mp 202°C (decomposed); $^1$H-NMR (300 MHz, $CD_3Cl$) (free base) δ 0.52 (m, 4H), 1.19 (m, 1H), 1.71 (m, 2H), 1.86 (m, 2H), 2.26 (m, 2H), 2.34 (m, 2H), 2.65 (m, 2H), 2.78 (m, 2H), 3.00 (m, 1H), 3.67 (b, 1H, $D_2O$ exchangeable), 4.67 (m, 1H), 6.65 (d, J=7.8 Hz,

1H), 6.75 (d, J=7.8 Hz, 1H), 7.52 (m, 1H), 8.45 (m,1H), 8.86 (m, 1H), 9.56 (s, 1H); $^{1}$H-NMR (300 MHz, $CD_3OD$) (dihydrochloride salt) δ 0.86 (m, 4H), 1.20 (m, 1H), 1.31 (m, 2H), 1.74 (b, 1H, $D_2O$ exchangeable), 2.03 (b, 1H, $D_2O$ exchangeable), 2.13 (m, 2H), 2.86 (m, 2H), 3.15 (m, 2H),3.33 (m, 2H), 3.41 (m, 2H), 3.59 (m, 1H), 4.08 (m, 1H), 5.39 (d, J=5.4 Hz, 1H), 5.63 (d, J=5.4 Hz, 1H), 6.75 (b, 1H, $D_2O$ exchangeable), 8.28 (m, 1H), 9.14 (m, 1H), 9.28 (m, 1H), 9.63 (s, 1H); $^{13}$C-NMR (75 MHz, $CD_3OD$) (free base) δ 3.30, 3.46, 9.00, 22.87, 26.56, 30.30, 35.29, 43.47, 50.85, 55.33, 58.86, 89.35, 93.97, 118.21, 119.76, 123.37, 123.75, 127.42, 137.42, 137.56, 139.31, 143.14, 149.96, 152.17, 163.37, 207.43; IR ($cm^{-1}$) 737.60, 1108.04, 1282.53, 1716.37, 2946.50; MS *m/z* (relative intensity, ion): 447.0 (100%, $(M+H)^+$).

**17-Cyclopropylmethyl-4,5α-epoxy-3-hydroxy-14β-*O*-(benzoylcarboxy)morphinan-6-one (20)**

Following procedure A, benzoyl chloride (281 mg, 2.0 mmol), naltrexone (300 mg, 0.9 mmol), DMF (5 mL), and TEA (0.56 mL, 405 mg, 4.0 mmol), are applied. The next step involving dilute $H_2SO_4$ and MeOH is unable to remove the benzyl group at the 3-position. The reaction mixture is concentrated and stored in freezer overnight. In order to remove the benzyl group at the 3-position, the 200 mg of the di-substituted product is dissolved in 20 mL of THF and 5 mL of a saturated $K_2CO_3$ aqueous solution that is diluted by half. The mixture is stirred overnight at room temperature. Next, the mixture is separated into a THF layer and water layer. The water layer is extracted with 40 mL of $CH_2Cl_2$ (3 times) and the combined organic layers are dried and concentrated. The

product is isolated and purified by column chromatography (200:1:0.04 and 100:1:0.04 $CH_2Cl_2$:MeOH:$NH_3H_2O$). About 40 mg (10.2% yield) of a light yellow powder is obtained and converted to hydrochloride salt. mp 161-165°C; $^1$H-NMR (300 MHz, $CDCl_3$) (free base) δ 0.60 (m, 4H), 1.25 (m, 1H), 1.88 (m, 2H), 2.18 (m, 2H), 2.42 (m, 2H), 2.62 (m, 2H), 2.68 (m, 2H), 2.98 (m, 2H), 3.05 (m, 1H), 3.27 (m, 1H), 4.72 (b, 1H, $D_2O$ exchangeable), 6.73 (d, J=8.1 Hz, 1H), 6.96 (d, J=8.1 Hz, 1H), 7.49 (m, 2H), 7.62 (m, 1H), 8.21 (m, 2H); $^1$H-NMR (300 MHz, $CD_3OD$) (monohydrochloride salt) δ 0.90 (m, 4H), 1.30 (m, 1H), 1.79 (b, 1H, $D_2O$ exchangeable), 1.95 (m, 2H), 2.10 (m, 2H), 2.47 (m, 2H), 2.74 (m, 2H), 2.84 (m, 2H), 2.90 (m, 2H), 3.01 (m, 1H), 3.33 (m, 1H), 4.88 (b, 1H, $D_2O$ exchangeable), 7.00 (d, J=9.1 Hz, 1H), 7.14 (d, J=9.1 Hz, 1H), 7.61 (m, 2H), 7.73 (m, 1H), 8.21 (m, 2H); $^{13}$C-NMR (75 MHz, $CD_3OD$) (monohydrochloride salt) δ 1.56, 4.34, 4.91, 22.87, 26.89, 30.03, 33.76, 56.98, 58.09, 61.64, 62.11, 69.12, 69.35, 89.12, 93.10, 96.46, 119.74, 122.50, 123.44, 129.31, 129.39, 132.18, 132.66, 133.52, 147.54, 163.72, 205.92; IR ($cm^{-1}$) 709.97, 1055.29, 1238.92, 1729.47, 3398.92; MS *m/z* (relative intensity, ion): 447.0 (100%, $(M+H)^+$).

**17-Cyclopropylmethyl-4,5α-epoxy-3-hydroxy-14β-*O*-(isoquinolinyl-3'-carboxy)morphinan-6-one (21)**

Following procedure B, 3-isoquinoline carboxylic acid (381 mg, 2.2 mmol), $SOCl_2$ (5 mL), naltrexone (341 mg, 1.0 mmol), DMF (5 mL), and TEA (0.61 mL, 445 mg, 4.4 mmol) is applied. Product is isolated by column chromatography (200:1:0.04 $CH_2Cl_2$:MeOH:$NH_3H_2O$) and 117 mg (23.6% yield) of a dark yellow powder is isolated

and converted to hydrochloride salt. mp 201-204°C; $^{1}$H-NMR (300 MHz, $CDCl_3$) (free base) δ 0.38 (m, 4H), 1.18 (m, 1H), 1.27 (m, 2H), 1.70 (m, 2H), 2.98 (m, 2H), 3.02 (m, 2H), 3.06 (m, 2H), 3.19 (m, 2H), 3.28 (m, 1H), 3.66 (b, 1H, $D_2O$ exchangeable), 4.74 (m, 1H), 6.78 (d, J=8.1 Hz, 1H), 7.07 (d, J=8.1 Hz, 1H), 7.89 (m, 3H), 8.06 (m, 1H), 8.46 (s, 1H), 8.73 (s, 1H); $^{1}$H-NMR (300 MHz, $CD_3OD$) (monohydrochloride salt) δ 0.84 (m, 4H), 1.15 (m, 1H), 1.30 (m, 2H), 1.73 (m, 2H), 2.04 (m, 2H), 2.33 (b, 1H, $D_2O$ exchangeable), 2.78 (m, 2H), 3.33 (m, 2H), 3.46 (m, 2H), 3.59 (m, 1H), 3.64 (b, 1H, $D_2O$ exchangeable), 4.03 (m, 1H), 7.01 (d, J=8.1 Hz, 1H), 7.21 (d, J=8.1 Hz, 1H), 8.01 (m, 3H), 8.25 (m, 1H), 8.50 (s, 1H), 8.87 (s, 1H); $^{13}$C-NMR (75 MHz, $CD_3OD$) (free base) δ 3.45, 3.62, 8.97, 22.61, 30.38, 30.79, 43.05, 50.25, 53.68, 58.79, 61.48, 69.63, 90.27, 119.05, 122.62, 125.01, 126.34, 128.16, 128.34, 129.20, 129.85, 130.19, 130.75, 131.66, 132.23, 136.64, 138.94, 147.36, 161.70, 207.23; IR ($cm^{-1}$) 781.33, 1182.05, 1724.96, 2920.65, 3392.46; MS *m/z* (relative intensity, ion): 497.4 (100%, $(M+H)^{+}$).

**17-Cyclopropylmethyl-4,5α-epoxy-3-hydroxy-14β-*O*-(quinolinyl-2'-carboxy)morphinan-6-one (22)**

Following the above procedure A, quinaldyl chloride (383 mg, 2.0 mmol), naltrexone (300 mg, 0.9 mmol), DMF (5 mL), and TEA (0.56 mL, 405 mg, 4.0 mmol), is applied. Product is isolated by column chromatography (50:1:0.04 $CH_2Cl_2$:MeOH:$NH_3H_2O$) and 76 mg (17.4% yield) of a white powder is obtained and converted to hydrochloride salt. mp 85-88°C; $^{1}$H-NMR (300 MHz, $CDCl_3$) (free base) δ 0.18 (m, 4H), 0.59 (m, 1H), 1.29 (m, 2H), 1.66 (m, 2H), 1.94 (m, 2H), 2.36 (m, 2H), 2.76 (m, 2H), 3.10 (m, 2H), 3.24 (m,

1H), 3.68 (b, 1H, $D_2O$ exchangeable), 4.73 (m, 1H), 6.61 (d, J=4.8 Hz, 1H), 6.62 (d, J=4.8 Hz, 1H), 6.76 (m, 1H), 6.79 (m, 1H), 7.29 (m, 1H), 7.52 (d, J=8.1 Hz, 1H), 7.61 (d, J=8.1 Hz, 1H), 7.86 (m, 1H); $^1$H-NMR (300 MHz, $CD_3OD$) (dihydrochloride salt) δ 0.82 (m, 4H), 1.28 (m, 1H), 1.71 (m, 2H), 1.94 (b, 1H, $D_2O$ exchangeable), 2.31 (b, 1H, $D_2O$ exchangeable), 2.92 (m, 2H), 3.07 (m, 2H), 3.24 (m, 2H), 3.43 (m, 2H), 3.56 (m, 2H), 4.07 (m, 1H), 4.20 (m, 1H), 5.08 (b, 1H, $D_2O$ exchangeable), 7.00 (d, J=8.1 Hz, 1H), 7.26 (d, J=8.1 Hz, 1H), 7.92 (m, 1H), 8.08 (m, 1H), 8.24 (m, 1H), 8.38 (d, J=8.4 Hz, 1H), 8.50 (d, J=8.4 Hz, 1H), 8.99 (m, 1H); $^{13}$C-NMR (75 MHz, $CD_3OD$) (free base) δ 3.39, 3.62, 8.96, 22.20, 30.18, 30.94, 35.79, 43.20, 50.60, 58.76, 61.56, 69.90, 90.06, 115.70, 117.66, 119.50, 121.09, 122.34, 123.52, 127.38, 128.51, 130.28, 131.41, 133.72, 138.64, 140.65, 143.11, 143.76, 163.00, 209.92; IR ($cm^{-1}$) 729.62, 1240.22, 1453.50, 1660.32, 1731.42, 3179.17; MS *m/z* (relative intensity, ion): 497.1 (100%, $(M+H)^+$).

**17-Cyclopropylmethyl-4,5α-epoxy-3-hydroxy-14β-*O*-(quinolinyl-3'-carboxy)morphinan-6-one (23)**

Following procedure B, 3-quinoline carboxylic acid (366 mg, 1.9 mmol), $SOCl_2$ (5 mL), naltrexone (307 mg, 0.9 mmol), DMF (5 mL), and TEA (0.51 mL, 364.3 mg, 3.5 mmol), is applied. Product is isolated by column chromatography (60:1:0.04 $CH_2Cl_2$:MeOH:$NH_3H_2O$) and 104 mg (21.7% yield) of a light yellow powder is obtained and converted to hydrochloride salt. mp 187°C (decomposed); $^1$H-NMR (300 MHz, $CDCl_3$) (free base) δ 0.38 (m, 4H), 0.93 (m, 1H), 1.80 (m, 2H), 2.05 (m, 2H), 2.28 (m, 2H), 2.40 (m, 2H), 2.70 (m, 2H), 3.08 (m, 2H), 3.15 (m, 1H), 3.28 (b, 1H, $D_2O$

exchangeable), 4.74 (m, 1H), 6.83 (d, J=8.1 Hz, 1H), 7.07 (d, J=8.1 Hz, 1H), 7.67 (m, 1H), 7.83 (m, 1H), 7.92 (m, 1H), 8.15 m, 1H), 9.07 (s, 1H), 9.61 (s, 1H); $^{1}$H-NMR (300 MHz, CDOH) (dihydrochloride salt) δ 0.86 (m, 4H), 1.20 (m, 1H), 1.86 (b, 1H, $D_2O$ exchangeable), 2.00 (b, 1H, $D_2O$ exchangeable), 2.12 (m, 2H), 2.25 (m, 2H), 2.75 (m, 2H), 3.02 (m, 2H), 3.15 (m, 2H), 3.33 (m, 2H), 3.49 (m, 1H), 4.25 (m, 1H), 7.08 (d, J=8.1 Hz, 1H), 4.95 (b, 1H, $D_2O$ exchangeable), 7.27 (d, J=8.1 Hz, 1H), 7.93 (m, 1H), 8.32 (m, 3H), 9.58 (s, 1H), 9.64 (s, 1H); $^{13}$C-NMR (75 MHz, $CD_3OD$) (dihydrochloride salt) δ 1.63, 4.42, 4.97, 13.57, 22.96, 26.93, 30.16, 33.87, 56.97, 61.44, 64.98, 69.37, 89.52, 120.07, 122.14, 123.29, 123.67, 127.06, 128.19, 128.44, 129.02, 129.70, 132.07, 134.83, 143.32, 144.14, 146.82, 147.10, 160.69, 206.38; IR ($cm^{-1}$) 761.94, 1188.51, 1724.96, 3386.00; MS *m/z* (relative intensity, ion): 497.1 (100%, $(M+H)^+$).

**17-Cyclopropylmethyl-4,5α-epoxy-3-hydroxy-14β-*O*-(napthalenyl-2'-carboxy)morphinan-6-one (24)**

Following procedure A, 2-napthoyl chloride (419.3 mg, 2.2 mmol), naltrexone (341 mg, 1.0 mmol), DMF (5 mL), and TEA (0.56 mL, 405 mg, 4.4 mmol), is applied. The next step involving dilute $H_2SO_4$ and MeOH is unable to remove the naptholene group at the 3-position. The reaction mixture is concentrated and stored in freezer overnight. About 387 mg of di-substituted product is obtained. So in order to remove the naptholene moiety at the 3-position, 200 mg of the di-substituted product is dissolved in 20 mL of THF and 5 mL of a saturated $K_2CO_3$ aqueous solution that is diluted by half. The mixture is stirred overnight at room temperature. Next the mixture is separated into a

THF layer and water layer. The water layer is extracted with 40 mL of $CH_2Cl_2$ (3 times) and the combined organic layers are dried and concentrated. The product is isolated by column chromatography (200:1:0.04 and 100:1:0.04 $CH_2Cl_2$:MeOH:$NH_3H_2O$). About 35 mg (7.1% yield) of a light brown powder was isolated and converted to hydrochloride salt. mp 137-140°C; $^1$H-NMR (300 MHz, $CDCl_3$) (free base) δ 0.40 (m, 4H), 1.25 (m, 1H), 1.93 (m, 2H), 2.75 (m, 2H), 3.04 (m, 2H), 3.38 (m, 2H), 3.45 (m, 2H), 3.70 (m, 2H), 3.88 (m, 1H), 4.04 (m, 1H), 5.09 (b, 1H, $D_2O$ exchangeable), 6.76 (d, J=8.1 Hz, 1H), 7.01 (d, J=8.1 Hz, 1H), 7.60 (m, 2H), 7.90 (m, 2H), 7.99 (m, 1H), 8.20 (m, 1H), 8.81 (s, 1H); $^1$H-NMR (300 MHz, $CD_3OD$) (monohydrochloride salt) δ 0.91 (m, 4H), 1.20 (m, 1H), 1.34 (m, 2H), 1.86 (b, 1H, $D_2O$ exchangeable), 2.16 (m, 2H), 2.53 (m, 2H), 3.53 (m, 2H), 3.89 (m, 2H), 4.07 (m, 2H), 4.19 (m, 1H), 4.39 (m, 1H), 4.77 (b, 1H, $D_2O$ exchangeable), 7.02 (d, J=8.1 Hz, 1H), 7.21 (d, J=8.1 Hz, 1H), 7.70 (m, 2H), 8.10 (m, 4H), 8.97 (s, 1H); $^{13}$C-NMR (75 MHz, $CD_3OD$) (monohydrochloride salt) δ 1.50, 4.39, 4.92, 22.86, 26.90, 33.79, 56.96, 61.65, 69.37, 76.69, 89.18, 93.17, 96.52, 119.17, 119.80, 122.32, 123.53, 124.37, 126.62, 127.04, 127.36, 127.72, 128.15, 128.70, 131.25, 121.53, 132.02, 132.78, 135.49, 164.81, 206.04; IR ($cm^{-1}$) 775.87, 1055.98, 1188.70, 1731.54, 3386.00; MS *m/z* (relative intensity, ion): 496.0 (100%, $(M+H)^+$).

## 3. Pharmacological Studies

### 3.1 Cell Culture

Cells expression the mu-, delta-, and kappa-opioid receptors are grown and harvested in order to test the affinities of the naltrexone derivatives. Chinese hamster ovary (CHO) cells that over expressed the mu-opioid receptor (Dr. Dana Selley's laboratories at VCU) and kappa-opioid receptor (Dr. Ping Law at University of Minnesota) are grown. For the delta-opioid receptor, four different cell lines that over expressed the delta-opioid receptor are utilized for testing the naltrexone derivatives. The first set of cell lines tested consisted of two CHO cell lines (Dr. Ping Law from the University of Minnesota and Dr. Liu-Chen at Temple University) and human embryonic kidney 293 (HEK) cells (Dr. Ping Law from the University of Minnesota). The final cell line used is the NG108-15 neurohybrid (Mouse Neuroblastoma x Rat Glioma hybrid) cell line because it naturally expresses the delta-opioid receptor (Dr. Dana Selley's laboratories at VCU).

#### A. Cell Culture Protocol

Similar protocols are used employed to grow and harvest all of the cell lines used for the pharmacology studies. However, there are some differences in media used for each cell line. Freezebacks of each cell line are obtained from their respective laboratories.

First, the cells are put into a 15 mL falcon tube with complete media and spun down at 5000 rpm for 5 minutes. Complete media consists of FBS (Fetal Bovine Serum,

USDA approved, Invitrogen), G418 (Genetecin, Invitrogen), and Penicillin/Streptomycin (Invitrogen). For the NG108-15 and HEK cell lines, 1.5M Hepes (Mediatech) is added for a final concentration of 15 mM. Plain media is just media with no additional additives.

After the cells are spun down, the supernatant is poured off and the pellet is re-suspended in 10 mL of complete media. Next, the cells are plated in a tissue dish (100 x 20 mm, Fischer) with complete media and placed in the incubator set at 37 °C with 5% $CO_2$ and 95% humidity. The cells are left until they were about 80% confluent and then passed from 1 to 4 tissue dishes by pouring off the old media and adding 4 mL of Trypsin with 0.05% EDTA (Invitrogen). The cells are put back into the incubator for 3 to 5 minutes until all the cells were detached from the tissue dish. Then 4 mL of complete media is added to the cells. Next, 2 mL of the cells in media are added to each tissue dish. Then the cells are placed back into the incubator until they are confluent, this takes about 1 to 2 days depending on the cell line. Two plates are then passed the same way from 2 to 8 tissue dishes. The other 2 tissue dishes are frozen down to create more freezebacks.

After the second passage there are 8 tissue dishes. When the cells are confluent, they are transferred into 8 flasks (175 $cm^2$, Corning) by pouring off the old media and adding 4 mL of trypsin. Then the cells from each tissue dish are added into separate flasks. About 25 mL of complete media is added to each of the flasks and placed back into the incubator. When the cells in the flasks are confluent, they are harvested by adding 6 mL of trypsin and put back into incubator for 10 to 15 minutes until all of the

cells detached from the flask. Then 6 mLs of complete media is added and the flasks were rinsed about 10 times to break up the cells. About 9 mL of cells are added into falcon tubes and 1 mL of cells was left in the bottom of each flask. Finally, 25 mL of complete media is added to the flasks and put back into incubator.

The cells in the falcon tubes are spun down at 5000 rpm for 5 minutes. The supernatant is poured off and the cells were re-suspended in 30 mL of 1X PBS (100mL of 10X PBS liquid concentrated in 900 mL deionized water, VWR) and spun down at 5000 rpm for 5 minutes. About 10 mL of TME with no NaCl is added and transferred into a polypropylene centrifuge tube. The cells are spun down again at 50,000 x g for 10 minutes at 4 °C. The supernatant is poured off and then 5 mL of TME with no NaCl is added and homogenized for 30 seconds. Next, a Bradford protein determination is run on the cells and the cells are divided into 3 mg portion in 2 mL cryovials (Corning) and frozen at -80 °C. The cells are passed until they reach their $20^{th}$ passage each time following the above procedure.

**B. Freezeback Protocol**

The freezebacks are created by pouring off the old media and adding 3 mLs of trypsin to each plate. When all of the cells detach from the tissue dish, they are put in a falcon tube and spun down at 5000 rpms for 5 minutes. The supernatant is poured off and 2 mL of a freezeback solution was added. The freezeback solution contains the appropriate media for the cells as well as 10% FBS and 10% sterile DMSO (Research

Organic Inc.). The cells are aliquoted into two 1 mL portions in cryovials and put into a -20 °C freezer for 30 minutes and then moved to the -80 °C freezer for long-term storage.

## C. Cell Media Recipe

Each of the cell lines used in the pharmacology studies has a different media recipe and two types of media were used for the cells. The CHO cell lines use DMEM/F12 (Invitrogen) and the HEK 293 and NG108-15 cell lines use DMEM (Invitrogen) media. The cell media also contains additives including FBS, G418, and Penicillin/Streptomycin.

A solution of 50 mg/mL of G418 is made by dissolving 5 g of G418 in 100 mL of HBSS (Hank's Balanced Salt Solution, Invitrogen) without $Ca^{2+}$ and $Mg^{2+}$ media. Then the pH of the solution is adjusted to 7.4 by the addition of 1N NaOH. The solution is stored in 10 mL portions in the -20 °C freezer till needed.

For the NG108-15 and DORHEK cells, a 1.5 M HEPEs solution is added. This is made by making a 1.5 M (35.7 g) HEPEs solution in 100 mL of deionized water. Then the solution is sterile filtered (Stericup Disposable Vacuum Filtration System, 22 μm, Millipore, Bedford, MA) under the hood. The solution is stored in 4 °C refrigerator until needed.

The FBS is prepared by thawing it overnight in 4 °C refrigerator. When the FBS is completely thawed, it is heat inactivated by placing it in a water bath set at 56 °C for 30 minutes. Then the FBS is aliquoted in 100 mL portions into autoclaved bottles. These bottles are then stored in the freezer set at -20 °C until needed.

The media for the DORHEK cells consists of DMEM media with 8% FBS (40 mL), 1% Penicillin/Streptomycin (5 mL), 1.5 mM Hepes (5 mL), and 0.2 mg/mL G418 (2 mL). The media prepared for the DORCHO cells consists of DMEM/F12 with 10% FBS (50 mL), 1% Penicillin/Streptomycin (5 mL) and 0.2 mg/mL G418 (2 mL).

The media prepared for the KORCHO and MORCHO cells consists of DMEM/F12 with 5% FBS (25 mL), 1% Penicillin/Streptomycin (5 mL) and 0.2 mg/mL G418 (2 mL). The DORCHO cells used the same media recipe except it contained 10% FBS (50mL) instead of 5% FBS.

For the NG108-15 cells the media is prepared similar to the DORHEK cells with DMEM media containing 10% FBS (50 mL), 1% Penicillin/Streptomycin (5 mL), 1.5 mM HEPEs (5 mL), and 0.2 mg/mL G418 (2 mL). For NG108-15 cells, 2 bottles of a 50X HAT supplement (final concentration 200 μM Hypoxanthine, 0.8 μM Aminopterin, and 32 μM thymidine, Hybrimax) is added by dissolving the HAT powder in 10 mL of deionized water and adding it directly to the media.

## 3.2 Preparation of Naltrexone and Naltrexamine Derivatives for Radiolabeled Binding Assays

The 14-*O*-heterocyclic substituted naltrexone derivatives and the 6-*N*-heterocyclic substituted naltrexamine derivates are prepared for the binding assays by drying them on a vacuum pump for at least 2 h. Then 2 mM stock concentrations of the compounds are prepared by first dissolving the compound in a drop of DMSO and using a vortex to mix the compound until it was completely dissolved. Then 1 mL of deionized water is added

and mixed again using a vortex. Finally, the compound is aliquoted into 50 µL portions and stored at -20 °C freezer till needed.

The above procedure is followed for all of the compounds except compound **17**. Compound **17** is insoluble in deionized water so it was dissolved in 70% DMSO and 30% deionized water to make the 2 mM stock solution.

### 3.3 Radiolabeled Binding Assays

#### A. Saturation or Scatchard Radiolabeled Binding Assay

The saturation ligand-binding assay is the main technique used in the determination of the availability of the receptors. In this assay, receptors are incubated with increasing concentrations of radiolabeled ligand. From this assay the Bmax, the density or the maximum number of binding sites, and Kd, dissociation constant of the radioligand, is determined.[101] The saturation assay is conducted for the KORCHO, DORCHO and DORHEK cell lines from the University of Minnesota. Other cell lines used includes MORCHO and NG108-15 cell lines from Dr. Selley's laboratories at Virginia Commonwealth University and DORCHO cells from Temple University but the saturation assay was not conducted for these cell lines.

The buffer that was used in this experiment is TME without NaCl (24.27 g Tris, 50 mM), 1.16 g $MgCl_2$ (3 mM), 0.312 g EGTA (0.2 mM), 4 L DI water and pH adjusted to 7.7 at room temperature). For this particular assay there will be 8 different concentrations of [$^3$H] radioligand ranging from 0.01 nM to 2.0 nM. All the concentrations are done in triplicate with each concentration having non-specific tubes

also in triplicate. The non-specific binding is measured with the addition of same ligand as the radioligand but not labeled with tritium. The total volume in each tube is 500 µL. For the total binding it will include the cells, radioligand, and TME without NaCl. For non-specific binding it will include all of the components in total binding as well as the addition of cold ligand.

Below is a general step-by-step protocol for the saturation binding assay. However, some changes are made in certain cases discussed in the discussion and results section.

**Preparation of Protein**

1. Remove cells from -80 °C freezer and thaw. Add about 5mL of TME buffer with no NaCl into the centrifuge tube for every cell aliquot used.

   **NOTE: Keep all buffers, compounds and cells on ice at all times!**
2. Vortex cells to make sure the cells are completely dissolved in the buffer.
3. Counterbalance the tubes by weight and centrifuge at 50,000 x g for 10 minutes at 10 °C.
4. Pour out the supernatant and keep the pellet. Re-suspend the pellet in about 3 to 4 mLs of the TME buffer with no NaCl for every tube of cells used.
5. Homogenize the cells to make sure they are completely dissolved in the buffer. Keep the cells on ice.

6. Conduct the Bradford Protein Determination Assay using BSA (Bovine Serum Albumin) as standards using a Beckman DU 640 Spectrophotometer.

**Saturation/Scatchard Assay**

1. Propylene culture tubes (12x75 mm) were numbered and placed in racks on ice.
2. First add the appropriate amount of TME with No NaCl to all the culture tubes. Note: Follow spreadsheet made with concentrations and amounts of drugs to add to the tubes. Normally final volume will be 500 µL per tube.
3. For this assay, there are 8 different concentrations of the radioligand used ranging from 0.05 to 2 nM. Each different concentration of radioligand will have a Non-specific and binding vials in triplicate, 6 tubes for each concentration of radioligand.

**Radioligand used for respective opioid receptor:**

**Mu = [$^3$H] Naloxone**

**Kappa = [$^3$H] NorBNI**

**Delta = [$^3$H] Naltrindol**

4. Make the non-specific with cold drug at 0.1 mM, final concentration will be 0.01 mM, and add 50 µL to the non-specific tubes. You will need about 1200 µL of cold drug for each rack.

**Non-specific used the following drugs for respective opioid receptor:**

**Mu = Naltrexone**

**Kappa = NorBNI**

**Delta = Naltrindol**

5. After selecting concentrations of radioligand to use, make a serial dilution to the appropriate concentrations. Make the drugs 10 times more concentrated than final desired concentration. Add 50 µL to the appropriate tubes.
6. Add 100 µL of cells to each tube. Vortex the tubes and place into the shaking water bath for 90 minutes at 30 °C.
7. Prepare standards by adding 50 µL of each concentration of radioligand to 4 mL of scintillation fluid (EconoSafe™ Economical Biodegradable Counting Cocktail) in 7 mL scintillation vials. You will need 3 tubes per concentration of radioligand so in total there will be 24 standards.
8. Fill blue racks with scintillation vials leaving the first and last slots open. You will need 3 blue racks for each rack of tubes.
9. Before the incubation was complete GF/B glass fiber filters (Brandel) were placed in the brandel harvester and rinsed with cold 50 mM Tris buffer (pH 7.2).

10. After 90 minutes, remove rack from water bath and incubation was quenched with cold 50 mM Tris buffer and aspirated and rinsed three times with cold 50 mM Tris.
11. Remove filter paper and transfer to scintillation tubes using puncher/filler. Fill tubes with 4 mL of scintillation fluid and cap.
12. Label tubes and shake for 30 to 60 mins.
13. The bound radioactivity was determined by liquid scintillation spectrophotometry (Beckman Coulter LS6500 Scintillation Counter).
14. Clean Brandel harvester with a little bit of 70% EtOH and rinse with lots of deionized water.

**B. One-Site Competition Binding Assay**

The main technique used to characterize the naltrexone derivatives synthesized in our laboratoies by a one-site competition binding assay. In this assay receptors are incubated with a constant concentration of radiolabeled ligand that is 0.75 to 1 times the Kd value determined in the saturation binding assay and various concentrations of the naltrexone derivatives. From this assay the Ki, the affinity of the unlabeled drug of interest for the receptor which uses the Cheng-Prusoff equation, and $EC_{50}$, the molar concentration of the unlabeled drug of interest that produces 50% inhibition of specific radioligand binding, is determined.[103]

For each naltrexone derivative, the one-site competition binding assay is done for the mu-, delta- and kappa-opioid receptors. For the mu-opioid receptor, the MORCHO

cells from Dr. Selley's laboratories (VCU) are used. The kappa-opioid receptor data uses KORCHO cells from the University of Minnesota. Both the mu- and kappa-opioid receptor data is analyzed using hill plot between 5 and 95 percent inhibition. The delta-opioid receptor data uses the DORHEK cells from the University of Minnesota for the 6-*N*-heterocyclic substituted naltrexamine derivatives. This set of data is analyzed using nonlinear regression using Prism, a statistical software package. The 14-*O*-heterocyclic substituted naltrexone derivatives delta-opioid receptor data uses the DORCHO cells from Temple University. This set of data is analyzed by using the hill plot between 5 and 95 percent inhibition.

The buffer uses in this assay is TME buffer without NaCl (24.27 g Tris 50mM), 1.16 g $MgCl_2$ (3 mM), 0.312 g EGTA (0.2 mM), 4 L DI water and pH adjusted to 7.7 at room temperature). The protein concentration ranges from 9 to 30 μg depending on the cells being used. For this assay, the concentration of the [$^3$H] radioligand will be 0.75 to 1 times the Kd value determined by the saturation assay. The non-specific binding is measured with the addition of the same ligand as the radioligand but not labeled with tritium. The total volume in each tube is 500 μL. For this assay, there are 3 types of tubes: total binding, non-specific binding, and drugs competition binding. For the total binding, it will include the cells, radioligand, and TME without NaCl. For non-specific binding, it will include all of the components in total binding as well as the addition of cold ligand. For each rack, 2 different drugs can be tested with 7 different concentrations. These tubes will include radioligand, cells, drug of interest and TME with no NaCl. All of these tubes are done in triplicate. A serial dilution of the drugs of

interest is made 10 times more concentrated than the final concentrations that ranged from 0.001 nM to 1000 nM. The concentration ranges can be narrowed down to get a more accurate Ki value.

The basic protocol is very similar to the saturation assay. The general step-by-step protocol for the competition binding assay can be seen below and some changes are made in certain cases discussed in the discussion and results section.

**Preparation of Protein**

1. Remove cells from -80°C freezer and thaw. Add about 5mL of TME buffer with no NaCl into the centrifuge tube for every cell aliquot used.

   **NOTE: Keep all buffers, compounds and cells on ice at all times!**
2. Vortex cells to make sure the cells are completely dissolved in the buffer.
3. Counterbalance the tubes by weight and centrifuge at 50,000 x g for 10 minutes at 10°C.
4. Pour out the supernatant and keep the pellet. Re-suspend the pellet in about 3 to 4 mLs of the TME buffer with no NaCl for every tube of cells used.
5. Homogenize the cells to make sure they are completely dissolved in the buffer. Keep the cells on ice.
6. Conduct the Bradford Protein Determination Assay using BSA (Bovine Serum Albumin) as standards using a Beckman DU 640 Spectrophotometer.

**One-site Competition Binding Assay**

1. Propylene culture tubes (12x75 mm) were numbered and placed in racks on ice.
2. First, add the appropriate amount of TME with No NaCl to all the culture tubes. Note: Follow spreadsheet made with concentrations and amounts of drugs to add to the tubes. Normally final volume will be 500 µL per tube.
3. Make the cold drug 10 x more concentrated than the final desired concentration in TME with no NaCl. So, the concentration should be 100 µM with a final concentration 10 µM. Add 50 µL to the appropriate tubes in triplicate. This is your non-specific.

   **Non-specific used the following drugs for respective opioid receptor:**

   **Mu = Naltrexone**

   **Kappa = NorBNI**

   **Delta = Naltrindol**
4. Make the dilutions of your drugs in TME with no NaCl and add 50 µL of drug to appropriate tubes. The drugs should be made 10 times more concentrated than the desired concentration. Also, in the beginning you should test a wide range before narrowing it down. **Note: You can do 2 drugs per rack in triplicate.**

5. Make the stock solution of the radioligand 10 times more concentrated than desired concentration in TME with no NaCl. Add 50 µL to all the tubes. **Note: The concentration of radioligand is normally 0.75 to 1 times of its Kd.**

**Radioligand used for respective opioid receptor:**

**Mu = [$^3$H] Naloxone**

**Kappa = [$^3$H] NorBNI**

**Delta = [$^3$H] Naltrindol**

6. Add 100 µL of cells to each tube. Vortex the tubes and place into the shaking water bath for 120 minutes at 30 °C.
7. Prepare standards by adding 50 µL of radioligand to 4 mL of scintillation fluid (EconoSafe™ Economical Biodegradable Counting Cocktail) in 7 mL scintillation vials in triplicate. Cap and label the standards.
8. Fill blue racks with scintillation vials leaving the first and last slots open. You will need 3 blue racks for each rack of tubes.
9. Before the incubation was complete, GF/B glass fiber filters (Brandel) were placed in the brandel harvester and rinsed with cold 50 mM Tris buffer (pH 7.2).
10. After 120 minutes, remove rack from water bath and incubation was quenched with cold 50 mM Tris buffer and aspirated and rinsed three times with cold 50 mM Tris.

11. Remove filter paper and transfer to scintillation tubes using puncher/filler. Fill tubes with 4 mL of scintillation fluid and cap.
12. Label tubes and shake for 30 to 60 minutes.
13. The bound radioactivity was determined by liquid scintillation spectrophotometry (Beckman Coulter LS6500 Scintillation Counter).
14. Clean Brandel harvester with a little bit of 70% EtOH and rinse with lots of deionized water.

**C. Functional [$^{35}$S] GTPγS Assay – Agonism of Compounds Compared with DAMGO**

The [$^{35}$S]GTPγS functional binding assay measures the level of G-protein activation following the binding of an agonist to a G-protein coupled receptor. This assay is useful to measure the functional activity of a ligand for a certain receptor including potency, efficacy and antagonistic affinity. Since this assay analyzes the earliest receptor-mediated events, the measures obtained from the agonist are not subject to amplification or other modulation that may occur further downstream from the receptor. From the functional [$^{35}$S] GTPγS binding assay we can determine the Emax, the maximum effect of the drug or the efficacy, and the $EC_{50}$, the molar concentration that produces 50% of the maximum possible effective response normally for an agonist or the potency. DAMGO, a full mu-opioid receptor agonist, is used to compare with our drugs. For this assay, we use TME with NaCl because $Na^+$ decreases spontaneous receptor activity.

In the assay, [$^{35}$S]GTPγS replaces the endogenous GTP that binds to the Gα subunit when the receptor is activated (**Figure 31**). Since the γ-thiophosphate bond is poorly hydrolyzed by GTPase, the G-protein is prevented from reforming the heterotrimer (**Figure 32**).[115] Therefore, the [$^{35}$S]GTPγS labeled $G_\alpha$ subunits accumulate and can be measured by counting the amount of [$^{35}$S]-label incorporated. The Gα subunit remains associated with the membrane by filtering the preparation through filters and counting the radioactivity retained on the filter.[101]

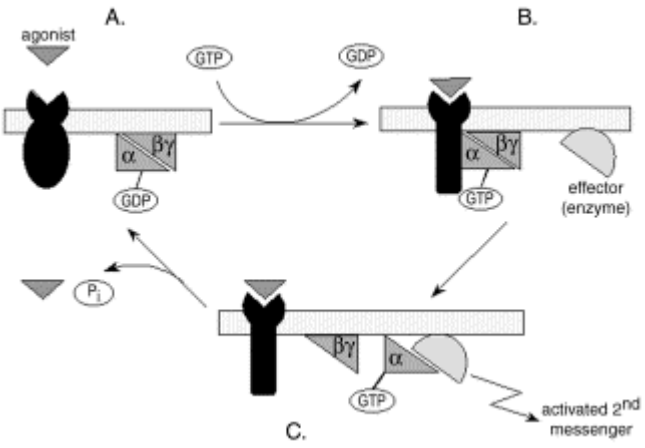


**Figure 31.** Guanine-nucleotide exchange in G-protein coupled receptor signaling cycle. (A) Low-affinity state of receptor where G-protein is uncoupled from the receptor. The agonist binds and induces receptor conformational change. (B) High-affinity state of receptor where the receptor is coupled to the G-protein, this is also known as the ternary complex. The ternary complex consists of an agonist, receptor and G-protein. Activation of receptor will release bound GDP and bind GTP. (C) The Gα subunit of the G-protein dissociates from the complex and interacts with downstream second messenger elements. The Gα subunit is turned off when the bound GTP undergoes a hydrolysis reaction to reform GDP and the receptor returns to inactive state.[108]

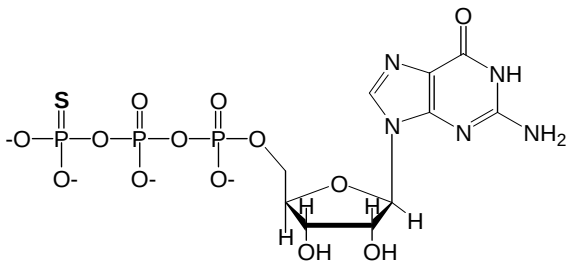

**Figure 32.** Chemical Structure of [$^{35}$S]GTPγS.

For each naltrexone derivative, a functional assay is done for the mu-opioid receptors. For the mu-opioid receptor, the MORCHO cells from Dr. Selley's laboratories (VCU) are used.

The buffer that is used in this assay is TME buffer with NaCl (24.27 g Tris 50 mM), 1.16 g $MgCl_2$ (3 mM), 0.312 g EGTA (0.2 mM), 28.38 g NaCl (100 mM), 4L DI water and pH adjusted to 7.7 at room temperature. The protein concentration ranges from 9 to 10 µg depending of MORCHO cells being used. For this assay, [$^{35}$S]GTPγS radioligand is used and the concentration of the radioligand is made to equal 125,000 DPMs (disintegrations per minute). The non-specific binding is measured with the addition of cold GTPγS or not labeled with [$^{35}$S]. The total volume in each tube is 500 µL. For this assay, there are 4 different conditions: basal, non-specific binding, DAMGO binding and drug binding. For the basal, it will include the cells, GDP, radioligand, and TME with NaCl. For non-specific binding, it will include all of the components in basal binding as well as the addition of cold GTPγS. For DAMGO, the tubes include DAMGO, GDP, cells and TME with NaCl. For each rack, 2 different drugs can be tested one with 6 different concentrations and one with 7 different concentrations. These tubes

will include radioligand, cells, GDP, drug of interest and TME with NaCl. All of these tubes are done in triplicate. A serial dilution of the drugs of interest was made 10 times more concentrated than the final concentrations that ranged from 0.001 nM to 10000 nM. After an idea of the value of the $EC_{50}$ has been determined, it is possible to narrow the concentration ranges to be around that value.

The general step-by-step protocol for the functional binding assay below and some changes are made in certain cases discussed in the discussion and results section.

**Preparation of Protein**

1. Remove cells from -80 °C freezer and thaw. Add about 5mL of TME buffer with NaCl into the centrifuge tube for every cell aliquot used.

**NOTE: Keep all buffers, compounds and cells on ice at all times!**

2. Vortex cells to make sure the cells are completely dissolved in the buffer.
3. Counterbalance the tubes by weight and centrifuge at 50,000 x g for 10 minutes at 10 °C.
4. Pour out the supernatant and keep the pellet. Re-suspend the pellet in about 3 to 4 mLs of the TME buffer with NaCl for every tube of cells used.
5. Homogenize the cells to make sure they are completely dissolved in the buffer. Keep the cells on ice.

6. Conduct the Bradford Protein Determination Assay using BSA (Bovine Serum Albumin) as standards using a Beckman DU 640 Spectrophotometer.

**GTPγS Functional Binding Assay**

1. Propylene culture tubes (12x75 mm) were numbered and placed in racks on ice.
2. First, add the appropriate amount of TME with NaCl to all the culture tubes. Note: Follow spreadsheet made with concentrations and amounts of drugs to add to the tubes. Normally final volume will be 500 µL per tube.
3. Make the cold GTPγS to 10 µM concentration (final concentration will be 1 µM) according to work up table in TME with NaCl and add 50 µL to the appropriate tubes in triplicate. Cold GTPγS is used to measure your non-specific.
4. Make the dilutions of your drugs and add 50 µL of drug to appropriate tubes. Note: The drugs should be 10 times more concentrated then the final concentration. Also, in the beginning you should test a wide range before narrowing it down. **Note: You can make 2 drug in triplicate for each rack.**
5. Make a 100 µM solution of GDP (final concentration will be 10 µM) in TME with NaCl and add 50 µL in to all the tubes.

**6.** Make the stock solution of the [$^{35}$S] GTPγS radioligand with TME with NaCl. Add 50 µL to all of the tubes. **Note: For 1 aliquot of [$^{35}$S]GTPγS, about 5 µL, you will need around 5 mL of TME with NaCl. Basically, you need to make your standards to be around 125,000 DPM so check by adding 50 µL to 4 mL of scintillation fluid (EconoSafe™ Economical Biodegradable Counting Cocktail) in 7 mL scintillation vials in triplicate and check with scintillation counter.**

7. Add 100 µL of cells to each tube. Vortex the tubes and place into the shaking water bath for 90 minutes at 30 °C.

8. Fill blue racks with scintillation vials leaving the first and last slot open. You will need 3 blue racks for each rack of tubes.

9. Before the incubation was complete GF/B glass fiber filters, (Brandel) were placed in the brandel harvester and rinsed with cold 50 mM Tris buffer (pH 7.2).

10. After 90 minutes, remove rack from water bath and incubation was quenched with cold 50 mM Tris buffer and aspirated and rinsed three times with cold 50 mM Tris.

11. Remove the rack from the water bath and aspirate the tubes and rinse 3 times with cold tris.

12. Remove filter paper and transfer to scintillation tubes using puncher/filler. Fill tubes with 4 mL of scintillation fluid and cap.

13. Label tubes and place in counter with a 9 hour delay use program 10 and place a rack with any 3 vials from any previous assay. **Note: Each vial will be counted for 3 hours.**
14. The bound radioactivity was determined by liquid scintillation spectrophotometry (Beckman Coulter LS6500 Scintillation Counter).
15. Clean Brandel harvester with a little bit of 70% EtOH and rinse with lots of deionized water.

**D. Functional [$^{35}$S]GTPγS Assay – Competition of Naltrexamine Derivatives with DAMGO**

Next, the step is to determine whether the 6-*N*-heterocyclic substituted naltrexamine derivatives were antagonists by conducting a functional [$^{35}$S] GTPγS assay where the drug of interest is competing against DAMGO, a full mu-opioid agonist. From this functional [$^{35}$S] GTPγS binding assay we can determine the Emax, the maximum effect of the drug or the efficacy, and the $EC_{50}$, the molar concentration that produces 50% of the maximum possible effective response normally for an agonist or the potency.[107] DAMGO, a full mu-opioid agonist, is used to compare with our drugs. For this assay, TME with NaCl is used because $Na^+$ decreases agonist binding and will barely affect antagonist binding.

For each naltrexone derivative, a functional assay is done for the mu-opioid receptors. For the mu-opioid receptor, the MORCHO cells from Dr. Selley's laboratories (VCU) is used.

The buffer that is used in this assay is TME buffer with NaCl (24.27 g Tris 50mM), 1.16 g $MgCl_2$ (3 mM), 0.312 g EGTA (0.2 mM), 28.38 g NaCl (100 mM), 4L DI water and pH adjusted to 7.7 at room temperature). The protein concentration ranges from 9 to 10 µg depending of MOR CHO cells being used. For this assay, [$^{35}$S]GTPγS radioligand is used and the concentration of the radioligand is made to equal 125,000 DPMs (disintegrations per minute). The non-specific binding is measured with the addition of cold GTPγS or not labeled with [$^{35}$S]. The total volume in each tube is 500 µL. For this assay, there are 4 types of tubes: basal, non-specific binding, DAMGO binding and drug binding. The basal includes the cells, GDP, radioligand, and TME with NaCl. For non-specific binding, it will include all of the components in Basel binding as well as the addition of cold GTPγS. For the set of DAMGO, tubes include DAMGO, GDP, cells and TME with NaCl. There are 7 different concentrations of DAMGO used ranging from 0.001 to 10 nM. The first set of tubes is just DAMGO and then the last set of 7 tubes is DAMGO at different concentrations with a single concentration of the drug of interest. Normally the concentration of the drug of interest is about 10 times its Ki value. For each rack, only 1 different drug can be tested. These tubes will include radioligand, cells, GDP, DAMGO, the drug of interest and TME with NaCl. All of these tubes are done in triplicate.

For these assays, the Ke value is determined for the drug of interest by comparing the right shift in the curve produced by the addition of the drug of interest to DAMGO.

The general step-by-step protocol for the functional competition binding assay of DAMGO and drug of interest can be seen below. Some changes are made in certain cases discussed in the discussion and results section.

**Preparation of Protein**

1. Remove cells from -80 °C freezer and thaw. Add about 5mL of TME buffer with NaCl into the centrifuge tube for every cell aliquot used.

   **NOTE: Keep all buffers, compounds and cells on ice at all times!**

2. Vortex cells to make sure the cells are completely dissolved in the buffer.
3. Counterbalance the tubes by weight and centrifuge at 50,000 x g for 10 minutes at 10 °C.
4. Pour out the supernatant and keep the pellet. Re-suspend the pellet in about 3 to 4 mLs of the TME buffer with NaCl for every tube of cells used.
5. Homogenize the cells to make sure they are completely dissolved in the buffer. Keep the cells on ice.
6. Conduct the Bradford Protein Determination Assay using BSA (Bovine Serum Albumin) as standards using a Beckman DU 640 Spectrophotometer.

**GTPγS Functional Binding Assay**

1. Propylene culture tubes (12x75 mm) were numbered and placed in racks on ice.

2. First, add the appropriate amount of TME with NaCl to all the culture tubes. Note: Follow spreadsheet made with concentrations and amounts of drugs to add to the tubes. Normally final volume will be 500 µL per tube.
3. Make the cold GTPγS to 10 µM concentration (final concentration will be 1 µM) according to work up table in TME with NaCl and add 50 µL to the appropriate tubes in triplicate. Cold GTPγS is used to measure your non-specific.
4. Make the dilutions of your drugs and add 50 µL of drug to appropriate tubes. Note: The drugs should be 10x more concentrated then the final concentration. Also in the beginning you should test a wide range before narrowing it down. **Note: You can make 2 drug in triplicate for each rack.**
5. Make a 100 µM solution of GDP (final concentration will be 10 µM) in TME with NaCl and add 50 µL in to all the tubes.
6. Make the stock solution of the [$^{35}$S] GTPγS radioligand with TME with NaCl. Add 50 µL to all of the tubes. **Note: For 1 aliquot of [$^{35}$S]GTPγS, about 5 µL, you will need around 5 mL of TME with NaCl. Basically, you need to make your standards to be around 125,000 DPM so check by adding 50 µL to 4 mL of scintillation fluid (EconoSafe™ Economical Biodegradable Counting Cocktail) in 7 mL scintillation vials in triplicate and check with scintillation counter.**

7. Add 100 µL of cells to each tube. Vortex the tubes and place into the shaking water bath for 90 minutes at 30 °C.
8. Fill blue racks with scintillation vials leaving the first and last slot open. You will need 3 blue racks for each rack of tubes.
9. Before the incubation was complete GF/B glass fiber filters (Brandel) were placed in the brandel harvester and rinsed with cold 50 mM Tris buffer (pH 7.2).
10. After 90 minutes, remove rack from water bath and incubation was quenched with cold 50 mM Tris buffer and aspirated and rinsed three times with cold 50 mM Tris.
11. Remove the rack from the water bath and aspirate the tubes and rinse 3 times with cold tris.
12. Remove filter paper and transfer to scintillation tubes using puncher/filler. Fill tubes with 4 mL of scintillation fluid and cap.
13. Label tubes and place in counter with a 9 h delay use program 10 and place a rack with any 3 vials from any previous assay. **Note: Each vial will be counted for 3 hours.**
14. The bound radioactivity was determined by liquid scintillation spectrophotometry (Beckman Coulter LS6500 Scintillation Counter).
15. Clean Brandel harvester with a little bit of 70% EtOH and rinse with lots of deionized water.

**4. Data Analysis of Pharmacological Studies**

The competition binding assays are used to determine the affinity of these 14-*O*-heterocyclic substituted naltrexone derivatives and 6-*N*-heterocyclic substituted naltrexamine derivatives for all three opioid receptors. From the assay, the $IC_{50}$ values are determined, and using the Cheng-Prusoff equation, the $IC_{50}$ values can be converted into Ki values (**Figure 33**).[103]

$$\mathbf{Ki = \frac{IC_{50}}{1 + (D/K_D)}}$$

**Figure 33.** Cheng-Prusoff equation. This is the equation to convert the $IC_{50}$ of a ligand to the Ki or the concentration required to produce 50% inhibition of the competing radioligand. The D represents the concentration of radioligand and the Kd is the dissociation constant of the radioligand binding to the receptor.[103]

A graphical representation, competition binding curve, is created consisting of the log concentration of the naltrexone derivative versus the percent of radioligand bound for each concentration of naltrexone derivative. Only the linear portion of the curve, where 5 to 95% of the radioligand is bound, is considered in determining the $IC_{50}$ value. $IC_{50}$ is determined where the concentration of the competitive ligand produces 50% inhibition of the competing radioligand (**Figure 34**).[116]

The standard error of the mean was determined for each compound and the ratio between delta- to mu-opioid receptors and kappa- to mu-opioid receptors was determined.

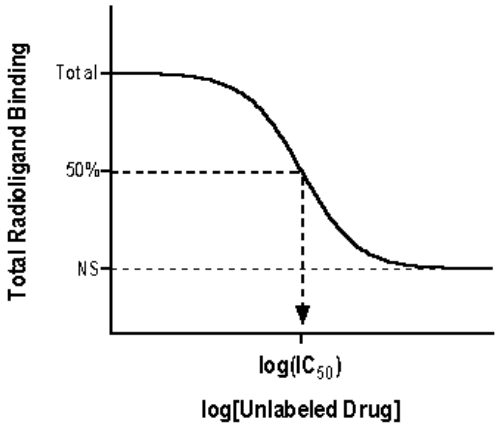


**Figure 34.** Competition binding curve. Binding of a single concentration of labeled ligand in the presence of various concentrations of unlabeled ligand. The $IC_{50}$ is determined where there is 50% radioligand bound to receptor.[117]

In order to characterize the agonistic activity of these naltrexone derivatives, a functional binding assay was conducted, and the 14-*O*-heterocyclic substituted naltrexone derivatives and 6-*N*-heterocyclic substituted naltrexamine derivatives Emax values are compared to the Emax value for DAMGO. Competition binding curves are constructed from the data where the log concentration of the unlabeled drug is on the x-axis and the percent stimulation of the receptor by the binding of [$^{35}$S]GTPγS is on the y-axis. From the curves, the potency, or $EC_{50}$, and the intrinsic efficacy, or Emax, are determined. The $EC_{50}$ is the molar concentration of an agonist to produce 50% of the maximal possible effect and the Emax is the maximum effect of the agonist.[106] DAMGO has an Emax value of 366% stimulation of receptor and represents 100% agonist activity. All of the naltrexone derivatives are compared to DAMGO's Emax value in order to determine whether these compounds are agonists, partial agonists or antagonist profiles. Since the measurement is taken at the first step of activation where GTP binds, amplification is not

a factor and provided the best source of information about ligand-induced events at the receptor.[118]

Stimulation of [$^{35}$S]GTPγS through binding of an agonist produces a sigmoidal concentration effect curve (**Figure 34**). Therefore, the effects of competitive antagonists can be measured using a similar [$^{35}$S]GTPγS assay. The shifts in the agonist concentration-effect curve for the [$^{35}$S]GTPγS binding in the presence of a single-concentration of antagonist can be measured. A dissociation constant, Ke, for the antagonist is determined from the right shift in the agonist concentration-effect curve (**Figure 35**). From the Ke, the reciprocal can be taken and defined as the affinity of the antagonist such that when the degree of shift of the agonist dose-response curve is 2 fold, the $-\log_{10}Ke=pA_2$ where Ke is in molar concentration. The $pA_2$ value is the apparent affinity that is the negative log of the molar concentration of antagonist that makes it necessary to double the concentration of the agonist needed to elicit the original submaximal response obtained in the absence of antagonist. This analysis assumes the antagonist is competitive and not dependent on how the antagonist acts.[106,107]

$$\textbf{Dose Ratio} = \frac{\textbf{[EC}_{\textbf{50}}\textbf{ DAMGO + Antagonist]}}{\textbf{[EC}_{\textbf{50}}\textbf{ DAMGO]}}$$

$$\textbf{Ke} = \frac{\textbf{[Antagonist]}}{\textbf{(Dose Ratio-1)}}$$

**Figure 34.** Determination of the dose ratio and dissociation constant (Ke). The dose ratio is determined from the $EC_{50}$ of DAMGO with a single concentration of antagonist present over the $EC_{50}$ of DAMGO by itself. The Ke is determined from the concentration of the antagonist divided by the dose ratio minus 1.[107]

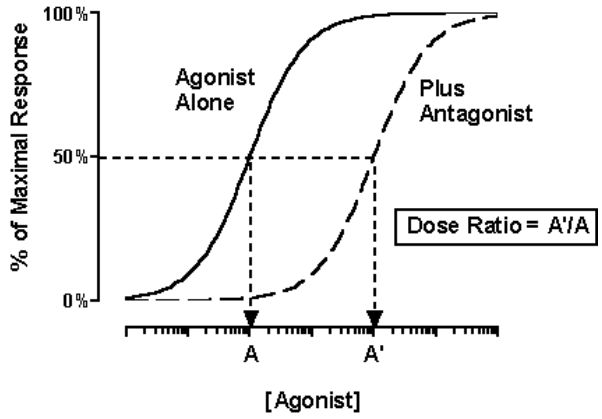


**Figure 35.** [$^{35}$S]GTPγS functional competition binding curve. Concntration curve of the binding of a full agonist at varying concentrations and the addition of a single concentration of antagonist to produce a right shift in the curve. A dose ratio can be calculated to determine the dissociation constant, Ke, for the antagonist.[117]

## 5. Molecular Modeling Studies

### 5.1 Homology Model of the Mu-Opioid Receptor

A homology model of the mu-opioid receptor was built based on the X-ray crystal structure of bovine rhodopsin (1U19) with a resolution of 2.2 Å.[109] A primary sequence alignment was conducted using Clustal X. Rhodopsin sequence was aligned with the human mu-opioid receptor sequence as well as human delta- and kappa-opioid receptors for a more accurate alignment. The helices were identified based the alignment in reference to the conserved residues in all GPCRs.[119] The bovine rhodopsin crystal structure was downloaded into Sybyl 7.1 from the Protein Data Bank. All seven helices of bovine rhodopsin were mutated and the N terminus and C terminus of mu-opioid receptor was cleaved off before Ile68 and after Pro355 respectively. Loop searches were conducted for EL (extracellular loops) 1, 2 and 3, IL (intracellular loop) 3 and the

beginning of TM (transmembrane) 2. It was very important to maintain the same backbone orientation of rhodopsin in the mu-opioid receptor homology model's EL2 and the TM helices part since they were involved in the binding pocket of most GPCRs. Once the mu-opioid receptor model was generated, SCWRL (Side Chain Placement with Rotamer Library) was used to minimize sidechain-backbone and sidechain-sidechain clashes. Since SCWRL broke the disulfide bond between cysteine amino acid residues 130 of TM3 and 180 of EL2, they were rejoined manually. Also, hydrogens are added and lone pairs of electrons were deleted. Then the receptor model conformation is minimized and the backbone validation was conducted using ProTable. ProTable program was used to check the geometry and stereochemistry of the backbone and sidechains of the receptor.

## 5.2 Binding Pocket Modification of the Mu-Opioid Receptor and Ligand Docking Studies

Compound **22** was manually docked into the binding pocket of MOR because it has a very high binding affinity to MOR (Ki = 1.439 nM) among all of the 14-*O*-heterocyclic substituted naltrexone derivatives. Site-directed mutagenesis data was used in order to position this compound within the mu-opioid receptor and to help characterize the binding pocket.[106,116] First, the protonated nitrogen near the cyclopropylmethyl group may form hydrogen bond or have ionic interaction with carboxyl group of Asp149 located on TM3 of MOR. It was reported that the Tyr150 residue locating also on TM3 might interact with the phenolic moiety at the third position of the naltrexone derivative.

The aromatic moiety Phe223 located on EL2 may also interact through hydrophobic interactions with the phenolic moiety at the third position of the naltrexone derivative. It has been reported that Trp320 located on TM7 has a hydrophobic interaction with the piperidinyl and cyclohexanonly rings in the naltrexone skeleton. Finally, Tyr328 also located on TM3 was shown to be an important recognition site for naltrexone through mutation to a phenyalanine which shows decreased binding affinity to naltrexone. Tyr328 might interact with the protonated amine and the C14 hydroxyl group of the naltrexone skeleton.

The compound was then merged into the receptor and locked into place. Another round of minimization is conducted to get the receptor into the lowest energy confirmation possible. The receptor is minimized for 100,000 iterations using Gasteiger-Hückel charges and a dielectric constant of 4.0.

Dynamic simulations were also run for 100,000 iterations, snapshots were taken every 25 fs, with Gasteiger-Hückel charges and a dielectric constant of 4.0. In addition to these normal settings for a molecular dynamics run of a membrane protein, an aggregate was setup around the ligand in order to keep the receptor from falling apart. Therefore, a radius of 8.0 Å is setup around the ligand and this area is the only part of the receptor-ligand complex that underwent dynamics simulation. When the simulation was complete, the last 2000 fs of the receptor was combined and minimized using the previous settings. The ligand was removed from the receptor and the 14-*O*-heterocyclic substituted naltrexone derivatives underwent docking studies.

All of the 14-*O*-heterocyclic substituted naltrexone derivatives were drawn into Sybyl 7.1 with a protonated amine and their conformations are minimized. GOLD (Genetic Optimization for Ligand Docking) 3.1 was used to perform docking studies for all of the ligands. The default settings were used and the active site radius was set to 15 Å measured from O1278, C1277, and O1279 from Asp149. Next, the distance constraints of 2 to 4 Å were set between O1278 to the positively charged nitrogen of the naltrexone derivatives. The best docking solutions of all the ligands were assessed using Sybyl 7.1.

Literature Cited

Literature Cited

1. Brownstein, M. A Brief History of Opiates, Opioid Peptides, and Opioid Receptors. *PNAS* **1993**, *90*, 5291-5393.

2. Kilpatrick, G.; Smith, T. Morphine-6-Glucuronide: Actions and Mechanisms. *Med. Res. Rev.* **2005**, *25*, 521-544.

3. Substance Abuse and Mental Health Services Administration, Office of Applied Studies, The NSDUH Report. Patterns and Trends in Non-medical Prescription Pain Relief Use: 2002 to 2005. *National Survey on Drug Use and Health* **2007**.

4. White, J.; Lopatko, O. Opioid Maintenance: A Comparative Review of Pharmacological Strategies. *Expert Opin. Pharmacother.* **2007**, *8*, 1-11.

5. Loh, H.; Liu, H.; Cavalli, A.; Yang, W.; Chen, Y.; Wei, L. Mu Opiod Receptor Knockout in Mice: Effects on Ligand-Induced Analgesia and Morphine Lethality. *Mol. Brain Res.* **1998**, *54*, 321-326.

6. Roozen, H.; De Waart, R.; Van Der Windt, D.; Van Den Brink, W.; De Jong, C.; Kerkhof, A. A Systematic Review of the Effectiveness of Naltrexone in the Maintenance Treatment of Opioid and Alcohol Dependence. *Eur. Neuropharm.* **2006**, *16*, 311-323.

7. Miotto, K.; McCann, M.; Basch, J.; Rawson, R.; Ling, W. Naltrexone and Dysphoria: Fact or Myth? *Am. J. Addict.* **2002**, *11*, 151-160.

8. Pfab, R.; Hirtl, C.; Zilker, T. Opiate Detoxification Under Anesthesia: No Apparent Benefit but Suppression of Thyroid Hormones and Risk of Pulmonary and Renal Failure. *J. Toxicol. Clin. Toxicol.* **1999**, *37*, 43-50.

9. Takemori, A.; Portoghese, P. Selective Naltrexone-Derived Opioid Receptor Antagonists. *Ann. Rev. Pharm. Toxicol.* **1992**, *32*, 239-269.

10. Gentilucci, L. New Trends in the Development of Opioid Peptide Analogues as Advanced Remedies for Pain Relief. *Curr. Top. Med. Chem.* **2004**, *4*, 19-38.

11. Pogozheva, I.; Przydzial, M.; Mosberg, H. Homology Modeling of Opioid Receptor-Ligand Complexes using Experimental Constraints. *AAPS Journal* **2005**, *7*, E434-E448.

12. Terenius, L. Stereospecific Interaction between Narcotic Analgesics and a Synaptic Plasma Memebrane Fraction of Rat Cerebral Cortex. *Acta Pharmacol. Toxicol.* **1973**, *32*, 317-320.

13. Pert, C.; Snyder, S. Opiate Receptor: Demonstration in Nervous Tissue. *Science* **1973**, *179*, 1011-1014.

14. Simon, E.; Hiller, J.; Edelman, I. Stereospecific Binding of the Potent Narcotic Analgesic [$^3$H] Etorphine to Rat-Brain Homogenate. *PNAS* **1973**, *70*, 1947-1949.

15. Lord, J.; Waterfield, A.; Hughes, J.; Kosterlitz, H. Endogenous Opioid Peptides: Multiple Agonists and Receptors. *Nature* **1977**, *267*, 495-499.

16. Mansour, A.; Taylor, L.; Fine, J.; Thompson, R.; Hoversten, M.; Mosberg, H.; Watson, S.; Akil, H. Key Residues Defining the Mu-Opioid Receptor Binding Pocket: A Site-Directed Mutagenesis Study. *J. Neurochem.* **1997**, *68*, 344-353.

17. Dhawan, B.; Cesselin, F.; Raghubir, R.; Reisine, T.; Bradley, P.; Portoghese, P.; Hamon, M. International Union of Pharmacology. XII. Classification of Opioid Receptors. *Pharmacol. Rev.* **1996**, *48*, 567-592.

18. Sim-Selley, L. Regional Difference in Adaptation of CNS Mu Opioid Receptors to Chronic Opioid Agonist Administration. *Curr. Neuropharm.* **2005**, *3*, 157-182.

19. Mansour, A.; Watson, S.; Akil, H. Opioid Receptors: Past, Present, and Future. *Trends Neurosci*. **1995**, *18*, 69-70.

20. Kane, B.; Svensson, B.; Ferguson, D. Molecular Recognition of Opioid Receptor Ligands. *AAPS Journal* **2006**,*8*, E126-E137.

21. Subramanian, G.; Paterlini, M.; Portoghese, P.; Ferguson, D. Molecular Docking Reveals a Novel Binding Site Model for Fentanyl at the Mu-Opioid Receptor. *J. Med. Chem.* **2000**, *43*, 381-391.

22. Connor, M.; Christie, M. Opioid Receptor Signalling Mechanisms. *Clin. Exp. Pharmacol. Physiol.* **1999**, *26*, 493-499.

23. Hamm, H. The Many Faces of G-Protein Signaling. *J. Biol. Chem.* **1998**, *273*, 669-672.

24. Spiegel, A. Mutations in G-Proteins and G-Protein-Coupled Receptors in Endocrine Disease. *J. Clin. Endocrinol. Metab.* **1996**, *81*, 2434-2442.

25. Taussig, R.; Iniguez-Lluhi, J.; Gilman, A. Inhibition of Adenylyl Cyclase by Gi alpha. *Science* **1993**, *261*, 218-221.

26. Svoboda, K.; Lupica, C. Opioid Inhibition of Hippocampal Interneurons via Modulation of Potassium and Hyperpolarization-activated cation (Ih) Currents. *J. Neurosci.* **1998**, *18*, 7084-7098.

27. Jan, L.; Jan, Y. Receptor-regulated Ion Channels. *Curr. Opin. Cell. Biol.* **1997**, *9*, 155-160.

28. Wilding, T.; Womack, M.; McCleskey, E. Fast Local Signal Transduction between the Mu Opioid Receptor and $Ca^{2+}$ Channels. *J. Neurosci.* **1995**, *15*, 4124-4132.

29. Mansour, A.; Khachaturian, H.; Lewis, M.; Akil, H.; Watson, S. Anatomy of CNS Opioid Receptors. *Trends Neurosci.*, **1988**, *11*, 308-314.

30. Minami, M.; Satoh, M. Molecular Biology of the Opioid Receptors: Structures, Functions, and Distributions. *Neurosci. Res.* **1995**, *23*, 121-145.

31. Mansour, A.; Fox, C.; Akil, H.; Watson, S. Opioid-receptor mRNA Expression in the Rat CNS: Anatomical and Functional Implications. *Trends Neurosci.* **1995**, *18*, 22-29.

32. Henriksen, G.; Wiloch, F. Imaging of Opioid Receptors in the Central Nervous System. *Brain* [Online early access]. doi:10.1093/brain/awm255. Published Online: Nov 29, 2007. http://brain.oxfordjournals.org/cgi/reprint/awm255v1 (accessed Mar 15, 2008).

33. Fields, H. State-dependent Opioid Control of Pain. *Nat. Rev. Neurosci.* **2004**, *5*, 565-575.

34. Fields, H. Understanding How Opioids Contribute to Reward and Analgesia. *Reg. Anesth. Pain Med.* **2007**, *32*, 242-246.

35. Bagnol, D.; Mansour, A.; Akil, H.; Watson, S. Cellular Localization and Distribution of Cloned Mu and Kappa Opioid Receptors in Rat Gastrointestinal Tract. *Neurosci.* **1997**, *81*, 579-591.

36. Mignat, C.; Wille, U.; Ziegler, A. Affinity Profiles of Morphine, Codeine, Dihydrocodeine and their Glucuronides at Opioid Receptor Subtypes. *Life Sci*. **1995**, *56*, 793-799.

37. Becker, A.; Grecksch, G.; Brodemann, R.; Kraus, J.; Peters, B.; Schroeder, H.; Thiemann, W.; Loh, H.; Hollt, V. Morphine Self-administration in Mu-opioid Receptor-deficient Mice. *Naunyn-Schmiedeberg's Arch. Pharmacol.* **2000**, *361*, 584-589.

38. Goodman, A.; Le Bourdonnec, B.; Dolle, R. Mu-Opioid Receptor Antagonists: Recent Developments. *Chemmedchem* **2007**, *2*, 1552-1570.

39. Pain. *Current Understanding, Emerging Therapies, and Novel Approaches to Drug Discovery* Bountra, C.; Munglai, R.; Schmidt, W., Eds.; Marcel Decker, New York, **2003**.

40. Williams, M.; Kowaluk, E.; Arneric, S. Emerging Molecular Approaches to Pain Therapy. *J. Med. Chem.* **1999**, *42*, 1481-1500.

41. Krishnan-Sarin, S.; Wand, G.; Li, X.; Portoghese, P.; Froehlich, J. Effects of Mu Opioid Receptor Blockade on Alcohol Intake in Rats Bred for High Alcohol Drinking. *Pharmacol. Biochem. Behav.* **1998**, *59*, 627-635.

42. Wentland, M.; Lu, Q.; Lou, R.; Bu, Y.; Knapp, B.; Bidlack, J. Synthesis and Opioid Receptor Binding Properties of a Highly Potent 4-Hydroxy Analogue of Naltrexone. *Bioorg. Med. Chem. Lett.* **2005**, *15*, 2107-2110.

43. Martin, W.; Jasinski, D.; Mansky, P. Naltrexone, An Antagonist for the Treatment of Heroin Dependence. Effects in Man. *Arch. Gen. Psychiat.* **1973**, *28*, 784-791.

44. Wall, M.; Brine, D.; Perez-Reyes, M. The Metabolism of Naltrexone in Man. *NIDA Res. Mono.* **1981**, *28*, 105-131.

45. Verebey, K. The Clinical Pharmacology of Naltrexone: Pharmacology and Pharmacodynamics. *NIDA Res. Mono.* **1981**, *28*, 147-158.

46. Gold, M.; Dackis, C.; Pottash, A.; Sternbach, H.; Annitto, W.; Martin, D.; Dackis, M. Naltrexone, Opioid Addiction, and Endorphins. *Med. Res. Rev.* **1982**, *2*, 211-246.

47. Headings, C. Vivitrex (Alkermes/Cephalon). *Curr. Opin. Invest. Drugs* **2006**, *6*, 81-88.

48. Yuen, K.; Peh, K.; Billa, N. Comparative Bioavailability Study of a Generic Naltrexone Tablet Preparation. *Drug Dev.Industrial Pharmacy* **1999**, *25*, 353-356.

49. Le Bourdonnec, B.; Belanger, S.; Cassel, J.; Stabley, G.; DeHaven, R.; Dolle, R. Trans-3,4-Dimethyl-4-(3-carboxamidophenyl)piperidines: A Novel Class of Mu-Selective Opioid Antagonists. *Bioorg. Med. Chem. Lett.* **2003**, *13*, 4459-4462.

50. Lewis, K. Analgesic Drugs. *Fundamentals of Anesthesia*, 2, Pinnock, C.; Smith, T.; Lin, T.; Jones, R., Eds.; Greenwich Medical Media Ltd.: London, 2003; 619-638.

51. Lewanowitsch, T.; Irvine, R. Naloxone and its Quatenary Derivatives, Naloxone Methiodide, have Differing Affinities for Mu, Delta, and Kappa Opioid Receptors in Mouse Brain Homogenates. *Brain Res.* **2003**, *964*, 302-305.

52. Umbricht, A.; Montoya, I.; Hoover, D.; Demuth, K.; Chiang, C.; Preston, K. Naltrexone Shortened Opioid Detoxification with Buprenorphine. *Drug Alcohol Depend.* **1999**, *56*, 181-190.

53. Eguchi, M. Recent Advances in Selective Opioid Receptor Agonists and Antagonists. *Med. Res. Rev.* **2004**, *24*, 182-212.

54. Henderson, C.; Reynolds, J. Acute Pulmonary Edema in a Young Male after Intravenous Nalmefene. *Anesth. Analg.* **1997**, *84*, 218-219.

55. Farren, C.; O'Malley, S. Occurrence and Management of Depression in the Context of Naltrexone Treatment of Alcoholism. *Am. J. Pscychiatry* **1999**, *156*, 1258-1262.

56. Márki, Á.; Monory, K.; Ötvös, F.; Tóth, G.; Krassnig, R.; Schmidhammer, H.; Traynor, J.; Roques, B.; Maldonado, R.; Borsodi, A. Mu-Opioid Receptor Specific Antagonist Cyprodime: Characterization by In Vitro Radioligand and [$^{35}$S]GTPγS Binding Assays. *Eur. J. Pharmacol.* **1999**, *383*, 209-214.

57. Schmidhammer, H.; Jennewein, H.; Krassnig, R.; Traynor, J.; Patel, D.; Bell, K.; Froschauer, G.; Mattersberger, K.; Jachs-Ewomger, C.; Jura, P.; Fraser, G.; Kalinin, V. Synthesis and Biological Evaluation of 14-Alkoxymorphinans. 11. 3-Hydroxycyprodime and Analgoues: Opioid Antagonist Profile in Comparison to Cyprodime. *J. Med. Chem.* **1995**, *38*, 3071-3077.

58. Ward, S.; Takemori, A. Relative Involvement of Mu, Kappa and Delta Receptor Mechanisms in Opiate-mediated Antinociception in Mice. *J. Pharmacol. Exp. Ther.* **1983**, *224*, 525-530.

59. Goldstein, A.; James, I. Site-directed Alkylation of Multiple Opioid Receptors. II. Pharmacological Selectivity. *Mol. Pharmacol.* **1984**, *25*, 343-348.

60. Comer, S.; Burke, T.; Lewis, J.; Woods, J. Clocinnamox: A Novel, Systematically-Active, Irreversible Opioid Antagonist. *J. Pharmacol. Exp. Ther.* **1992**, *262*, 1051-1056.

61. Takemori, A.; Larson, D.; Portoghese, P. The Irreversible Narcotic Antagonistic and Reversible Agonistic Properties of the Fumaramate Methyl Ester Derivative of Naltrexone. *Eur. J. Pharmacol.* **1981**, *70*, 445-451.

62. Takemori, A.; Portoghese, P. Affinity Labels for Opioid Receptors. *Ann. Rev. Pharmacol.* **1985**, *25*, 193-223.

63. Sayre, L.; Larson, D.; Takemori, A.; Portoghese, P. Design and Synthesis of Naltrexone-derived Affinity Labels with Nonequilibrium Opioid Agonist and Antagonist Activities. Evidence for the Existence of Different Mu-Receptor Subtypes in Different Tissues. *J. Med. Chem.* **1984**, *27*, 1325-1335.

64. Portoghese, P.; Kouhen, R.; Law, P.; Loh, H.; Le Bourdonnec, B. Affinity Labels as Tools for the Identification of Opioid Receptor Recognition Sites. *Il Farmaco,* **2001**, *56*, 191-196.

65. Broadbear, J.; Sumpter, T.; Burke, T.; Husbands, S.; Lewis, J.; Woods, J.; Traynor, J. Methocinnamox is a Potent, Long-Lasting, and Selective Antagonist of Morphine-Mediated Antinociception in the Mouse: Comparison with Clocinnamox, β-Funaltrexamine, and β-Chlornaltrexamine. *J. Pharmacol. Exp. Ther.* **2000**, *294*, 933-940.

66. Lewis, J.; Smith, C.; McCarthy, P.; Walter, D.; Kobylecki, R.; Myers, M.; Haynes, A.; Lewis, C.; Waltham, K. New 14-Aminomorphinones and Codeinones. *NIDA Res. Monogr.* **1988**, *90*, 136-143.

67. Verber, D.; Freidinger, R.; Schuenk-Perlow, D.; Paleveda, W.; Holly, F.; Stracham, R.; Nutt, R.; Arison, B; Homnick, C.; Randall, W.; Glitzer, M. A Potent Cyclic Hexapeptide Analogue of Somatostatin. *Nature* **1981**, *292*, 55-58.

68. Pardridge, W.; Eisenberg, J.; Yamada, T. Rapid Sequestration and Degradation of Somatostatin Analogues by Isolated Brain Microvessels. *J. Neurochem.* **1985**, *44*, 1178-1184.

69. Pelton, J.; Guyla, K.; Hruby, V.; Duckles, S.; Yamamura, H. Conformationally Restricted Analogues of Somatostatin with High Mu-Opiate Receptor Specificity. *PNAS* **1985**, *82*, 236-239.

70. Kazmierski, W.; Wire, W.; Lui, G.; Knapp, R.; Shook, J.; Burks, T.; Yamamura, H.; Hruby, V. Design and Synthesis of Somatostatin Analogues with Topographical Properties that Lead to Highly Potent and Specific Mu-Opioid Receptor Antagonists with Greatly Reduced Binding at Somatostatin Receptors. *J. Med. Chem.* **1988**, *31*, 2170-2177.

71. Abbruscato, T.; Thomas, S.; Hruby, V.; Davis, T. Blood-Brain Barrier Permeability and Bioavailability of a Highly Potent and Mu-Selective Opioid Receptor Antagonist CTAP: Comparison with Morphine. *J. Pharmacol. Exp. Ther.* **1997**, *280*, 402-409.

72. Knapp, R.; Kazmierski, W.; Hruby, V.; Yamamura, H. Structural Characteristics of Two Highly Selective Opioid Peptides. *BioEssays* **1989**, *10*, 58-61.

73. Wang, Z.; Bilsky, E.; Porreca, F.; Sadee, W. Constitutive Mu-Opioid Receptor Activation as a Regulatory Mechanism Underlying Narcotic Tolerance and Dependence. *Life Sci.* **1994**, *54*, PL339-PL350.

74. Egleton, R.; Abbruscato, T.; Thomas, S.; Davis, T. Transport of Opioid Peptides into the Centeral Nervous System. *J. Pharm. Sci.* **1998**, *87*, 1433-1439.

75. Raynor, K.; Kong, H.; Chen, Y.; Yasuda, K.; Yu, L.; Bell, G.; Reisine, T. Pharmacological Characterization of the Cloned Kappa-, Delta-, and Mu-Opioid Receptors. *Mol. Pharmacol.* **1994**, *45*, 330-334.

76. Toll, L.; Berzetei-Gurske, I.; Polgar, W.; Brandt, S.; Adapa, I.; Rodriguez, L.; Schwartz, R.; Haggart, D.; O'Brien, A.; White, A.; Kennedy, J.; Craymer, K.; Farrington, L.; Auh, J. Standard Binding and Functional Assays Related to Medications Development Divison Testing for Potential Cocaine and Opiate Narcotic Treatment. *NIDA Res. Monogr.* **1998**, *178*, 440-466.

77. Portoghese, P. Impact of Recombinant DNA Technology and Molecular Modeling on the Practice of Medicinal Chemistry: Structure-Activity Analysis of Opioid Ligands. *Am. J. Pharm. Educ.* **1999**, *63*, 342-347.

78. Schwyzer, R. ACTH: A Short Introductory Review. *Ann. N. Y. Acad. Sci.* **1977**, *297*, 3-26.

79. Portoghese, P. The Role of Concepts in Structure-Activity Studies of Opioid Ligands. *J. Med. Chem.* **1992**, *35*, 1927-1937.

80. Portoghese, P.; Nagase, H.; Maloney-Huss, K.; Lin, C.; Takemori, A. Role of Spacer and Address Components in Peptidomimetic Delta-Opioid Receptor Antagonists Related to Naltrindole. *J. Med. Chem.* **1991**, *34*, 1715-1720.

81. Portoghese, P. An Approach to the Design of Receptor-Type-Selective Non-Peptide Antagonists of Peptidergic Receptors: Delta Opioid Antagonists. *J. Med. Chem.* **1991**, *34*, 1757-1762.

82. Jones, R.; Portoghese, P. 5'-Guanidinonaltrindole, a Highly Selective and Potent Kappa-Opioid Receptor Antagonist. *Eur. J. Pharmacol.* **2000**, *396*, 49-52.

83. Portoghese, P. Molecular Recognition at Kappa Opioid Receptors. *Pure Appl. Chem.* **2001**, *73*, 1387-1391.

84. Jones, R.; Hjorth, S.; Schwartz, T.; Portoghese, P. Mutational Evidence for a Common Kappa Antagonist Binding Pocket in the Wild-type Kappa and Mutant Mu[K303E] Opioid Receptors. *J. Med. Chem.* **1998**, *41*, 4911-4914.

85. Hjorth, S.; Thirstrup, K.; Grandy, D.; Schwartz, T. Analysis of Selective Binding Epitopes for the Kappa-opioid Receptor Antagonist Nor-binaltorphine. *Mol. Pharmacol.* **1995**, *47*, 1089-1094.

86. Sagara, T.; Egashira, H.; Okamura, M.; Fujii, I.; Shimohigashi, Y.; Kanematsu, K. Ligand Recognition in Mu-Opioid Receptor: Experimentally Based Modeling of Mu-Opioid Receptor Binding Sites and their Testing by Ligand Docking. *Bioorg. Med. Chem.* **1996**, *4*, 2151-2166.

87. Zhang, Y.; Sham, Y.; Rajamani, R.; Gao, J.; Portoghese, P. Homology Modeling and Molecular Dynamics Simulations of the Mu Opioid Receptor in a Membrane-Aqueous System. *Chembiochem* **2005**, *6*, 853-859.

88. Dietrich, G.; Gaibelet, G.; Capeyrou, R.; Butour, J.; Pontet, F.; Emorine, L. Implication of the First and Third Extracellular Loops of the Mu-Opioid Receptor in the Formation of the Ligand Binding Site: A Study Using Chimeric Opioid/Angiotension Receptors. *J. Neurochem.* **1998**, *70*, 2106-2111.

89. Li, G.; Aschenbach, L.; Cassidy, M.; Stevens, D.; Gabra, B.; Selley, D.; Dewey, W.; Westkaemper, R.; Zhang, Y. Design, Synthesis and Biological Evaluation of Pyridinyl and Isoquinolinyl Formaidyl 6α and 6β-Naltrexamine Derivatives as Mu-Opioid Receptor Selective Antagonists. *J. Med. Chem* **2008**, submitted.

90. Grffin, J.; Larson, D.; Portoghese, P. Crystal Structure of α- and β-Fuanltrexamine: Conformational Requirement of Fumaramate Moiety in the Irreversible Blockage of Mu-Opioid Receptors. *J. Med. Chem.* **1986**, *29*, 778-783.

91. Sayre, L.; Larson, D.; Fries, D.; Takemori, A.; Portoghese, P. Importance of Carbon 6 Chirality in Conferring Irreversible Opioid Antagonism to Naltrexone-Derived Affinity Lables. *J. Med. Chem.*. **1983**, *26*, 1229-1235.

92. Linder, C.; Fishman, J. Narcotic Antagonists. 1. Isomeric Sulfate and Acetate Esters of Naloxone (*N*-Allylnoroxymorphone). *J. Med. Chem.* **1973**, *16*, 535-555.

93. Simon, E.; Fan, L.; Hiller, J.; Seyed-Mozaffari, A.; Schultz, A.; Archer, S. Photoaffinity Ligands for the Mu-Opioid Receptor. *Life Sci.* **1993**, *53*, 1173-1178.

94. Smith, M.; March, J. Aliphatic Nucleophilic Substitution. *March's Advanced Organic Chemistry: Reactions, Mechanisms, and Structure*, Eds. 5; John Wilay & Sons Inc.: New York, 2001; pp 389-674.

95. Pizey, J. Dimethylformaide, Lithium Aluminium Hydride, Mercuric Oxide, Thionyl Chloride. *Synthetic Reagents*, Vol. 1; Ellis Horwood Ltd: New York, 1974.

96. Bernardo, P.; Chai, C. Friedel-Crafts Acylation and Metalation Strategies in the Synthesis of Calothrixins A and B. *J. Org. Chem.* **2003**, *68*, 8906-8909.

97. Dorp, E.; Yassen, A.; Dahan, A. Naloxone Treatment in Opioid Addiction: the Risks and Benefits. *Expert Opin. Drug Saf.* **2007**, *6*, 125-132.

98. Okamoto, I.; Nabeta, M.; Minami, T.; Nakashima, A.; Morita, N.; Takeya, T.; Masu, H.; Azumaya, I.; Tamura, O. Acid-induced Conformational Switching of Aromatic *N*-methyl-*N*-(2-pyridyl)amides. *Tetrahedron Lett.* **2007**, *48*, 573-577.

99. Klee, W.; Nirenberg, M. A Neuroblastoma x Glioma Hybrid Cell Line with Morphine Receptors. *PNAS* **1974**, *71*, 3474-3477.

100. Simonds, W.; Burke, T.; Rice, K.; Jacobson, A.; Klee, W. Purification of the Opiate Receptor of NG108-15 Neuroblastoma-glioma Hybrid Cells. *PNAS* **1985**, *82*, 4974-4978.

101. Assay Guidance Manual Version 5.0, **2008**, Eli Lilly and Company and NIH Chemical Genomics Center. http://www.ncgc.nih.gov/guidance/manual_toc.html (accessed April 4, 2008).

102. Jong, L.; Uges, D.; Franke, J.; Bischoff, R. Receptor-Ligand Binding Assays: Technologies and Applications. *J. Chromatogr. B* **2005**, *829*, 1-25.

103. Cheng, H. The Power Issue: Determination of KB or Ki from IC50. A Closer Look at the Cheng-Prusoff Equation, the Schild Plot and Related Power Equations. *J. Pharmacol. Toxicol. Methods* **2001**, *46*, 61-71.

104. Bradford, M. A Rapid and Sensitive Method for the Quantitation of Microgram Quantities of Protein Utilizing the Principle of Protein Dye-binding. *Anal. Biochem.* **1976**, *72*, 248-254.

105. Sikkema, J.; de Bont, J.; Poolman, B. Mechanisms of Membrane Toxicity of Hydrocarbons. *Microbiol. Rev.* **1995**, *59*, 201-222.

106. Neubig, R.; Spedding, M.; Kenakin, T.; Christopoulos, A. International Union of Pharmacology Committee on Receptor Nomenclature and Drug Classification. XXXVIII. Update on Terms and Symbols in Quantitative Pharmacology. *Pharmacol. Rev.* **2003**, *55*, 597-606.

107. Harrison, C.; Traynor, J. The [$^{35}$S]GTPγS Binding Assay: Approaches and Applications in Pharmacology. *Life Sci.* **2003**, *74*, 489-508.

108. Schild, H. An Ambiguity in Receptor Theory. *Br. J. Pharmacol.* **1975**, *53*, 311.

109. Baldwin, J.; Schertier, G.; Unger, V. An Alpha-Carbon Template for the Transmembrane Helices in the Rhodopsin Family of the G-Protein-Coupled Receptor. *J. Mol. Biol.* **1997**, *272*, 144-164.

110. Thompson, J.; Gibson, T.; Plewniak, F.; Jeanmougin, F.; Higgins, D. The Clustal X Windows Interface: Flexible Strategies for Multiple Sequence Alignment Aided by Quality Analysis Tools. *Nulceic Acids Res.* **1997**, *25*, 4876-4882.

111. Bower, M.; Cohen, F.; Dunbrack, R. Prediction of Protein Side-Chain Rotamers from a Backbone-Dependent Rotamer Library: A New Homology Modeling Tool. *J. Mol. Biol.* **1997**, *267*, 1268-1282.

112. Verdonk, M.; Cole, J.; Hartshorn, M.; Murray, C.; Taylor, R. Improved Protein-Ligand Docking using GOLD. *Proteins* **2003**, *52*, 609-623.

113. Rónai, A.; Gyires, K.; Schmidhammer, H.; Hostzafi, S.; Borsodi, A.; Spetea, M.; Friedmann, T.; Riba, P.; Fürst, Z. In Vitro and In Vivo Pharmacology of Novel Naltrindole-Related Compounds. *Med. Sci. Monit*. **1997**, *3*, 1-5.

114. Sterious, S.; Walker, E. Potency Differences for D-Phe-Cys-Tyr-D-Trp-Arg-Thr-Pen-Thr-$NH_2$ as an Antagonists of Peptide and Alkaloid Mu-Agonists in an Antinociception Assay. *J. Pharmacol. Exp. Ther.* **2003**, *304*, 301-309.

115. Bidlack, J.; Parkhill, A. Methods in Molecular Biology. In *G-Protein Signaling: Methods and Protocols*. Smrcka, A., Eds.; Humana Press: Totowa, 2004; Vol. 237, pp 135-144.

116. Molusky, H.; Christopoulos, A. *Fitting Models in Biological Data using Linear and Nonlinear Regression: A Pratical Guide to Curve Fitting*; GraphPad Software Inc: San Diego, CA, 2003.

117. Williams, A.; Michel, A.; Feniuk, W.; Humphrey, P. Somatostatin5 Receptor-Mediated [$^{35}$S]Guanosine-5'-*O*-(3-thio)triphosphate Binding: Agonist Potencies and the Influence of Sodium Chloride in Intrinsic Efficacy. *Mol. Pharmacol.* **1997**, *51*, 1060-1069.

118. Traynor, J.; Nahorski, S. Modulation by Mu-Opioid Agonists of Guanosine-5'-O-(3-[$^{35}$S]thio)triphosphate Binding to Membranes from Human Neuroblastoma SH-SY5Y Cells. *Mol. Pharmacol.* **1995**, *47*, 848-854.

119. Bissantz, C.; Bernard, P.; Hilbert, M.; Rognan, D. Protein-Based Virtual Screening of Chemical Databases: II. Are Homology Models of the G-Protein Coupled Receptors Suitable Targets? *Proteins: Structure, Function and Genetics* **2003**, *50*, 5-25.

# VITA

Lindsey Carol Kikuyo Aschenbach wlas born on December 19, 1980 to parents Masaru and Deborah Aschenbach. Lindsey graduated from Virginia Tech in July 2004 with a Bachelor of Science degree in Biochemistry. She joined the Medicinal Chemistry department in the School of Pharmacy at Virginia Commonwealth University in August 2005.